



Aleksander Krupkowski  
Institute of Metallurgy and Materials Science  
Polish Academy of Sciences



Marian Smoluchowski Institute of Physics  
Faculty of Physics, Astronomy and Applied Computer Science  
Jagiellonian University

PhD thesis

## **Synthesis and characterization of polystyrene scintillators and their application in positron emission tomography**

**M.Sc. Łukasz Kapłon**

Supervisor: Prof. Paweł Moskal, Ph.D., D.Sc.

Faculty of Physics, Astronomy and Applied Computer Science  
Jagiellonian University

Co-supervisor: Andrzej Kochanowski, Ph.D.

Faculty of Chemistry, Jagiellonian University

Cracow 2017

Copyright© Jagiellonian University, Cracow, Poland

All rights reserved.

Any part of this book may not be reproduced or distributed by any means without written permission of the author. Contact to the author: lukasz.kaplon@gmail.com.

Aleksander Krupkowski Institute of Metallurgy and Materials Science  
Polish Academy of Sciences  
25 Reymonta Street  
30-059 Cracow, Poland  
[www.imim.pl](http://www.imim.pl)

Marian Smoluchowski Institute of Physics  
Faculty of Physics, Astronomy and Applied Computer Science  
Jagiellonian University  
Prof. Stanisława Łojasiewicza 11 Street  
30-348 Cracow, Poland  
[www.if.uj.edu.pl](http://www.if.uj.edu.pl)  
[www.fais.uj.edu.pl](http://www.fais.uj.edu.pl)

Jagiellonian Positron Emission Tomography Group

<http://koza.if.uj.edu.pl/>



## Abstract

The aim of the thesis was to develop polystyrene scintillator for use in the novel time of flight Jagiellonian Positron Emission Tomography (J-PET) scanner being elaborated for the whole-body imaging. To achieve this goal, polystyrene based plastic scintillators with the different chemical compositions were produced and characterized. Spectroscopic and optical properties of these polystyrene scintillators were measured. Structure of manufactured plastic scintillators were studied using two methods: powder X-ray diffraction (PXRD) and differential scanning calorimetry (DSC).

Optimization of the conditions of styrene polymerization for the production of gamma radiation detectors was conducted. As a result of the work presented in this thesis the time-temperature cycles were established: (i) for polymerization in small cylinders as well as (ii) for polymerization in the glass mold allowing to manufacture long plastic scintillator strips. This thesis presents also a new method developed for the fast quality control of plastic scintillator strips. The method was successfully applied during J-PET prototype building.

Light output, decay time, emission spectra and technical attenuation length were measured to develop best composition of polystyrene scintillator. Among the polystyrene scintillators synthesized in the framework of this thesis it was established that:

- (i) polystyrene scintillator with 2% BPBD primary solute and 0.06% POPOP wavelength shifter possess the best timing properties with decay time of  $1.51 \pm 0.02$  ns that is in the range of the decay time of the best commercial scintillators as e.g. BC-420 (1.5 ns), BC-404 (1.8 ns) and EJ-230 (1.5 ns) used in the J-PET tomograph;
- (ii) polystyrene scintillator with 2% PPO primary solute and 0.03% bis-MSB and 0.03% POPOP wavelength shifters is characterized by the best light output of over 11200 photons per megaelectronvolt (MeV) which is comparable with light output of BC-420 with value 10240 photons per MeV.

# Abstrakt

Celem tej pracy było opracowanie scyntylatora polistyrenowego używanego w nowatorskim skanerze Jagiellońskiej Pozytonowej Emisyjnej Tomografii (J-PET) rozwijanym pod kątem obrazowania całego ciała. Aby osiągnąć ten cel, wyprodukowano i scharakteryzowano polimerowe scyntylatory oparte na polistyrenie z różnymi składami chemicznymi. Zmierzono spektroskopowe i optyczne właściwości tych polistyrenowych scyntylatorów. Struktura wyprodukowanych polimerowych scyntylatorów była zbadana z użyciem dwóch metod: proszkowej rentgenografii strukturalnej (PXRD) i skaningowej kalorymetrii różnicowej (DSC).

Przeprowadzono optymalizację warunków polimeryzacji styrenu do produkcji detektorów promieniowania gamma. Jako rezultat pracy przedstawionej w tej rozprawie doktorskiej zostały ustalone cykle czas-temperatura: (i) dla polimeryzacji w małych cylindrach jak również (ii) dla polimeryzacji w szklanych formach pozwalających wyprodukować paski polimerowych scyntylatorów o dużych rozmiarach. Ta rozprawa doktorska zawiera także nową metodę opracowaną dla szybkiej kontroli jakości pasków polimerowych scyntylatorów. Opracowana metoda została pomyślnie zastosowana podczas budowy prototypu tomografu J-PET.

W celu opracowania najlepszej kompozycji dokonano pomiarów wydajności świetlnej, czasu zaniku sygnału, widma emisji i technicznej długości wygaszania światła. Pośród scyntylatorów polistyrenowych zsyntezowanych w ramach tej pracy doktorskiej ustalono, że:

- (i) polistyrenowy scyntylator o składzie chemicznym 2% BPBD pierwszego dodatku i 0.06% POPOP przesuwacza długości fali posiada najlepsze właściwości czasowe z czasem zaniku sygnału  $1.51 \pm 0.02$  ns, który jest porównywalny z czasami zaniku sygnału komercyjnych scyntylatorów np. dla BC-420 (1.5 ns), BC-404 (1.8 ns) i EJ-230 (1.5 ns) użytych w tomografii J-PET;
- (ii) polistyrenowy scyntylator o składzie chemicznym 2% PPO pierwszego dodatku oraz 0.03% bis-MSB i 0.03% POPOP przesuwaczy długości fali cechuje się najlepszą wartością wydajności świetlnej ponad 11200 wyemitowanych fotonów światła na megaelektronowolt (MeV) energii zdeponowanej, wydajność ta jest porównywalna z wydajnością świetlną komercyjnego scyntylatora BC-420 o wartości 10240 fotonów na MeV.

# Table of contents

Abstract .....	3
Acknowledgments .....	6
List of symbols and abbreviations.....	7
1. Introduction .....	9
2. Theory and practice of plastic scintillators production .....	12
2.1. Introduction.....	12
2.2. Comparison of scintillators and its application in PET .....	15
2.3. Positron emission tomography scanners.....	17
2.4. Mechanism of energy transfer in plastic scintillators.....	20
2.5. Chemical components and basic properties of plastic scintillators .....	25
2.6. Components effect on plastic scintillator optical characteristics .....	35
2.7. Methods of industrial production: cell casting, injection molding, extrusion .	39
3. Thesis and objectives of the work .....	44
4. Synthesis of polystyrene scintillators.....	45
4.1. Cylinders .....	45
4.2. Plates .....	49
5. Measurement of polystyrene scintillator structure .....	55
5.1. Glass transition temperature .....	55
5.2. Amorphous state of polystyrene .....	59
6. Quality control of plastic scintillators .....	62
7. Measurement of plastic scintillators optical properties .....	69
7.1. A method for light attenuation length measurement .....	70
7.2. Emission spectra .....	77
7.3. Relative light output.....	81
7.4. Decay time .....	85
8. Discussion and conclusions .....	89
9. Appendix A.....	92
10. References .....	97

## Acknowledgments

I would like to express my sincerest gratitude to my supervisor Prof. Paweł Moskal from Institute of Physics of the Jagiellonian University for his valuable advice and motivating guidance.

I convey my special thanks to my co-supervisor Andrzej Kochanowski, Ph.D. from Department of Chemical Technology at Faculty of Chemistry of the Jagiellonian University for his polymer knowledge and technical suggestions.

Acknowledgments also belong to the Professors from Aleksander Krupkowski Institute of Metallurgy and Materials Science, Polish Academy of Sciences for materials science education.

I am truly grateful for all support in experimental work I have received from:

- Marcin Molenda, Ph.D., D.Sc. and Piotr Łątka, Ph.D., Department of Chemical Technology at Faculty of Chemistry of the Jagiellonian University;
- research collaborators from Jagiellonian Positron Emission Tomography Group, especially Kamil Dulski for help with fitting function in decay time measurement, Wojciech Migdał for mechanical machining of scintillators and design of polymerization mold;
- Krzysztof Pazdan, Department of Biomaterials, Faculty of Materials Science and Ceramics of the AGH University of Science and Technology;
- Łukasz Orzeł, Ph.D., Department of Inorganic Chemistry at Faculty of Chemistry of the Jagiellonian University.

The author was a scholar within the project *Doctus – Lesser Poland Scholarship Fund for PhD Students* co-financed by the European Union under the European Social Fund (contract number ZS.4112-79/12).

This thesis also contains some results obtained in the projects with financial support by the Polish National Center for Development and Research through grant INNOTECH-K1/IN1/64/159174/NCBR/12, the Foundation for Polish Science through MPD program and the EU and MSHE Grant No. POIG.02.03.00-161 00-013/09.

## List of symbols and abbreviations

2 $\theta$	scattering angle
3D	three-dimensional
Al <sub>2</sub> O <sub>3</sub>	aluminum oxide
APD	avalanche photodiode
a.u.	arbitrary unit
BaF <sub>2</sub>	barium fluoride
BAL	bulk attenuation length
BC-XXX	organic scintillator from Saint-Gobain Crystals
BGO	bismuth germanium oxide
bis-MSB	1,4-bis(2-methylstyryl)benzene
BPBD	2-(4-tert-butylphenyl)-5-(4-biphenyl)-1,3,4-oxadiazole
°C	Celsius degree
C	scintillators optical homogeneity parameter
CAS	Chemical Abstract Service registry number
CdWO <sub>4</sub>	cadmium tungstate
Cs-137	caesium-137 radioactive isotope
CT	computed tomography
d	density
deg	degree
DM-POPOP	1,4-bis(4-methyl-5-phenyl-2-oxazolyl)benzene
DSC	differential scanning calorimetry
dSiPM	digital silicon photomultiplier
$\Phi_f$	fluorescence quantum yield
EJ-XXX	organic scintillator from Eljen Technology
FWHM	full width at half maximum
$\gamma$	gamma photon
g	gram
GSO	gadolinium oxyorthosilicate
h	hour
HV	high voltage
J-PET	Jagiellonian positron emission tomography
keV	kiloelectronvolt
LaBr <sub>3</sub> (Ce)	cerium doped lanthanum bromide
LOR	line of response
LSO	lutetium oxyorthosilicate
LYSO	lutetium yttrium oxyorthosilicate
$\lambda_{\text{abs}}$	wavelength of maximum absorption
$\lambda_{\text{em}}$	wavelength of maximum emission
MBq	megabecquerel
MeV	megaelectronvolt
mm	millimeter

mol	mole
MRI	magnetic resonance imaging
mV	millivolt
mW	milliwatt
$n$	refractive index at wavelength of maximum emission
Na-22	sodium-22 radioactive isotope
NaI(Tl)	thallium doped sodium iodide
nm	nanometer
ns	nanosecond
PbWO <sub>4</sub>	lead tungstate
PET	positron emission tomography
ph	light photon
PMMA	poly(methyl methacrylate)
PMT	photomultiplier tube
ppm	parts-per-million
PPO	2,5-diphenyloxazole
POPOP	1,4-bis(5-phenyl-2-oxazolyl)benzene
PS	polystyrene
ps	picosecond
PTP	p-terphenyl
PVT	polyvinyltoluene
PXRD	powder X-ray diffraction
SiPM	silicon photomultiplier
SPECT	single photon emission computed tomography
$\tau$	decay time constant
TAL	technical attenuation length
TBC	4-tert-butylcatechol
TCSPC	time-correlated single photon counting
$T_g$	glass transition temperature
TOF	time of flight
UV	ultraviolet
W	watt
WLS	wavelength shifter
wt%	percentage by weight
XRD	X-ray diffraction
YAP	yttrium aluminium perovskite
Z	atomic number
$Z_{\text{eff}}$	effective atomic number
ZnS(Ag)	silver doped zinc sulfide



# 1. Introduction

Scintillator converts radiation into light. Scintillators can be divided into three main groups: inorganic, organic and composite. These scintillation materials are used for alpha, beta, gamma, neutron and X-rays radiation registering. They are also widely used in high energy physics experiments for particles detection and in medical diagnostics. Other important applications are homeland security, detecting and measuring radioactive contamination, nondestructive inspection of different kind of materials, oil and gas industry as detectors for gamma ray logs, astrophysics, space instrumentation and detection of cosmic rays.

Medical diagnostics is one of the most important application of scintillators. Scintillators have found use in such devices as positron emission tomography (PET), single photon emission computed tomography (SPECT) and computed tomography (CT) scanners. Commercial PET and CT scanners are based on inorganic crystals such as bismuth germanium oxide (BGO), lutetium oxyorthosilicate (LSO) and lutetium yttrium oxyorthosilicate (LYSO) [1], [2]. Crystal scintillators are arranged in a ring surrounding the patient. Such tomography scanners containing inorganic crystals are expensive. The high price makes it economically impossible to construct and use in hospitals tomography scanners allowing to diagnose the whole body of the patient at the same time. Yet, the whole-body PET tomography would significantly improve the diagnostic possibilities. The long axial coverage in whole-body PET scanners can yield a sensitivity gain of 30 ~ 40 times that of current scanners [3], [4]. The high sensitivity can be used for high-throughput scans and offers the potential to perform a whole-body examination in a single breath-hold. Such scans would drastically reduce the smearing of images caused by the motion of the organs due to the patients breathing. The increased sensitivity will also allow imaging at very low radiation doses (down to an injected dose of ~10 MBq compared to about 300 MBq dose needed at present) [3]. It will allow application of PET to pediatric and adolescent populations, studying and monitoring chronic disease, and much more. Moreover it can conducts dynamic PET imaging with simultaneous total-body coverage as compared to the current multi-bed multi-pass imaging protocol with large temporal gaps.

Therefore, there are various attempts to develop a new technology that would make it possible to build total-body tomography scanners. Development of a cost-effective whole-body PET scanner is a technological challenge and there are various non-standard techniques being tested such as detectors based on straw tubes drift chambers [5], [6] or large area resistive plate chambers [7], [8]. Total-body PET scanner is also being built from crystals within the \$15.5 million EXPLORER project [3], [4]. However the whole-body PET based on crystals seems to be impractical for the application in hospitals due to the extremely high costs.

An alternative solution, of the whole-body PET scanner was recently proposed at the Jagiellonian University [9]. Plastic scintillator is a transparent to visible light polymer material emitting blue light when excited by ionizing radiation. Plastic

scintillators are suitable for application in time of flight (TOF) detectors due to their short response time and the possibility of production in various shapes and sizes and are one- to two-orders of magnitude less expensive (per volume) than LSO crystals used in the modern PET scanners.

Novel PET scanner, developed at Jagiellonian University is referred to as Jagiellonian positron emission tomograph (J-PET) [10]. J-PET scanner can have a large field of view (up to about 2 meters) and a superior time of flight (TOF) resolution by application of fast plastic scintillators instead of organic crystals [11]. J-PET scanner based on plastic scintillators constitutes a promising solution in view of the TOF resolution and construction of the scanner allowing for simultaneous imaging of the whole human body. J-PET solution with the axially arranged strips of plastic scintillators read out only at the ends gives opportunity to increase the diagnostic chamber without significant increase of the cost of the whole scanner.

Two new solutions were recently proposed for detecting gamma quanta originating from positron annihilation in the human body. The first method involves the use of plastic scintillator strips arranged in the form of a barrel [12], called “strip-PET”, and the second proposed method is based on plastic scintillator plates combined with arrays of photomultipliers, called “matrix-PET” [13]. The main difference in the detection principle between traditional PET and J-PET is the utilization of time properties of the scintillators instead of signal amplitudes. Plastic scintillators have at least one order of magnitude shorter decay time than inorganic crystals. This feature allows improvement of the resolution of TOF determination in a strip-PET apparatus [14]. It is also important to stress that diagnostic chamber is free of any electronic devices and magnetic materials, thus giving unique possibility for simultaneous imaging of PET and magnetic resonance imaging (MRI) [15] as well as PET and computed tomography (CT) [16] in a way different from so far developed configurations. Though the general concepts of the production of such materials are known, the know-how of the synthesis of such materials in an effective way without various defects is not disclosed by the companies.

The work presented in this thesis constitutes an attempt to the improvement of polystyrene scintillator properties for new type of positron emission tomography (J-PET) scanners based on polymer scintillators. The main objective of this dissertation is to optimize conditions of synthesis and processing of polystyrene for the production of gamma radiation detectors and to develop a method for the fast and effective quality control of the produced scintillators. Long strips and plates of plastic scintillators are needed for J-PET scanner construction. The main objective was realized by sub-objective comprising: developing the best possible composition of the fluorescent additives in polystyrene scintillator for the detection of gamma radiation; temperature and time optimization of polystyrene polymerization cycle; matching optical properties of plastic scintillators with spectral characteristic of light detectors used in PET scanners.

The manuscript is organized in the following parts:

- 1<sup>st</sup> chapter introduces into main purpose of this thesis;
- 2<sup>nd</sup> chapter collects state of the art in plastic scintillators and PET scanners: describes various groups of scintillators and two types of PET scanners, theory behind converting radiation into light in plastic scintillators, properties of polymers and fluorescent substances used as scintillators components, four methods of polymers processing;
- 3<sup>rd</sup> chapter outlines thesis and objectives of the PhD work;
- 4<sup>th</sup> chapter describes synthesis of polystyrene scintillators in cylinder and plate shapes; thermal initiated bulk polymerization process in bigger volumes needs different time-temperature cycle than the one used in small cylinder synthesis due to difficult heat removing from thicker plates; two different time-temperature cycle were developed;
- 5<sup>th</sup> chapter contains description and results from two methods used in measurements of polystyrene structure: differential scanning calorimetry to check thermal stability and obtain glass transition temperature of polystyrene scintillator and powder X-ray diffraction to check amorphous state of polystyrene;
- 6<sup>th</sup> chapter comprises the description of plastic scintillators quality control method developed during J-PET scanner building;
- 7<sup>th</sup> chapter contains principles of operation, schematics of instruments, results and its discussion from measurements of plastic scintillators optical properties such as light attenuation length, emission spectra, relative light output, decay time constant and variation of the photon energy spectrum while they propagate through the plastic scintillator strip;
- 8<sup>th</sup> chapter summarizes research and development work;
- 9<sup>th</sup> chapter contains emission spectra of plastic scintillators;
- 10<sup>th</sup> chapter gathers bibliography form the PhD thesis.

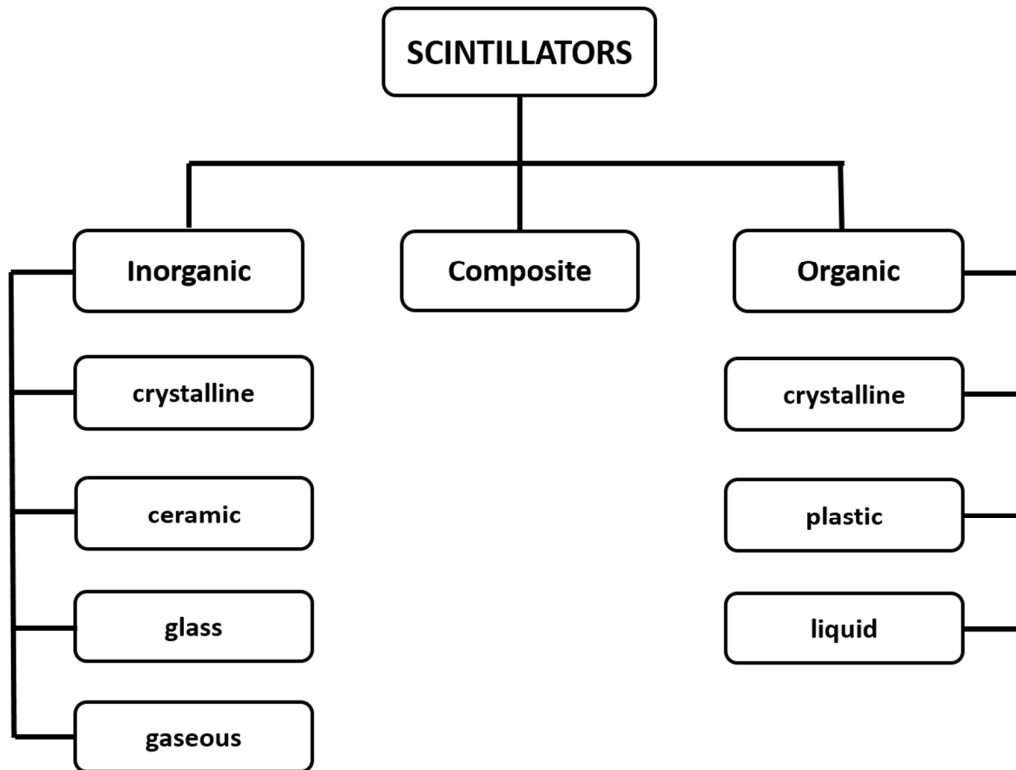
## 2. Theory and practice of plastic scintillators production

### 2.1. Introduction

Scintillator is a material emitting light when excited by ionizing radiation [17]. This phenomenon is called scintillation. Scintillators are significant components in solid state radiation detectors, called scintillating counters. They are usually build from scintillator (converts radiation to light), light detector (converts light to electrical signal), readout electronic (amplifies, discriminates and counts these signals), voltage supply and data storage system. Scintillator materials have been widely used as detectors of alpha, beta, gamma radiation and other particles in science and industry. For example they are applied in:

- neutron and high energy particle physics experiments [18];
- astrophysics, space instrumentation and indirect detection of cosmic rays [19];
- materials science in scanning electron microscopy (SEM), transmission electron microscopy (TEM), x-ray diffraction (XRD);
- identifying of isotopes in high resolution spectroscopy [20];
- positron emission lifetime spectroscopy [21], [22], [23], [24];
- accelerator mass spectrometry and its applications in archaeology, geology and environmental research;
- detecting and measuring radioactive contamination: survey meters, isotope identifiers, area and contamination monitors;
- monitoring nuclear materials in nuclear power plants;
- homeland security applications – detecting, locating and identifying of hidden radioactive threats in border crossings, airports and seaports [25];
- metal recycling: conveyor and gateway/portal monitors;
- nondestructive inspection of different kind of materials;
- oil and gas industry as detectors for gamma ray logs [26];
- medicine in Gamma camera, computed tomography (CT), single photon emission computed tomography (SPECT) and positron emission tomography (PET) [27].

Scintillators can be divided into three main groups: inorganic, organic and composite (Figure 1). Website [28] contains summary list of over 500 different scintillators, some experimental and some well-established. They exist in form of solid crystals, plastics, ceramics, glasses and powders; liquid solutions and gases.



**Figure 1. Types of scintillators**

Inorganic group consists of commonly used monocrystalline scintillators activated with metals ions like: thallium doped sodium iodide NaI(Tl), bismuth germanium oxide BGO, cadmium tungstate CdWO<sub>4</sub>; cerium activated gadolinium oxyorthosilicate GSO, yttrium aluminium perovskite YAP, lutetium oxyorthosilicate LSO; unactivated barium fluoride BaF<sub>2</sub>, glass scintillators: cerium activated lithium glass and terbium activated glass; polycrystalline silver doped zinc sulfide ZnS(Ag). There are also gaseous scintillators consisting of nitrogen and the noble gases helium, argon, krypton, and xenon.

Organic scintillators are divided into:

- plastic – solid solutions of fluorescent compounds in polymers containing aromatic molecules into polymer chain (e.g. polystyrene [29], polyvinyltoluene [30]);
- liquid solutions of fluorescent compounds in solvents like toluene, xylene, dioxane, phenylcyclohexane, triethylbenzene, hexafluorobenzene, mineral oil and decalin [31];
- pure crystals of aromatic hydrocarbon compounds, most popular are anthracene, stilbene and p-terphenyl [32].

Another classification of organic scintillators contains six principal types:

- unitary systems
  - pure crystals (e.g. anthracene, stilbene);
  - pure liquids, (e.g. xylene, benzene) and pure plastics (e.g. polystyrene) they scintillation efficiency is too low for them to be of practical use;

- binary systems
  - liquid solutions (e.g. p-terphenyl in xylene)
  - plastic solutions (e.g. p-terphenyl in polystyrene)
  - crystal solutions (e.g. anthracene in naphthalene);
- ternary systems
  - liquid solutions (e.g. p-terphenyl and POPOP in xylene)
  - plastic solutions (e.g. p-terphenyl and POPOP in polystyrene) [33].

Composite scintillator is a material made from two or more constituent materials with significantly different physical or chemical properties that, when combined, produce a material with characteristics are different from the individual components. Examples are gadolinium fluoride nanoparticles in polystyrene matrix [34], gadolinium oxide-polyvinyltoluene nanocomposites [35], crystalline grains of stilbene or p-terphenyl doped by 1,4-diphenyl-1,3-butadiene [36], polystyrene blends with low-melting inorganic crystals [37], cadmium telluride quantum dots in poly(vinyl alcohol) or poly(methyl methacrylate) polymer matrices [38], hafnium silicate nanoparticles incorporated in polystyrene matrix [39], quantum-dots (CdSe/ZnS) and 2,5-diphenyloxazole (PPO) doped polystyrene based scintillators [40].

The ideal scintillator should possess the following properties:

- it should convert the kinetic energy of radiation into detectable light with a high scintillation efficiency;
- scintillation conversion should be linear: the light yield should be proportional to deposited energy over as wide a range as possible;
- scintillator should be transparent to the wavelength of its own emission for good light collection;
- the decay time of the induced light should be short so that fast signal pulses can be generated;
- the material should be of good optical quality and subject to manufacture in sizes large enough to be of interest as a practical detector;
- its index of refraction should be near that of glass (~1.5) to permit efficient coupling of the scintillation light to light detector [17].

## 2.2. Comparison of scintillators and its application in PET

Basic physical and spectral properties of selected scintillators are listed in Table 1. The most important properties are light yield (the more emitted light the better scintillator) and decay time constant (the lower value or shortest decay time the better scintillator). Light yield or light output is a conversion efficiency of radioactive energy deposited in scintillator into light and is expressed in light photons generated per megaelectronvolt (ph/MeV) of deposited energy. Some authors compare light yield relative to anthracene crystal light output taken as 100% and then it is called relative light yield or relative light output. Decay time is time over which the light signal from scintillator decreased to 1/e of its maximum value. Wavelength of maximum emission is maximum peak in emission spectrum. Other important property is light attenuation length, over which the light signal passing through scintillator is attenuated to 1/e of its original value. For plastic scintillators this varies from 0.1 to 4 meters.

**Table 1. Properties of selected scintillators. Data gathered from [19], [41].**

Scintillator	Light yield [ph/MeV]	Decay time [ns]	Wavelength of maximum emission [nm]	Refractive index	Density [g/cm <sup>3</sup> ]	Price [US\$/cm <sup>3</sup> ]
Inorganic						
Nal(Tl)	37 700	230	415	1.85	3.67	6
<sup>6</sup> Li glass	2 000	60	390-430	1.56	2.60	1 500
BaF <sub>2</sub>	10000/1400	630/0.8	315/220	1.50	4.88	15
YAP	18 000	27	350	1.94	5.55	100
LSO	30 000	40	420	1.82	7.40	60
LYSO	32 000	40	420	1.81	7.10	70
BGO	8 200	300	480	2.15	7.13	35
PbWO <sub>4</sub>	100/31	10/30	420/425	2.20	8.28	6
LaBr <sub>3</sub> (Ce)	63 000	16	380	1.90	5.08	500
Organic plastic						
BC-420	12 240	1.5	391	1.58	1.03	0.11-0.32
BC-422Q	2 200	0.7	370	1.58	1.03	
BC-452	6 400	2.1	424	1.58	1.08	3
BC-454	9 600	2.2	425	1.58	1.03	11-12
Organic liquid						
BC-505	16 000	2.5	425	1.50	0.88	0.07-0.25
BC-509	4 000	3.1	425	1.40	1.61	
BC-521	12 000	4.0	425	1.50	0.89	
Organic crystalline						
Stilbene	14 000	3.5	390	1.64	1.22	-
Anthracene	20 000	30	445	1.62	1.25	-
P-terphenyl	27 000	3.7	420	1.65	1.23	-

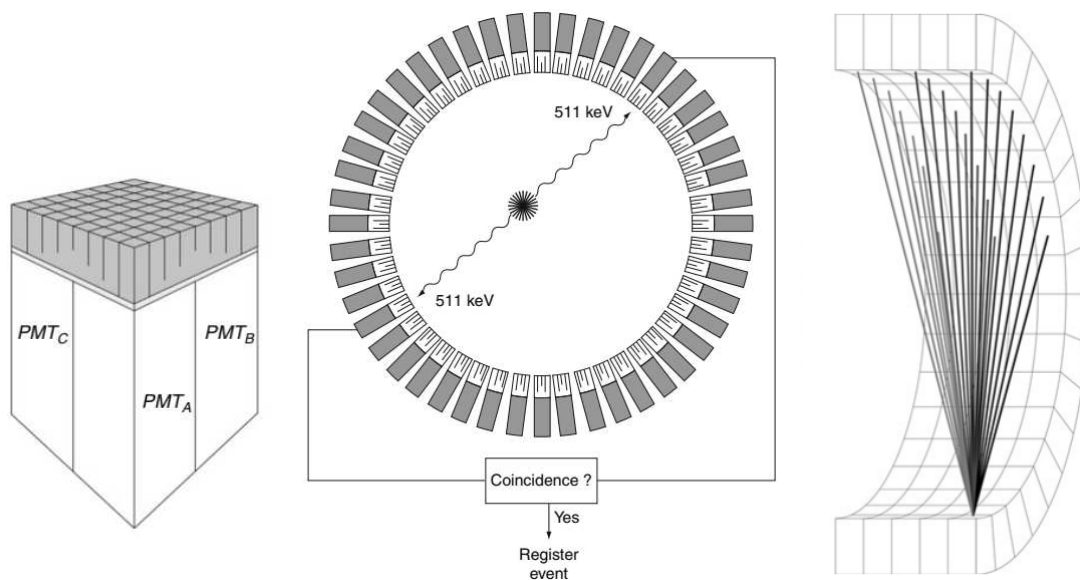
Commercial positron emission tomography (PET) scanners are based on inorganic crystals [1], [2], [42] such as bismuth germanium oxide (BGO), lutetium oxyorthosilicate (LSO) and lutetium yttrium oxyorthosilicate (LYSO). These crystals have high density allowing to absorb gamma quanta in small volume of the detector mainly by photoelectric effect. LSO and LYSO emit about three times more light than plastic scintillators but its decay time is one order of magnitude longer (see Table 1).

Plastic scintillators are suitable for application in time of flight (TOF) detectors due to their short response time and the possibility of production in various shapes and sizes. The achievable time resolution of a PET scanner depends on the decay and rise time of light signals produced in scintillators and on the amount of light reaching the photomultipliers. The decay time of a typical plastic scintillator ranges from 1.4 ns to 2.4 ns and light output amounts to approximately 10,000 photons/MeV of absorbed energy (Table 1). A large attenuation length of up to 4 meters allows the transportation of light from the center to the edges of the scintillator strips with small losses. The maximum of emission spectra is observed at around 420 nm and this value matches well with the quantum efficiency of typical photomultiplier tubes (PMT) [43].



### 2.3. Positron emission tomography scanners

Positron emission tomography (PET) is a research and diagnostic imaging method used in research to study biology and disease and clinically as a routine diagnostic imaging tool. PET is used to image the in vivo 3D distribution of an injected radiotracer - molecule labeled with a positron-emitting radionuclide such as fluorodeoxyglucose. In a typical PET imaging examination, a small amount of radiotracer is injected into the patient body. The patient is then placed into a PET scanner, which is designed to detect the high energetic photons (511 keV) that are emitted as a result of the positron-electron annihilation decay. By using an image reconstruction, a 3D image is created which represents the distribution of the radiotracer in the patient [19].

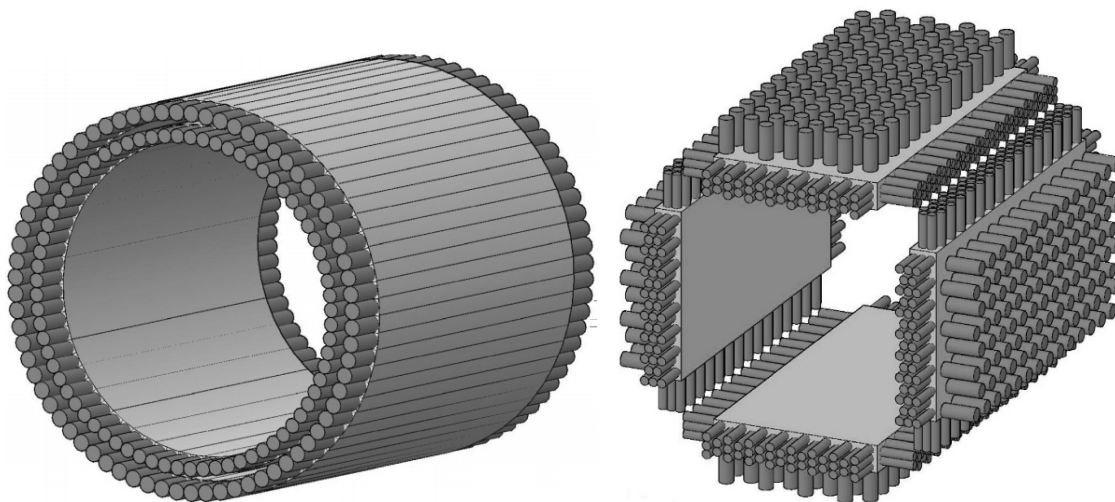


**Figure 2. Principle of the traditional PET scanner. An array of detector elements is created from a large block of scintillation material, which is coupled to four PMTs (left figure). A great number of detectors are arranged into rings around the object to be imaged (middle figure). 3D image of few detector rings with coincidences between a large number of detector elements (right figure). [19]**

A typical PET scanner (Figure 2) is composed of an array of crystal scintillation detectors surrounding an imaging volume. When a positron annihilates two detectors are hit by a gamma photon within a coincidence time window (6–15 ns), one coincidence event is counted. By connecting detectors that recorded two coincident photons, a line called the “line of response” (LOR) is created. The coincidence counts from many parallel LOR are combined to produce a single projection and several projections from a ring PET system are needed to reconstruct a 3D image corresponding to the radiotracer distribution in the body [44].

Commercial PET scanners are based on inorganic crystals such as BGO, LSO, and LYSO. However, two new solutions (Figure 3), called Jagiellonian-PET (J-PET), were recently proposed for detecting gamma quanta originating from positron

annihilation in the human body [9]. The first method involves the use of plastic scintillator strips connected with two photomultipliers on both sides arranged in the form of a barrel [12], [45], called “strip-PET”. The second proposed method is based on plastic scintillator plates combined with arrays of photomultipliers, called “matrix-PET” [13]. The main difference in the detection principle with respect to the commercial PETs is the utilization of time properties of the scintillators instead of signal amplitudes (Table 2).



**Figure 3. Schematic view of two possibilities of arrangement of scintillation elements and photomultipliers for the diagnostic chambers of double layer strip-PET (left) and matrix-PET (right) detector systems [13]**

A single detector module of the strip-PET detector consists of a plastic scintillator strip read out by photomultiplier tubes or silicon photomultipliers at both ends. The detector is built out from strips of plastic scintillators forming a diagnostic chamber as shown schematically in the left panel of Figure 3.

Concept of matrix-PET is based on using the large and thick organic scintillators blocks as a detector of gamma quanta instead of crystal scintillators used in current commercial PET scanners. Its uniqueness constitutes the solution of light collection allowing for the conversion to the electric signal of direct light. The idea is demonstrated schematically in right panel of Figure 3. This method allows to achieve a time resolution which is not affected by the deformation of light pulses due to reflections at scintillators surfaces. Such PET detector would consist of organic scintillator plates. The plates could be set in many ways so as to cover the whole body of the patient.

**Table 2. Differences between traditional TOF PET-CT/PET-MRI and novel strip J-PET scanners. Data combined from [1], [2], [11].**

Parameters	Traditional PET	Strip J-PET
Type of scintillator	crystals LSO, LYSO, BGO	plastics BC-404, BC-420, EJ-230
Physical phenomenon	photoelectric effect	Compton scattering
Measured property	energy of gamma photon + time of flight	time of flight
Granularity of detector	high	low
Number of scintillators	13,824 to 32,444 crystals	192 strips
Scintillator size [mm <sup>3</sup> ]	e.g. 4x4x20; 6.3x6.3x30	e.g. 6x24x500; 5x19x300
Photo-detector	PMT, SiPM, dSiPM, APD	PMT, SiPM
Number of PMTs	256 to 768	384
Detection efficiency	high	low
Detector's acceptance	low	high
Axial length [mm]	157 to 260	500
Used electronics	analog	digital
Signal triggering	triggering	triggerless data acquisition
TOF resolution* [ps]	345 to 550	320
Simultaneous imaging of the whole human body	no	yes
Simultaneous imaging of PET-MRI	yes	yes
Simultaneous imaging of PET-CT	no	yes

\* coincidence resolving time.

J-PET scanner can have a large field of view (up to about 2 meters) and a superior TOF resolution by application of fast plastic scintillators instead of organic crystals. PET scanner based on plastic scintillators constitutes a promising solution in view of the TOF resolution and construction of the scanner allowing for simultaneous imaging of the whole human body. Plastic scintillators have at least one order of magnitude shorter decay time than inorganic crystals. This feature allows the improvement of the resolution of TOF determination in a strip PET apparatus, which is presently being developed by the Jagiellonian-PET collaboration [14], [46], [47], [48], [49], [50], [51], [52], [53], [54], [55]. Diagnostic chamber is free of any electronic devices and magnetic materials, thus giving unique possibility for simultaneous imaging of PET and magnetic resonance imaging (MRI) [15] as well as PET and computed tomography (CT) [16] in a way different from so far developed configurations.

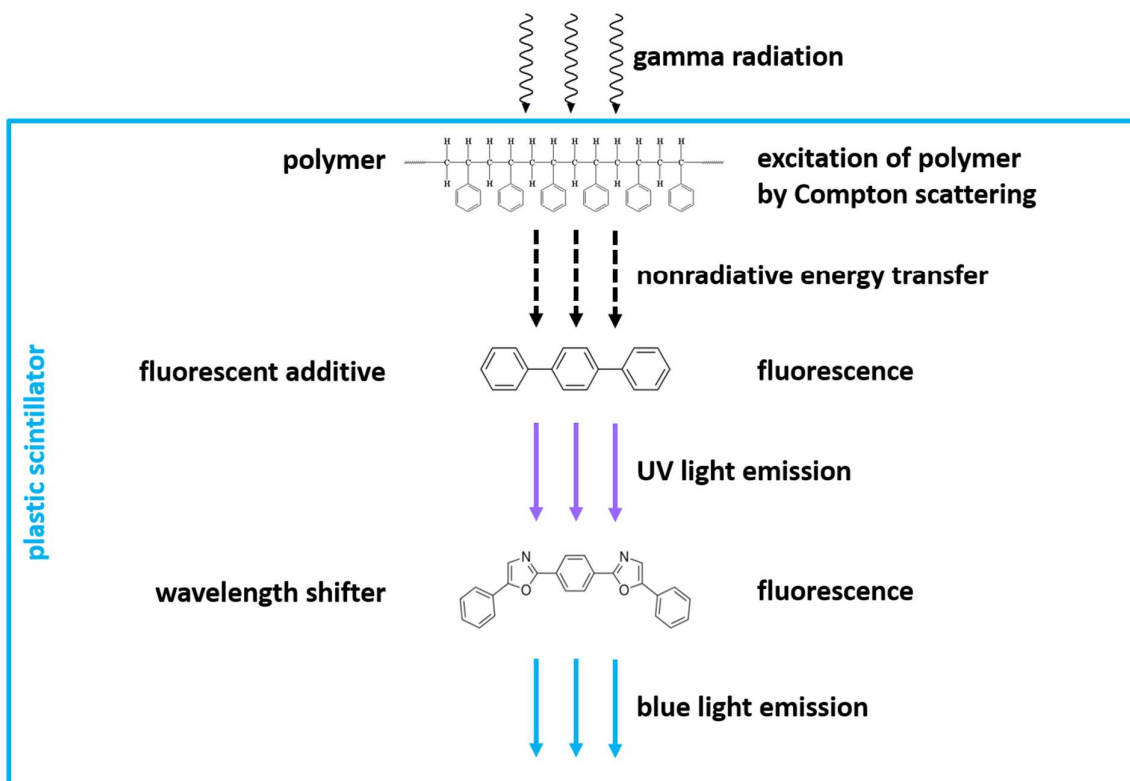
## 2.4. Mechanism of energy transfer in plastic scintillators

Typical plastic scintillator is a solid solution of two kinds of fluorescent compounds: first additive (primary fluor) and second additive (called wavelength shifter or secondary fluor) in polymer matrix. Ternary plastic scintillators (polymer + primary fluor + wavelength shifter) are most commercially available however there is also binary scintillator [56] (polymer + primary fluor) with one fluorescent additive [57], [58].

Role of the polymer in plastic scintillator is to absorb radiation and transport produced light through scintillator volume to light detector. Polymers must be transparent to visible light. Examples of most commonly used polymers are polyvinyltoluene (PVT), polystyrene (PS) and poly(methyl methacrylate) (PMMA).

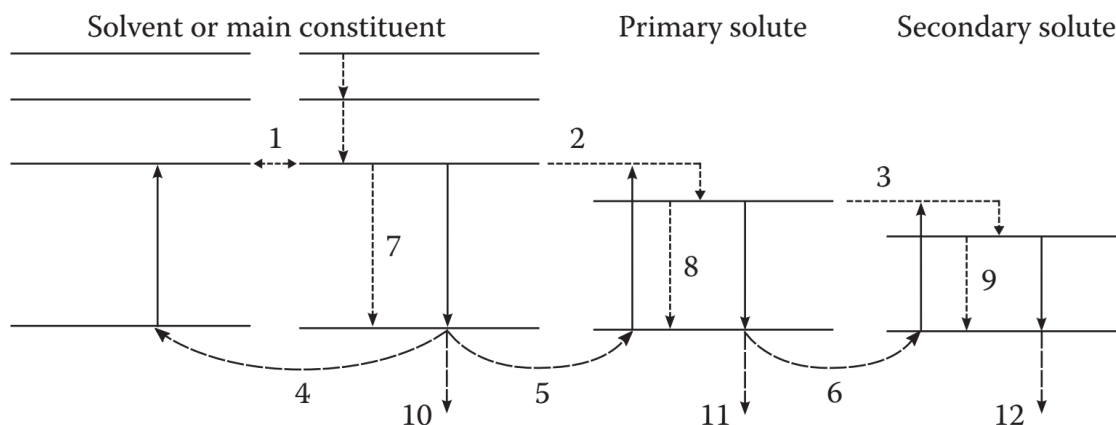
Ionization in the plastic base produces UV photons with short attenuation length (several mm). Longer attenuation lengths are obtained by dissolving a primary fluor in high concentration (1% by weight) into the base, which is selected to efficiently re-radiate absorbed energy at wavelengths where the base is more transparent [59]. The primary fluor has a second important function. The decay time of the scintillator base material can be quite long – in pure polystyrene it is 16 ns, for example. The addition of the primary fluor in high concentration can shorten the decay time by an order of magnitude and increase the total light yield. At the concentrations used (1% and greater), the average distance between a fluor molecule and an excited base molecule is around 10 nm, much less than a wavelength of light. At these distances the predominant mode of energy transfer from base to fluor is not the radiation of a photon, but a resonant dipole-dipole interaction, first described by Förster, which strongly couples the base and fluor.

Low density about 1.1 g/cm<sup>3</sup> and low average effective atomic number ( $Z_{\text{eff}} \sim 5.6$ ) of plastic scintillator cause gamma radiation interaction mainly by Compton scattering. Gamma quanta passing through plastic scintillator interact with electrons in polymer and eject electrons. These electrons have part of gamma quanta energy and they excite other parts of polymer backbone. Excited polymer transfers part of its energy to fluorescent additive (Figure 4) by nonradiative means – without light emission. In next step fluorescence additive absorbs this energy and gives back its portion by radiative transfer - fluorescence in ultraviolet light. Last step involves absorption of this UV light by wavelength shifter and blue light emission also through fluorescence. Whole process occurs in short time from  $10^{-10}$  to  $10^{-7}$  seconds [60]. Fluorescence additives are used as “wavelength shifters” to shift scintillation light from UV to a more convenient wavelength matched with light detectors.



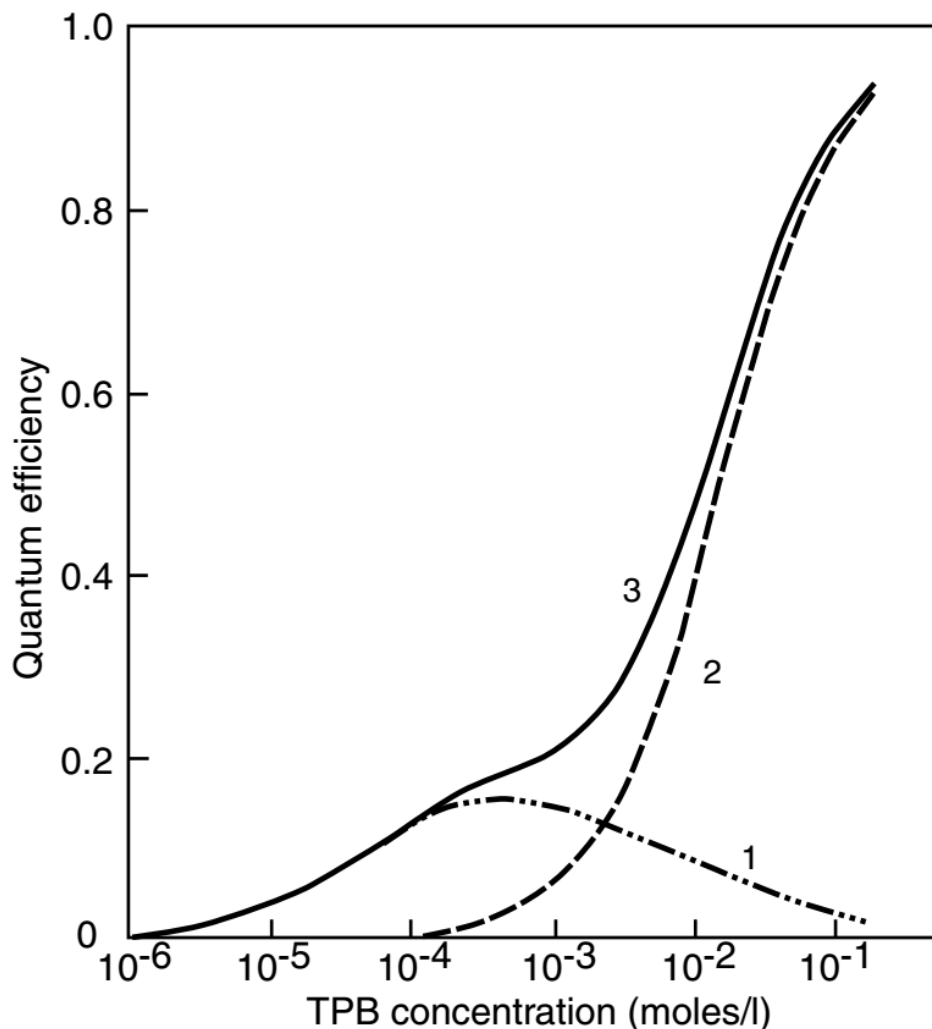
**Figure 4. Flow diagram of energy transfer mechanism in ternary plastic scintillators excited by gamma radiation. Ternary means that the plastic scintillator is composed of polymer base, first fluorescent additive and second fluorescent additive (wavelength shifter).**

More detailed energy flow processes between the components of plastic scintillator are presented in Figure 5 which contains fragments of Jablonski diagram for three ingredients of ternary scintillator. Polymer chains (solvent or matrix for fluorescent additives in plastic scintillator) are excited by radiation followed by nonradiative energy transfer to primary solute (first fluorescent additive). The process is called Förster resonance energy transfer [61] and is due to resonant dipole-dipole interaction between energy donor (polymer) and acceptor (primary solute) in within 10 nm distance [62]. The effectiveness of this process is inversely proportional to  $r^6$ , where  $r$  is distance between donor and acceptor, and proportional to concentration of the fluorescent additive in the polymer. The result of such energy transfer is excitation of primary solute followed by fluorescence (ultraviolet light emission). In the wavelength shifter, the initial excitation takes place via the absorption of a photon and de-excitation by emission of a longer wavelength photon. Thus, in the last step ultraviolet light is absorbed by wavelength shifter and emitted in blue wavelength by fluorescence.



**Figure 5. Detailed scheme of energy transfer and de-excitation processes in ternary plastic scintillator. Horizontal lines denote energy levels of compounds. Solvent or main constituent denotes polymer. Secondary solute denotes wavelength shifter. The processes are numbered following the description in the text below. The figure is adapted from [63].**

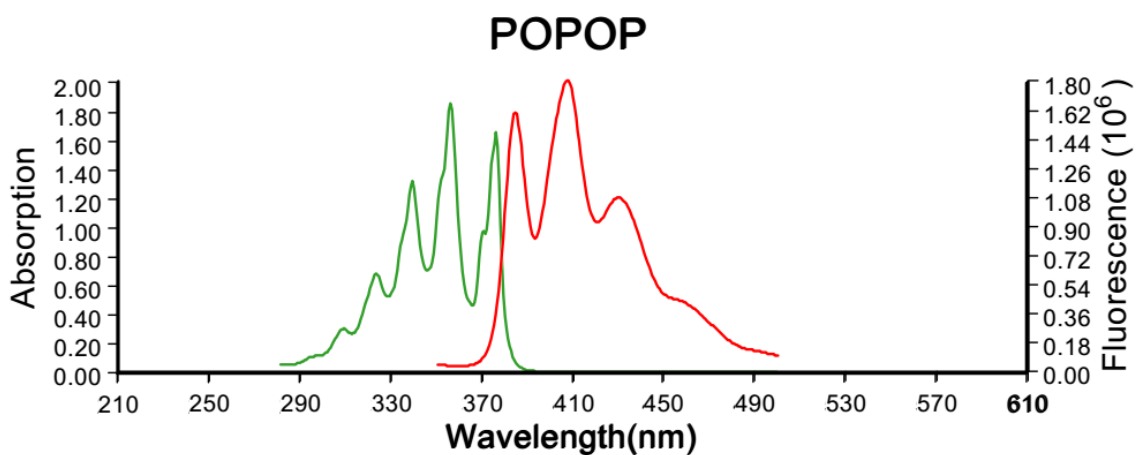
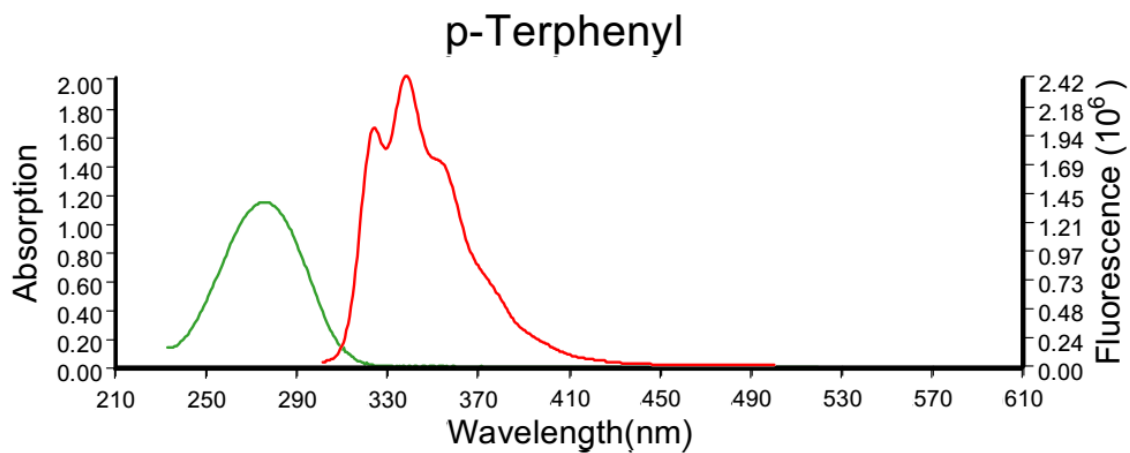
Nonradiative transfer in ternary plastic scintillator is possible from a molecule of solvent (polymer) to either another molecule of this type (label 1 in Figure 5) or a molecule of the primary solute (label 2). Then energy transfer can occur from the primary solute to the secondary solute (wavelength shifter, label 3). Radiative transfer is also possible between the three components (labels 4–6). The visible photon emitted by the polymer is absorbed instead of escaping the scintillator and contributing to the scintillation signal. Internal quenching can happen for any of the components in ternary systems, reducing the scintillation efficiency (labels 7–9). Another consequence of the presence of three types of molecules is that the emission of visible light can come from one or other ingredients of the system (labels 10–12). It then produces more or less extended spectra on the wavelength axis, with one or multiple peaks [63].



**Figure 6. Quantum efficiency of energy transfer from polymer to the primary fluorescent additive in the polystyrene - 1,1,4,4-tetraphenylbutadiene (TPB) plastic scintillator: 1 – radiative transfer, 2 – nonradiative transfer, 3 – total transfer [64]**

Radiative and nonradiative energy transfers are connected with fluorescent additives concentration in polymer (Figure 6). Effective energy transfer from polymer to first fluor requires high concentration of this fluor about  $10^{-2}$  mol. Förster resonance energy transfer is proportional to concentration of the fluorescent additive in the polymer. On the other hand wavelength shifters concentration in scintillator is about 50 to 100 smaller than first fluor. There are optimal concentration of wavelength shifter, adding to much will cause fluorescence quenching of emitted light.

Effective energy transfer from fluorescent additive to wavelength shifter is determined by high fluorescence quantum yield of these substances. Furthermore first fluors emission spectrum should strongly overlap with wavelength shifters absorption spectrum as it is shown in Figure 7 where p-terphenyl is first fluor and POPOP is wavelength shifter.



**Figure 7. Absorption (green curves) and emission spectra (red curves) of two fluorescent compounds used in ternary plastic scintillators. P-terphenyl emission spectrum overlaps with POPOP absorption spectrum [65]**



## 2.5. Chemical components and basic properties of plastic scintillators

Polymers usually contain aromatic molecules in polymer chain, for example benzene rings with or without substituents, naphthalene and biphenyl substituents (Table 3). This configuration with aromatic substituents in polymer chain and in fluorescent additives ensures good energy transfer of absorbed radiation and its conversion to light.

The selected polymer base must be able to be purified and processed in quantities of hundreds to thousands of kilograms at a reasonable cost. Commercially most used polymers for scintillator synthesis are polyvinyltoluene (PVT), polystyrene (PS) and poly(methyl methacrylate) (PMMA). A comparison of scintillators made with PVT, PS and PMMA plus naphthalene, with equivalent fluor concentrations, produced relative signal intensities of 1.0, 0.88 and 0.38, respectively [66].

Other important physical property of polymers is glass-transition temperature ( $T_g$ ) above 100°C to obtain plastic scintillator in solid state at room temperature. If polymers glass-transition temperature is below room temperature then scintillator is in form of rubber (see silicone rubber PMPS in Table 3).

Refractive index ( $n$ ) about 1.5 is matched to refractive index of glass in light detector (usually photomultiplier tubes). This ensures effective transition of light from scintillator to detector without light loss on reflections.

Wavelength of maximum emission ( $\lambda_{em}$ ) of polymer ranges between 300 and 400 nm and it is matched to wavelength of maximum absorption ( $\lambda_{abs}$ ) in primary fluorescent substances.

Because polymers constitute about 96-98% of scintillators mass its density ( $d$ ) is also density of scintillator and is relatively low (1.00 to 1.36 g/cm<sup>3</sup>) compared to inorganic crystal scintillators (3.2 to 8.3 g/cm<sup>3</sup>).

**Table 3. Polymers used as a base for plastic scintillators production. Data gathered from [67], [68], [69].**

Name, common abbreviation, CAS number	$T_g$ [°C]	$d$ [g/cm <sup>3</sup> ]	$n$	$\lambda_{em}$ [nm]	Application and comments
poly(vinyltoluene), PVT, 9017-21-4	93-118	1.02	1.59	315	most used commercially, possess the best properties as polymer base for scintillators [66]
polystyrene, PS, 9003-53-6	100	1.04-1.065	1.59	310	used commercially for plastic scintillator base [29], [70], [71], [72], [73] and for plastic scintillating fibers [74], [75]

Name, common abbreviation, CAS number	T <sub>g</sub> [°C]	d [g/cm <sup>3</sup> ]	n	λ <sub>em</sub> [nm]	Application and comments
poly(methyl methacrylate), PMMA, 9011-14-7	105	1.19	1.49	-	used commercially with 10-20% naphthalene cosolvent [76] as Plexipop [77] and for production transparent light guides [78], [79]
poly(vinylxylene), PVX	-	-	-	-	excellent radiation resistance base for scintillators [80]
poly(4-methyl-1-pentene), PMP, 25068-26-2	240	0.838	1.46	-	polymer resistant to temperatures up to 200°C [81]
poly(4-vinylbiphenyl), PVBP, 25232-08-0	138	-	-	-	used for copolymerization in scintillator resistant to temperatures up to 150°C [82]
poly(4- <i>tert</i> -butylstyrene), PTBS, 26009-55-2	126-131	-	-	-	used for copolymerization in scintillator resistant to temperatures up to 130°C [82]
poly( <i>N</i> -vinyl carbazole), PVK, 25067-59-8	227	1.184	1.68	420	photoconductive polymer in OLED technology mixed with Bi and Ir complexes to obtain scintillator [83]
polycarbonate, PC, 25037-45-0	145	1.2	1.58	350	pure polymer is a scintillator [84]
poly(ethylene terephthalate) PET, 25038-59-9	78	1.33	1.57	385	pure polymer from PET bottles is a scintillator [85]
poly(ethylene-2,6-naphthalate), PEN, 25853-85-4	122	1.36	1.65	425	pure polymer is a scintillator [86]; trade name Scintirex [87]
polysulfone, PSU, 25135-51-7	187	1.24	1.63	380	pure polymer is a scintillator [88]
poly(ether sulfone), PESU, 25608-63-3	225	1.37	1.65	350	pure polymer is a scintillator [89]
poly(phenyl sulfone), PPSU, 25608-64-4	220	1.29	1.67	390	pure polymer is a scintillator [90]
poly(dimethyl- <i>co</i> -diphenylsiloxane), PMPS,	-33÷ -22	1.079- 1.115	1.47- 1.55	270 – 320	crosslinked silicone rubber with high radiation resistance [91]

Name, common abbreviation, CAS number	T <sub>g</sub> [°C]	d [g/cm <sup>3</sup> ]	n	λ <sub>em</sub> [nm]	Application and comments
9005-12-3					
poly(2-vinylnaphthalene), PVN, 28406-56-6	135- 145	-	1.68	400	copolymer for PMMA based scintillator [92]
poly(styrene- <i>co</i> -3-hydroxy-4'-ethenylflavone)	106- 132	-	-	550	example of styrene and fluorescent compound copolymer [93]

The polymer itself, though, is not useful as a scintillator because its fluorescent yield is very low, it is not transparent to its own emission light over any appreciable distance (<10 mm), and its UV light (300-350 nm) emission spectrum is too short to match the common photodetectors. Addition of a fluorescent substance such as oligophenylenes, oxazoles, oxadiazoles, pyrazolines, proton transfer compounds or luminescent metal complexes makes an efficient scintillator.

The addition of primary fluor at a concentration of 0.3 to 5% by weight and wavelength shifter from 0.001 to 0.1% by weight makes plastic scintillator emitting blue or green light. Higher concentration of primary fluorescent dyes up to 30 wt% of PPO has been found to be useful in plastic scintillator with efficient neutron-gamma pulse shape discrimination [94]. Examples of commercial scintillator compositions:

- UPS 923A: polystyrene doped with 2% PTP and 0.03% POPOP [95]
- BC-400: polyvinyltoluene doped with PTP and POPOP [96]
- BC-404: polyvinyltoluene doped with 3.5% PTP and 0.05% DPS [96]
- BC-422: polyvinyltoluene doped with <5% PBD [57]
- BC-428: polyvinyltoluene doped with BBQ [97].

As it was already mentioned before, the energy deposited by radiation to polymer base is transferred in non-radiative process (Förster resonance energy transfer) to primary fluor which emits ultraviolet light. That UV light is adsorbed by wavelength shifter and emitted in visible part of light spectrum. Typical wavelength of emitted light for first additive is 340 to 400 nm (Table 4) and for wavelength shifter is 410 to 430 nm (Table 5). Most commercial plastic scintillators emit blue light that is well matched to photomultiplier tubes maximal quantum efficiency around 400 nm [43]. Addition of wavelength shifter increase also bulk attenuation length from 0.1 meter for scintillator with only primary fluor to about four meters for ternary combination of fluorescent compounds in polymer.

**Table 4. Fluorescent compounds emitting UV light for scintillators production. Bibliography for fluorescent compounds comparison: [98], [99], [100], [101], [102], [103], [104].**

Name	Common abbreviation	CAS number	$\lambda_{\text{abs}}$ [nm]	$\lambda_{\text{em}}$ [nm]	$\Phi_f$	$\tau$ [ns]
2,5-diphenyl-1,3,4-oxadiazole	PPD	725-12-2	283	355	0.9	1.5
p-terphenyl	PTP	92-94-4	288; 276	335; 339	0.85	1.2
2-phenyl-5-(4-biphenyl)-1,3,4-oxadiazole	PBD	852-38-0	305; 302	360- 365	0.8	1.2
2-(4-tert-butylphenyl)-5-(4-biphenyl)-1,3,4-oxadiazole	BPBD	15082-28-7	308	365; 368	0.85	1.2
2,5-diphenyloxazole	PPO, DPO	92-71-7	308; 303	365; 361; 375	0.8	1.6
2-(1-naphthyl)-5-phenyl-1,3,4-oxadiazole	$\alpha$ -NPD	897-18-7	318	370	0.7	2
4,4"-di-t-amyl-p-terphenyl	DAT	121838-04-8	-	375	-	-
2,5-bis(4-biphenyl)-1,3,4-oxadiazole	BBD	2043-06-3	314; 315	373; 380	0.85	1.4
4,4"-bis[(2-butyloctyl)oxy]-p-quaterphenyl	BIBUQ	18434-08-7	306; 307; 313	381; 388	0.93	0.9
2-(4-biphenyl)-5-phenyloxazole	BPO	852-37-9	330	390	-	-
5-phenyl, 2-(4-biphenyl)-oxazole	PBO	852-36-8	-	-	-	-
2-(4-biphenyl)-6-phenylbenzoxazole	PBBO	17064-47-0	327; 330	395; 396; 403	-	-
7,7'-diphenyl-9,9,9',9'-tetrapropyl-2,2'-Bi-9H-fluorene	O408, Oligo 408	131549-47-8	-	410	-	2.5
	O415, Oligo 415	-	-	415	-	2.5
pyrene	-	129-00-0	340	390- 480	0.32	290

**Table 5. Fluorescent compounds emitting visible light (wavelength shifters) for scintillators production. Bibliography for fluorescent compounds comparison: [98], [99], [100], [101], [102], [103], [104].**

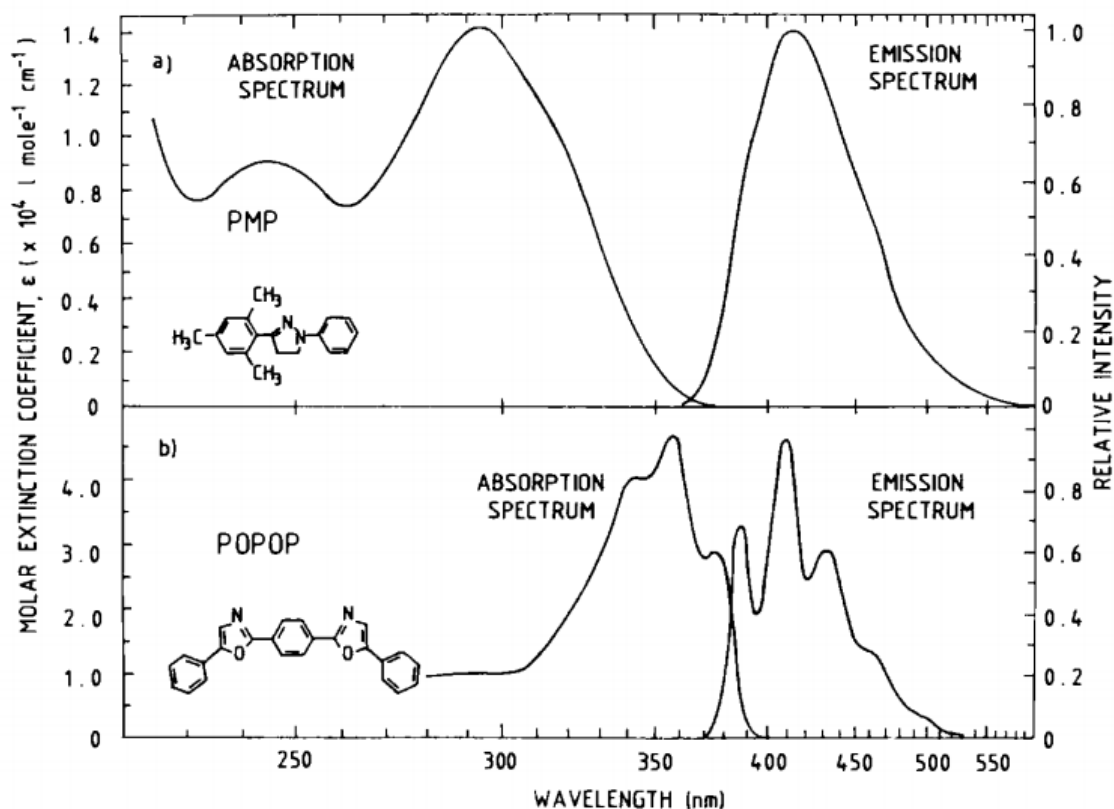
Name	Common abbreviation	CAS number	$\lambda_{\text{abs}}$ [nm]	$\lambda_{\text{em}}$ [nm]	$\Phi_f$	$\tau$ [ns]
2-(1-naphthyl)-5-phenyloxazole	$\alpha$ -NPO	846-63-9	345	400	0.8	2
2,5-di(4-biphenyl)oxazole	BBO	2083-09-2	340	410-412	0.75	1.4
trans-4,4'-diphenylstilbene	DPS	2039-68-1	337	410	0.8; 1.0	1.1
1,4-bis(5-phenyl-2-oxazolyl)benzene	POPOP	1806-34-4	365	415-417	0.85	1.3
1,4-bis(2-methylstyryl)benzene	bis-MSB	13280-61-0	347-350	420	0.96	1.6
2,5-bis(5-tert-butyl-benzoxazol-2-yl)thiophene	BBOT	7128-64-5	370	430	0.74	1.1
1,4-bis(4-methyl-5-phenyl-2-oxazolyl)benzene	DMPOPOP	3073-87-8	370	430	0.93	1.5
1,1,4,4-tetraphenyl-1,3-butadiene	TPB	1450-63-1	345	458; 465	0.43	1.8
9,10-diphenylanthracene	DPA	1499-10-1	366-375	430	0.95-1.0	7.3
1H,5H,11H-[1]benzopyrano[6,7,8-ij]quinolizin-11-one,2,3,6,7-tetrahydro-10-(3-pyridinyl)	Coumarin 510	87349-92-6	425	496	-	7.6
2,3,6,7-tetrahydro-9-(trifluoromethyl)-1H,5H,11H-[1]benzopyrano(6,7,8-ij)quinolizin-11-one	Coumarin 540A, Coumarin 153	53518-18-6	408	490	0.98	5.4
3-(2-N-methylbenzimidazolyl)-7-N,N-diethylaminocoumarin	Coumarin 515, Coumarin 30	41044-12-6	413; 420	480	-	7.5
3-(2-benzimidazolyl)-7-(diethylamino)coumarin	Coumarin 7	27425-55-4	433; 460	493; 510	-	-
1,6-diphenyl-1,3,5-hexatriene	DPH	1720-32-7	-	-	-	-
7H-benzimidazo[2,1-a]benz[de]isoquinoline-7-one	BBQ	-	400	470	-	18
benzoxanthene (xanthenic acid) derivative	Y11 (K27)	-	430	469; 530	0.7	11.8

The photophysical properties of a compound are determining factors in its selection for use in a scintillator formula. There are several performance requirements for fluors:

- suitable optical spectra – emission spectra of primary fluor must overlap with absorption spectra of wavelength shifter;
- low light self-absorption for high light transmission, if absorption and emission spectra of fluorescent compound are not overlapping then transmission of emitted light is possible for longer distance;
- high extinction coefficient ( $> 10,000$ ) to minimize the amount required for good energy transfer;
- high quantum yield ( $\Phi_f > 0.6$ ) for efficient energy transfer and high light output;
- short decay time: 2-3 ns for blue emitters and up to 12 ns and longer for green emitters;
- radiation hardness allows operation at high radiation doses for several years
- high solubility in monomer allows for uniform mixing of the additive in the solution and to achieve the required concentration: for primaries, at least 10 grams per liter, and for wavelength shifters at least 0.1 gram per liter;
- temperature tolerance: must be able to withstand processes going through 100-180 °C;
- chemical stability: must be compatible with all the other components in the solution and must not be susceptible to radical attack during the polymerization itself;
- the additives do not inhibit polymerization of the monomers;
- photostability: many fluors are light sensitive, and this must be taken into account when they are being handled;
- cost: fluor must possess all above requirements and be obtainable at an acceptable cost, less than \$10,000 per kilogram.

Most commonly used first fluorescent additives are 2,5-diphenyloxazole (PPO), p-terphenyl (PTP), 2-(4-tert-butylphenyl)-5-(4-biphenyl)-1,3,4-oxadiazole (BPBD) and wavelength shifters are 1,4-bis(5-phenyl-2-oxazolyl)benzene (POPOP), 1,4-bis(2-methylstyryl)benzene (bis-MSB), 1,4-bis(4-methyl-5-phenyl-2-oxazolyl)benzene (DM-POPOP).

Some compounds (Table 6), such as 3-mesityl-1-phenyl-4,5-dihydro-1H-pyrazole (PMP) [105] can absorb energy from the plastic base and emit in the blue in one step. Other fluors, such as 3-hydroxyflavone (3HF) and 2-(2-hydroxyphenyl)benzothiazole (HBT) by means of intramolecular proton transfer, can absorb energy from the plastic base and emit in the green in one step [106].



**Figure 8. Comparison of absorption and emission spectra of fluorescent compound PMP with large Stokes shift (a) and wavelength shifter POPOP (b) [107]**

These compounds show large Stokes shift (Figure 8) - the difference between positions of the band maxima of the absorption ( $\lambda_{\text{abs}}$ ) and emission ( $\lambda_{\text{em}}$ ) spectra of the same electronic transition (fluorescence) and can provide high light transmission in plastic scintillators volume. They are some of the most radiation-tolerant plastic scintillator formulas but they have smaller fluorescence quantum yield and longer decay time constant in comparison with standard fluors.

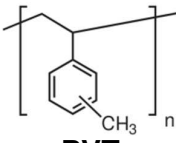
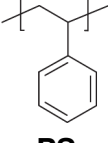
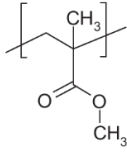
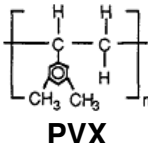
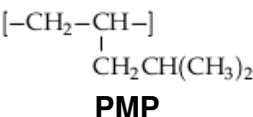
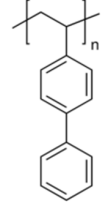
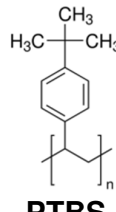
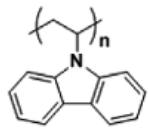
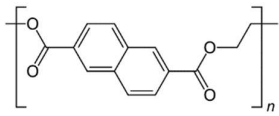
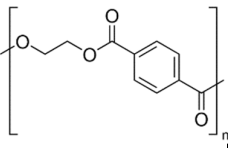
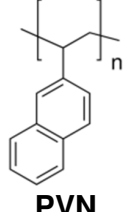
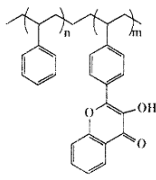
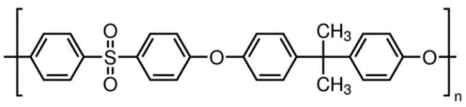
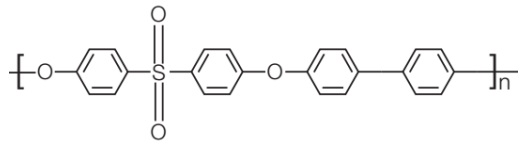
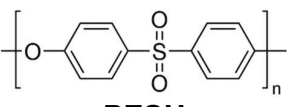
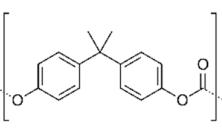
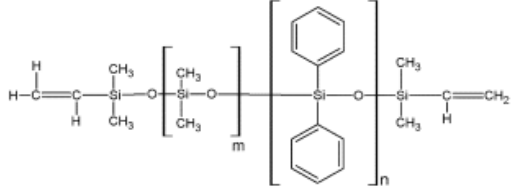
**Table 6. Fluorescent substances with high Stokes shift**

Name	Common abbreviation	CAS number	$\lambda_{\text{abs}}$ [nm]	$\lambda_{\text{em}}$ [nm]	$\Phi_f$	$\tau$ [ns]
	MOPOM	-	333	420	-	2
3-mesityl-1-phenyl-4,5-dihydro-1H-pyrazole	PMP	60078-97-9	295	425	0.88	3
2,2'-bipyridyl-3,3'-diol	BPD	36145-03-6	355	495	0.31	3.8
2-(2-hydroxyphenyl)benzothiazole	HBT	3411-95-8	340	530	0.35	3.9
3-hydroxyflavone	3HF	577-85-5	350	530	0.42	8.5

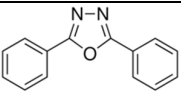
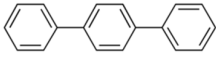
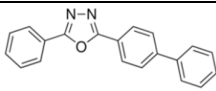
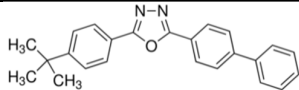
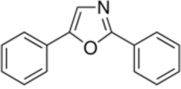
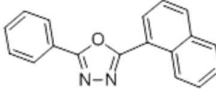

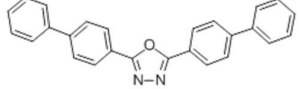
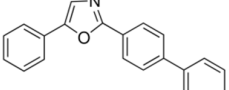
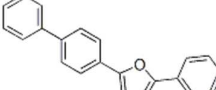
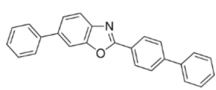
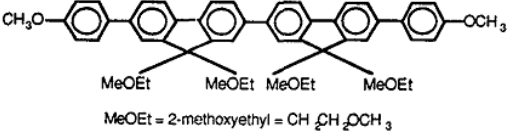
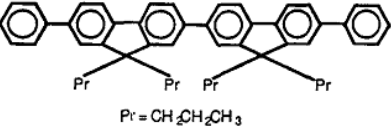
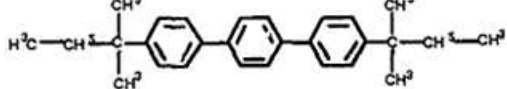
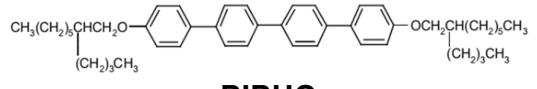
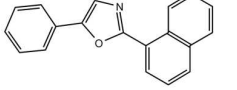
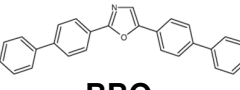
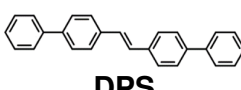
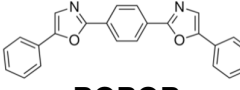
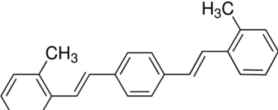
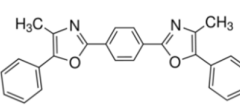
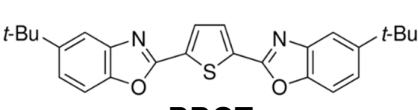
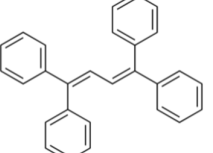
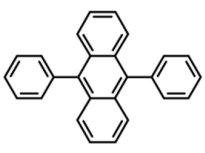
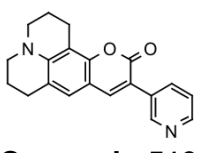
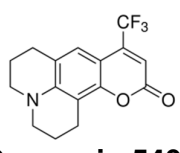
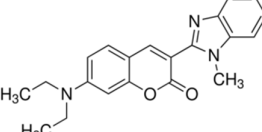
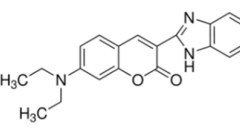
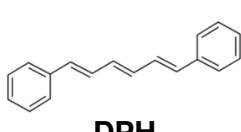
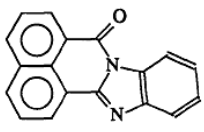
There are also polystyrene based plastic scintillators doped with phosphorescent iridium(III) complexes [108], polyvinyltoluene based scintillators doped with iridium complex, Flrpic [109], mixed-ligand complexes of gadolinium carboxylates containing unsaturated bonds in plastic scintillators [110]. Metal complexes have long decay time about 1000 ns and green emission spectrum (500 nm). They are very slow in time property due to light emission by phosphorescence.

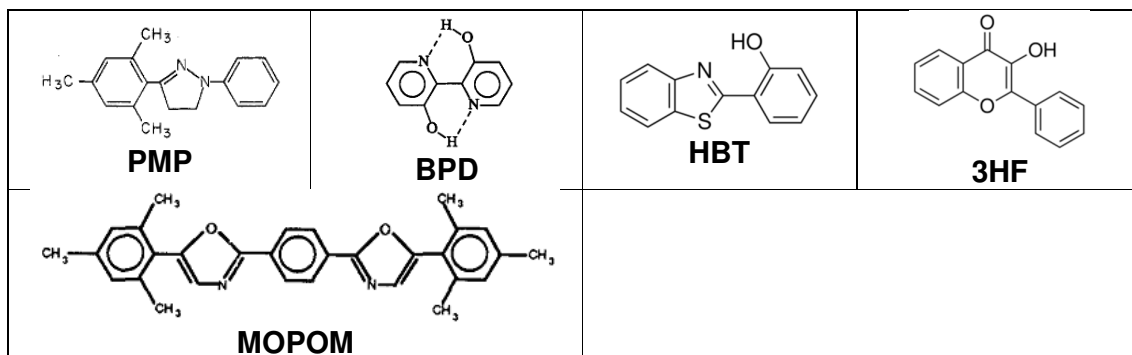
In Table 7 structural formulas of polymers and various groups of fluorescent additives are gathered. Note that most of these substances have aromatic rings in their chemical structure.

**Table 7. Structural formulas of polymers and fluorescent substances used in plastic scintillator manufacturing. Explanation of abbreviations are in previous tables with properties of those substances.**

Polymers			
 <b>PVT</b>	 <b>PS</b>	 <b>PMMA</b>	 <b>PVX</b>
 <b>PMP</b>	 <b>PVBP</b>	 <b>PTBS</b>	 <b>PVK</b>
 <b>PEN</b>	 <b>PET</b>	 <b>PVN</b>	 <b>poly(styrene-co-3-hydroxy-4'-ethenylflavone)</b>
 <b>PSU</b>	 <b>PPSU</b>		
 <b>PESU</b>	 <b>PC</b>	 <b>PMPS</b>	



Primary fluorescent additives			
 <b>PPD</b>	 <b>PTP</b>	 <b>PBD</b>	 <b>BPBD</b>
 <b>PPO</b>	 <b>α-NPD</b>	 <b>pyrene</b>	 <b>BBD</b>
 <b>BPO</b>	 <b>PBO</b>	 <b>PBBO</b>	
 <b>O415</b> MeOEt = 2-methoxyethyl = CH <sub>2</sub> CH <sub>2</sub> OCH <sub>3</sub>		 <b>O408</b> Pr = CH <sub>2</sub> CH <sub>2</sub> CH <sub>3</sub>	
 <b>DAT</b>		 <b>BIBUQ</b>	
Secondary fluorescent additives – wavelength shifters			
 <b>α-NPO</b>	 <b>BBO</b>	 <b>DPS</b>	 <b>POPOP</b>
 <b>bis-MSB</b>	 <b>DM-POPOP</b>	 <b>BBOT</b>	
 <b>TPB</b>	 <b>DPA</b>	 <b>Coumarin 510</b>	 <b>Coumarin 540A</b>
 <b>Coumarin 515</b>	 <b>Coumarin 7</b>	 <b>DPH</b>	 <b>BBQ</b>
Fluorescent substances with high Stokes shift			



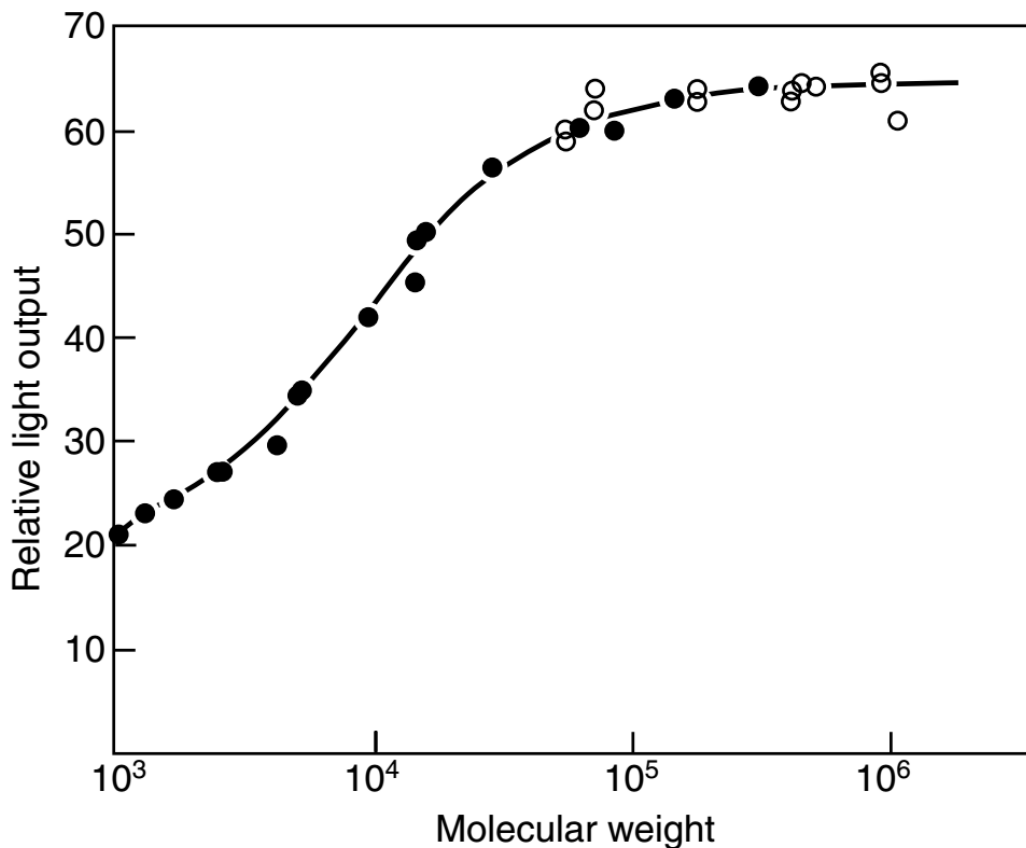
Furthermore the plastic scintillator may include other additives and polymer modifiers, for example:

- co-solvents naphthalene and 1,1,3-trimethyl-3-phenylindane in PMMA-based scintillators [76];
- fluorescence quencher benzophenone to improve timing properties [111], [112];
- release agent zinc stearate to prevent polymer from bonding to mold surfaces during polymerization [113];
- preservative butylated hydroxytoluene (BHT) or Ethanox 330 to prevent oxidation of polymer in scintillator [113];
- plasticizers silicone oil [114] and diphenyl ether [115] to accelerate diffusion and recombination of radicals during annealing after irradiation of the radiation hard scintillator;
- components which enhance absorption of neutrons, e.g. boron [116], [117], [118], lithium [119], [120] and gadolinium [121], [122] - these elements have large cross section to neutron absorption;
- components which enhance absorption of gamma radiation, e.g. tin [123], [124], [125], [126], lead [127], [128] and bismuth [129], [130] - these metals have high atomic number (50, 82, 83 respectively) and absorb gamma quanta with higher probability than carbon and hydrogen (with atomic number 6 and 1, respectively) from which plastic scintillators are built.

## 2.6. Components effect on plastic scintillator optical characteristics

The spectral properties of fluorescent additives discussed in previous sections concerned individual compounds. In the case of plastic scintillators, one takes into account the mutual influence of the components (polymer matrix, primary additive, and wavelength shifter) determining the spectral characteristics of the scintillator as a whole.

As the molecular weight of the polymer base of the scintillator increases to a certain limiting value (e.g.  $10^5$  for polyvinyltoluene), the light output increases (Figure 9). This is explained by the increased quantum output of fluorescence for macromolecules with a larger molecular weight. Other conditions being the same, a higher light output is characteristic of scintillators with narrower molecular-mass distribution pattern of the polymer base [131]. Plastic scintillators should be uniform and isotropic, and for this reason only amorphous polymers are employed as their base.



**Figure 9. Relative light output of polyvinyltoluene scintillator as a function of the molecular weight of polymer [132].**

Figure 10 presents the light output of polystyrene scintillators as influenced by the nature of the primary luminescent additive and its concentration. Figure 10 shows

that in all cases, the light output increases with increasing concentration of the primary additive up to the certain value (specific for each activator) where the light output attains maximum and starts to decrease with the further increase of the activator concentration. Decrease in light output at increased concentrations of the additives is due to the concentration-quenching phenomenon. For wavelength shifter (Figure 11) there is similar dependency - light output increases with increasing concentration and with concentration higher than 0.05% slow decreases in light output is observed.

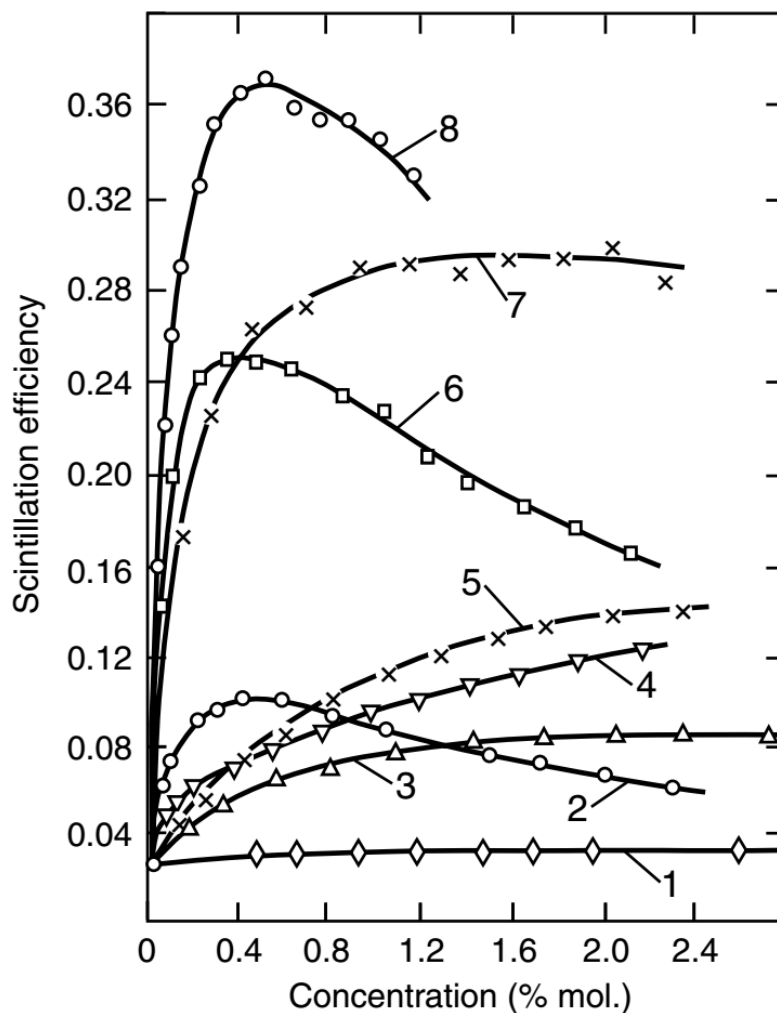
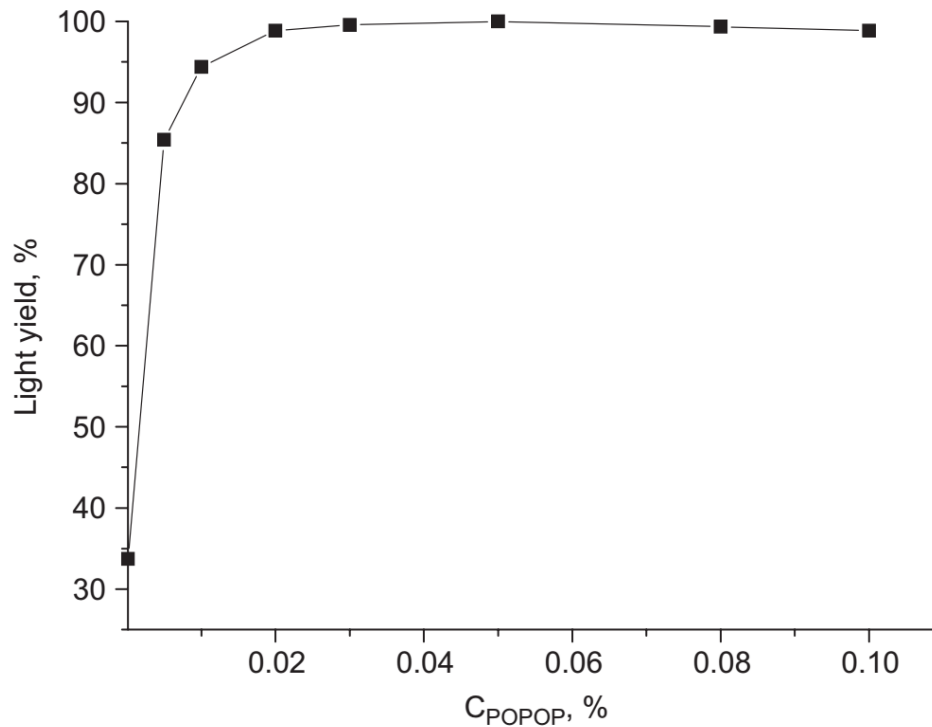


Figure 10. Light output of plastic scintillators (relative to anthracene) as influenced by the nature and concentration of the primary luminescent additive: (1) diphenyl, (2) stilbene, (3) naphthalene, (4) diphenylbutadiene, (5) anthracene, (6) PPO, (7) p-terphenyl; and (8) tetraphenylbutadiene [133].



**Figure 11. Relative light yield of 30 x 15 mm<sup>2</sup> polystyrene based plastic scintillator samples versus POPOP concentration under p-terphenyl concentration at 2.0% [134]**

Scintillators decay time dependency from the fluorescent additive concentrations are shown in Figure 12. With increasing concentrations of primary solutes in polymer base rapid reduction in the decay time to some minimum value is observed. A further increase in the concentration does not change decay time constant of these scintillators.

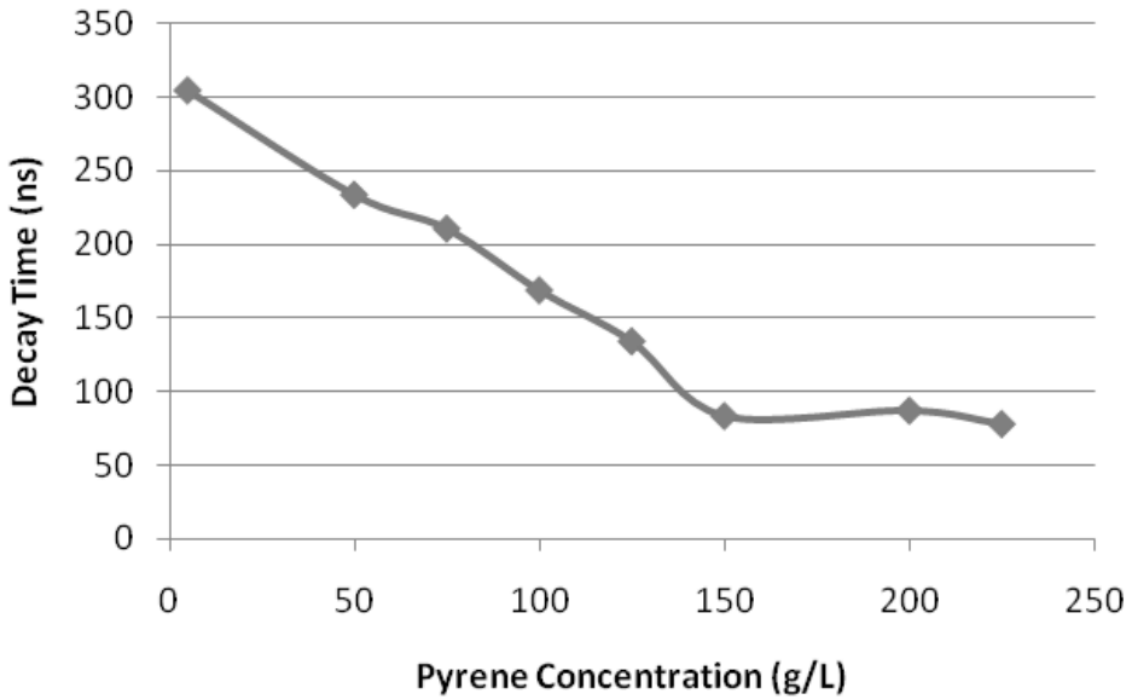
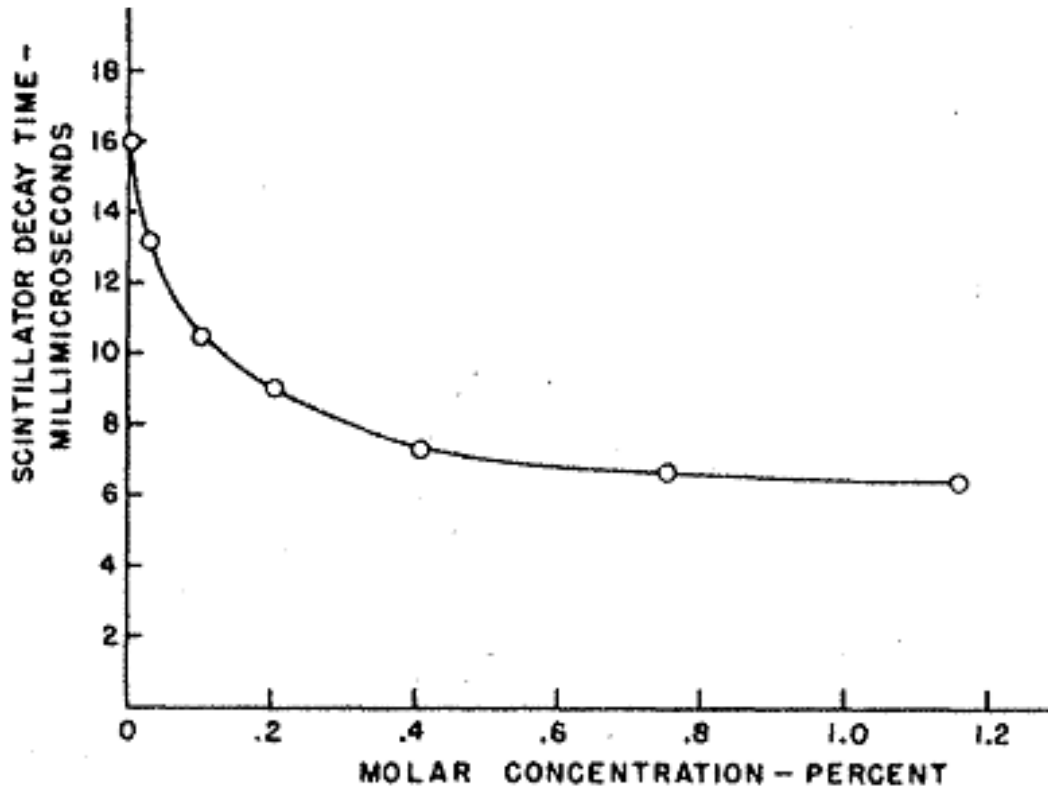
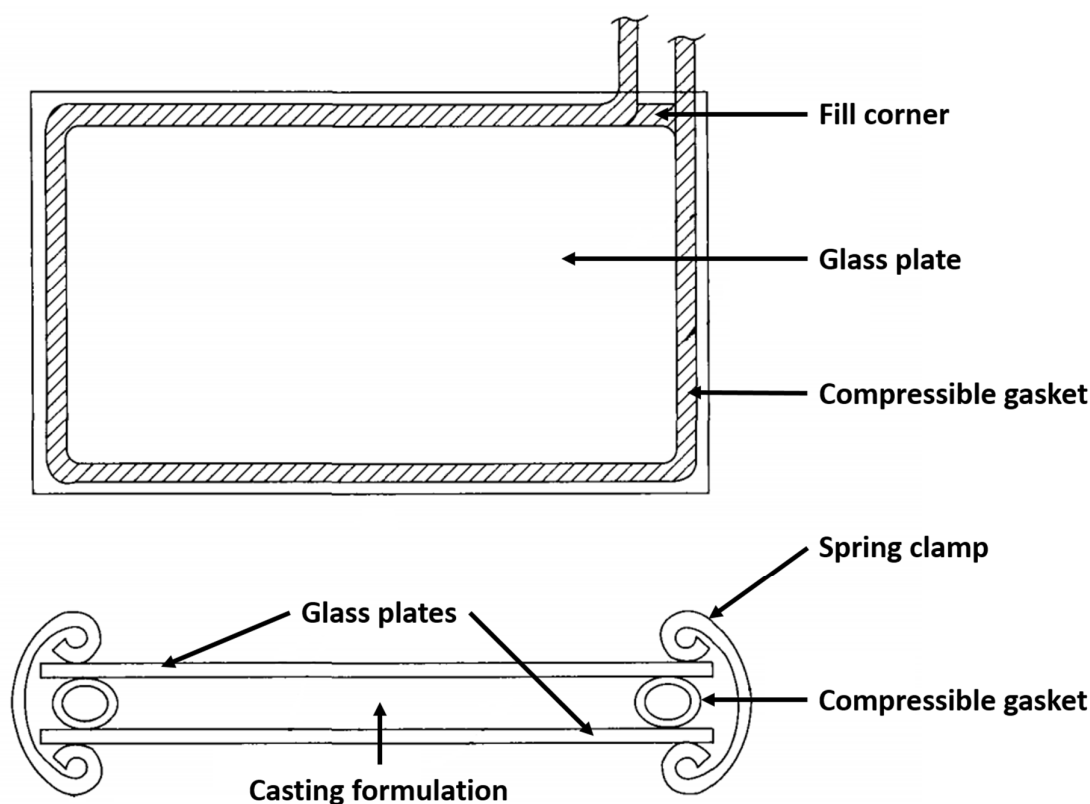


Figure 12. Scintillation decay time versus tetraphenylbutadiene (TPB) concentration in polystyrene scintillator (top) [135] and versus pyrene concentration in polyvinyltoluene scintillator (bottom) [136]

## 2.7. Methods of industrial production: cell casting, injection molding, extrusion

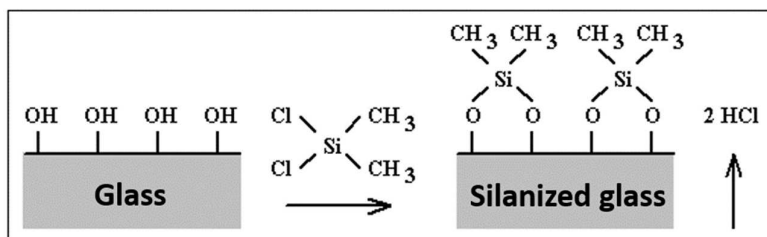
There are three main polymer manufacturing methods realized at the industrial scale that are applied to the production of plastic scintillators [137]. The best results are obtained in batch cell casting and this method is commonly used to make commercial scintillators. The other two methods concerning the production of polymers at the industrial scale are the injection molding technique and the extrusion technique. Both involve mixing a solid polymer pellets with fluorescent additions and use expensive equipment. There is also fourth method that merges cell casting with extrusion.



**Figure 13. Face view (top) and edge view (bottom) of conventional cell casting mold configuration. Scheme adapted from [138]**

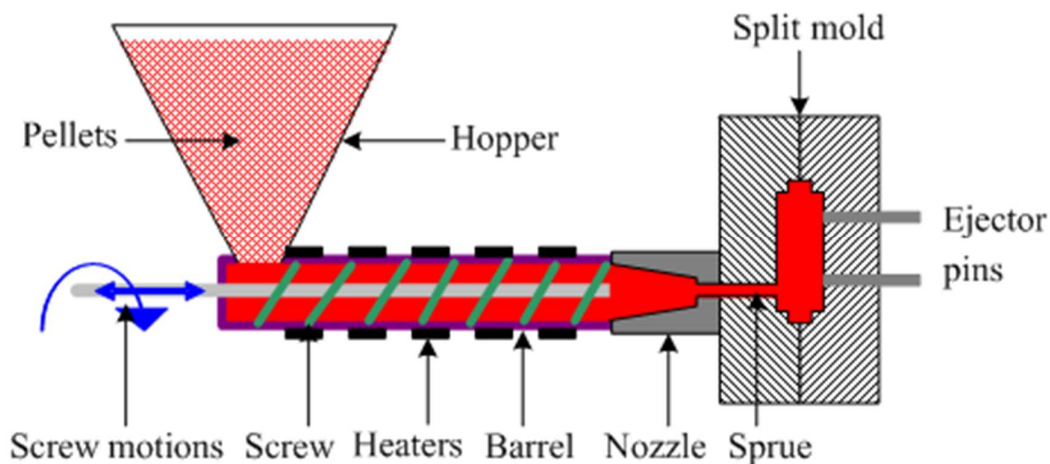
Batch cell casting is a process where a liquid monomer with dissolved dopants is poured into a mold and heated to rigid solid plastic (Figure 13). In the first step, the monomer is purified on activated alumina sorbent. The sorbent removes impurities such as inhibitor and water from the monomer. Dissolved oxygen and other gases are removed from the solution by degassing under reduced pressure. Before pouring the solution into the mold, the surface of the mold is treated with a solution of dichlorodimethylsilane in chloroform. This procedure is called silanization [61] and

allows the prevention of adherence of the polymer sample to the glass mold by formation of the antiadhesive layer (Figure 14).



**Figure 14. Silanization reaction for glassware. The figure is adapted from [139].**

The mold is then placed in the furnace under a heating cycle that takes place for approximately 5 days. After a few days the heating scintillator is cooled, annealed, and mechanically cut and polished. In this way, it is possible to obtain scintillators in shapes of blocks, plates, sheets, rods and bars. More complicated profiles may be manufactured by lathe work.



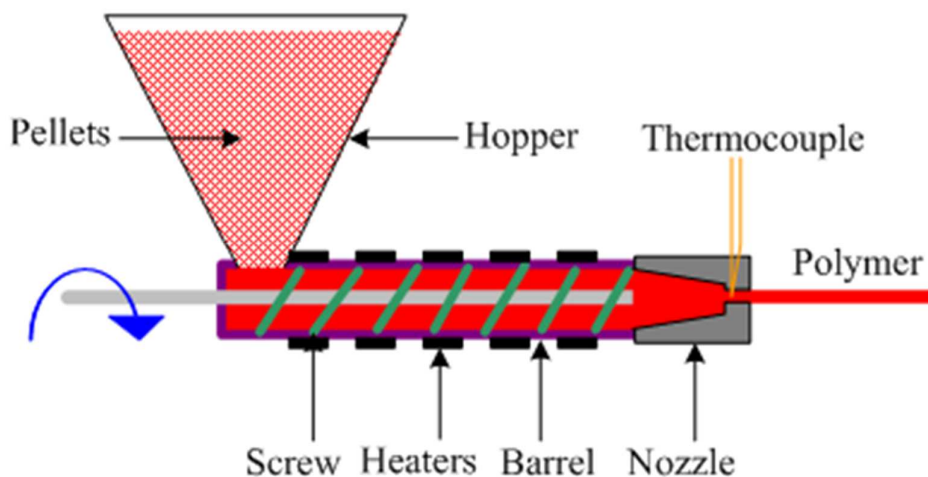
**Figure 15. Schematic of typical screw-injection molding machine [140]**

The injection molding technique is widely used in industry. Most plastic goods and packages are produced with this technique. Application of the injection molding technique for mass production of scintillation tiles was first developed in the early 1980s [141]. With this process, optically transparent granulated polystyrene is mixed with scintillation dopants. Then the mixture is loaded into a molding machine hopper, where it is continuously directed into a heated screw cylinder while being mixed (Figure 15). At the exit of the cylinder the temperature reaches approximately 200°C and the melted polystyrene accumulates in its nozzle. As it becomes full, an injection into the mold starts. It lasts for approximately 3 seconds at a pressure of approximately 700 atmospheres. After mold cooling up to approximately 50°C, it opens and the tile is taken away. The whole cycle lasts for less than 2 minutes per tile.

The production rate is high and the cost is a small fraction of the cost of a commercial scintillator. In addition, no secondary mechanical operation is needed for



the final product. Scintillators produced with the injection molding technique have inferior light yields and poorer optical properties compared with cast scintillators. It is related to the speed of the cooling rate of the scintillator being too high, which results in optical heterogeneity. Moreover, a very high temperature during manufacturing causes degradation of the polymer.



**Figure 16. Schematic of typical screw-extrusion machine [140]**

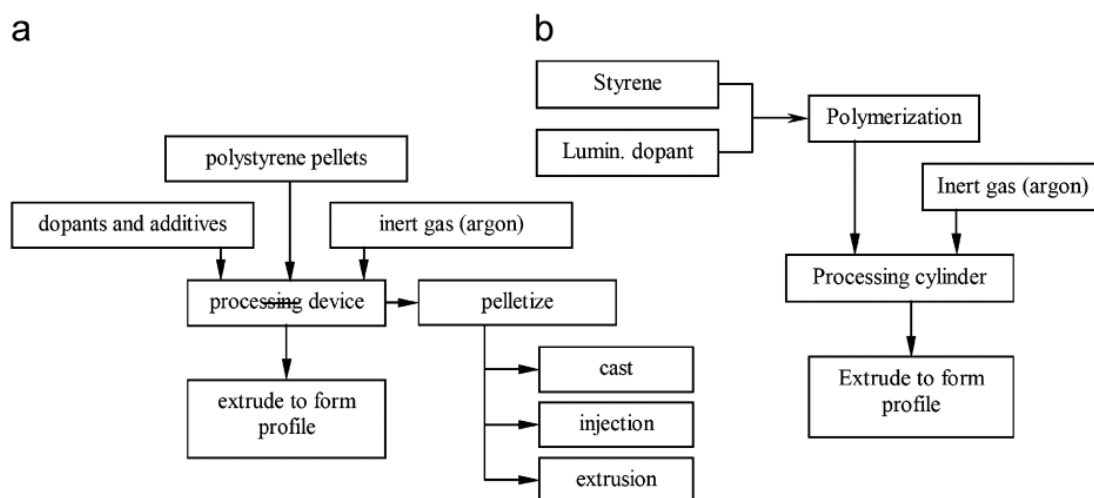
The extrusion technique was first applied to plastic scintillator detectors in 1980 [142] and produced a polystyrene-based scintillator with good light yield, but demonstrated a relatively poor light attenuation length. Twenty years later, another attempt was performed in order to make better scintillators with lower costs [143]. This method is a continuous in-line compounding and extrusion process (Figure 16).

Similar to the injection molding technique, polymer pellets are mixed with fluorescence dopants and loaded to a molding machine hopper with heaters and mixing steps. At the end of the machine there is a profile dye instead of mold. The extruder function is to melt, mix, and deliver the scintillator material to the profile dye. All steps are done under argon gas to prevent degradation of the polymer. After extrusion, the material immediately enters the vacuum-sizing tool mounted in a long chilled water tank. In this vacuum-sizing tank, differential pressure draws the semi-molten material to final dimensions. The material is further cooled in a second water-chilled section. The resulting scintillator has a shape of a long strip with a cross-section of the dye.

Extruded scintillators also have poor optical properties. The reason for low quality of extruded scintillator strips is presence of oxygen in polymer matrix while processing. During the storage, oxygen from air penetrates into polymer pellets and then leads to oxidation under high temperature in extrusion processing device.

The main idea of method that merges cell casting with extrusion concept was to obtain a scintillator using extrusion method but from the melt of polymerized plastic except of polymer pellets [144]. The other feature was to exclude screwing device from production scheme. Instead of that inert gas pressure was used as a driving force for

extrusion process. According to the flowchart in Figure 17, the new method consists of two stages: preparation of scintillating materials by bulk polymerization and extrusion under the inert gas pressure. Preparation stage includes input quality control of raw materials (styrene and luminescent dopants), clarification of raw material if necessary; preparation of scintillating composition; removing solute oxygen from styrene; and conducting thermal bulk polymerization. After reaction, the scintillating polymer was not cooled down to room temperature and loaded into extrusion device in melt state. During the all process oxygen contact with the reaction mixture was excluded. Extrusion stage includes melt scintillating composition is loaded into extrusion cylinder; inert gas pressure pushes the polymer through an extrusion die which forms shape and size of strip. For better uniformity of polymer feeding gear pump in extrusion line was used.



**Figure 17. Comparison of standard extrusion technology utilizes polymer pellets (a) and method of extrusion without screw uses bulk polymerized monomer solution (b) [144]**

A comparison of the described methods is presented in Table 8. Only one technique, cell casting, is commonly applied to fabricate plastic scintillators in industry and in research and development laboratories. This method seems to be suitable for the manufacturing of plastic scintillators, revealing properties which will fulfill the requirements of novel J-PET scanner applications.

**Table 8. Comparison of industrial methods for production of plastic scintillators**

<b>Technique</b>	<b>Advantages</b>	<b>Drawbacks</b>
Cell casting: thermal bulk polymerization from monomer	<ul style="list-style-type: none"><li>▪ best polymer quality and scintillator performance;</li><li>▪ smooth scintillator surfaces from mold;</li><li>▪ easily mechanical machined</li></ul>	<ul style="list-style-type: none"><li>▪ high manufacturing costs;</li><li>▪ time-consuming process;</li><li>▪ complicated reaction preparation</li></ul>
Injection molding from polymer pellets	<ul style="list-style-type: none"><li>▪ low cost;</li><li>▪ ability to produce complicated shapes</li><li>▪ mass production of many elements in short time</li></ul>	<ul style="list-style-type: none"><li>▪ optical heterogeneities;</li><li>▪ mechanical stresses inside the polymer;</li><li>▪ much lower scintillator performance: light attenuation length and light yield</li></ul>
Extrusion from polymer pellets	<ul style="list-style-type: none"><li>▪ low cost;</li><li>▪ ability to produce long strips with any cross-section</li><li>▪ mass production of many elements in short time</li></ul>	<ul style="list-style-type: none"><li>▪ optical heterogeneities;</li><li>▪ mechanical stresses inside the polymer;</li><li>▪ much lower scintillator performance: light attenuation length and light yield</li></ul>
Extrusion without screw from thermal bulk polymerized monomer	<ul style="list-style-type: none"><li>▪ polymer quality and scintillator performance same as in cell casting;</li><li>▪ low cost;</li><li>▪ ability to produce long strips with any cross-section</li></ul>	<ul style="list-style-type: none"><li>▪ time-consuming process;</li><li>▪ complicated reaction preparation;</li><li>▪ mechanical stresses inside the polymer</li></ul>

### 3. Thesis and objectives of the work

The work presents an attempt to improve the polystyrene scintillators properties for new type of positron emission tomography (PET) scanners based on plastic scintillators.

Considering presented literature review, the following thesis has been formulated:

**Developed polystyrene scintillator materials have properties allowing their use in new types of PET scanners which are based on plastic scintillators.**

To prove the proposed thesis, the main objective of this dissertation was aimed at optimization of the conditions of synthesis and processing of polystyrene for the production of gamma radiation detectors.

The main objective was realized by sub-objective compromising:

- development of the best possible composition of the fluorescent additives in polystyrene scintillator for the detection of gamma radiation: achieving the maximum light output and the shortest decay time of manufactured polymer scintillators
- matching optical properties of polystyrene scintillators with spectral characteristic of light detectors used in J-PET scanner
- time-temperature cycle optimization for styrene polymerization in small glass ampoules
- time-temperature cycle optimization for styrene polymerization in casting sheet between glass plates
- development of a method for the fast and effective quality control of the produced plastic scintillators.

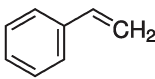
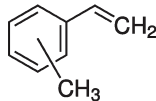
In the framework of this thesis the quality assurance method was developed and successfully applied for the validation of plastic scintillator strips purchased for the construction of the first full scale J-PET prototype, as well as for the construction of the presently built J-PET tomograph with the SiPM readout.

## 4. Synthesis of polystyrene scintillators

### 4.1. Cylinders

As a first step of the laboratory research, in order to measure spectroscopic properties of plastic scintillators small cylinders were synthesized with the following dimensions: 25 mm in diameter and 25 mm height. For research and development purposes, styrene as a monomer was chosen to produce polystyrene scintillators. A styrene monomer has low cost, is commercially available, and scintillators obtained on this basis have almost the same properties as for polyvinyltoluene. The monomer styrene (99.8%) was obtained from Brenntag [145] and monomer methylstyrene was obtained from Sigma-Aldrich [146]. Basic physical and chemical properties of these monomers are listed in Table 9.

**Table 9. Selected properties of monomers used in plastic scintillator synthesis**

Monomer	Styrene	Vinytoluene
Synonyms of the name	phenylethylene, vinylbenzene	methylstyrene
CAS number	100-42-5	25013-15-4
Structural formula		
Molar mass [g/mol]	104.15	118.18
Density at 20°C [g/cm <sup>3</sup> ]	0.910	0.893
Melting temperature [°C]	-31	-77
Boiling point [°C]	145-146	168
Purity [%]	>99.8	98.5; mix of isomers: 60% meta, 40% para and 1% ortho
Content of TBC polymerization inhibitor [ppm]	10-15	45-55
Storage temperature [°C]	2-8	2-8

Polymerization inhibitor 4-tert-butylcatechol (TBC) from monomer was removed on glass column filled with activated alumina (aluminum oxide, Al<sub>2</sub>O<sub>3</sub>) [147]. Sorbent balls have 2 to 5 mm in diameter [148]. This sorbent removes also water and other impurities like ethylbenzene and benzaldehyde [149]. Primary and secondary solutes were purchased from Sigma-Aldrich [150] and were not purified (>99% purity grade, suitable for scintillation).

Synthesis of samples was performed in glass ampoules 25 mm in diameter and 140 mm height. Before polymerization ampoules were treated 12 hours with 30% (volume concentration) solution of dichlorodimethylsilane in chloroform to prevent

sticking of scintillator samples to glass. After this procedure called silanization ampoules were rinsed in turn with chloroform, acetone, distilled water and were dried in an oven.

Primary and secondary solutes were weighted and dissolved in an appropriate volume of styrene monomer in composition from Table 10. To accelerate dissolution of secondary solutes styrene with solutes was heated in closed glass vessel up to temperature 60 °C. Prepared solution was poured into glass ampoule and argon gas was blown through Teflon pipe submerged in solution for 15 minutes. Oxygen in air can dissolve into top part of scintillators and cause yellow tint during polymerization. Removing oxygen from monomer solution prevents also decrease of light yield of plastic scintillators by fluorescence quenching caused by oxygen and inhibition of polymerization in early steps of polymerization cycle. Inert gas like argon prevents these phenomena. Finally ampoules were sealed under argon gas atmosphere using flame burner.

**Table 10. Chemical compositions of polystyrene scintillator samples. Values in weight percent.**

Sample No.	Primary solute	Secondary solute
1	2% PPO	0.06% POPOP
2		0.06% DM-POPOP
3		0.06% bis-MSB
4		0.03% POPOP + 0.03% DM-POPOP
5		0.03% DM-POPOP + 0.03% bis-MSB
6		0.03% bis-MSB + 0.03% POPOP
7		0.02% POPOP + 0.02% DM-POPOP + 0.02% bis-MSB
8	2% PPO	0.06% POPOP
9	2% PTP	
10	2% BPBD	
11	1% PPO + 1% PTP	
12	1% PTP + 1% BPBD	
13	1% BPBD + 1% PPO	
14	0.67% PPO + 0.67% PTP + 0.67% BPBD	
15	2% PPO	-
16	2% PTP	-
17	2% BPBD	-
18	-	0.06% POPOP
19	-	0.06% DM-POPOP
20	-	0.06% bis-MSB

Thermal activated bulk polymerization process was performed in electric split tubular furnace on stand (Figure 18) with automatic control of temperature with an accuracy of 1 °C [151]. Furnace is divided into four independent heating zones with temperature regulation from room temperature to 250 °C and seven time-temperature

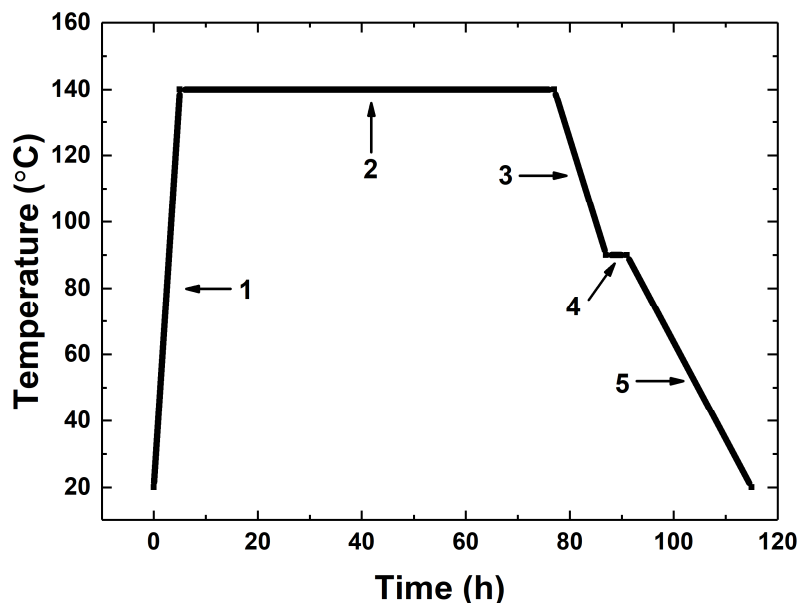
steps per cycle. Reactor with vertical pipe shape has 65 mm diameter and total four zones length is 780 mm. These dimensions allow to produce up to 8 cylinders with maximum 25 mm diameter in one polymerization cycle with the same temperature profile or with four different temperature programs. The following parameters were controlled: temperature, time, heating and cooling rate in each zone. All parameters are programmable from a computer and can be saved on-line to a personal computer with the thermal history of each zone.



**Figure 18. Split tubular furnace on stand used for plastic scintillator cylinders synthesis [151]**

Experimental studies on the polymerization process were performed to evaluate the optimal time and temperature cycle conditions. A series of experiments have been performed in order to find the most optimal temperature cycle which would lead to the synthesis of the sample without optical defects such as bubbles inside plastic scintillator volume and cracks on surfaces. A resulting best temperature cycle is shown in Figure 19. Polymerization was carried out with following steps:

1. heating from room temperature 20 °C to 140 °C in 5 hours, 24 °C/h,
2. polymerization at 140 °C during 72 hours,
3. cooling from 140 °C to 90 °C in 10 hours, 5 °C/h,
4. annealing in 90 °C for 4 hours,
5. cooling from 90 °C to room temperature in 24 hours, 2.5 °C/h.



**Figure 19. Most optimal temperature cycle established for cylinders polymerization. Description in the text.**

Polymerization starts in first step during fast heating. Small samples require a rapid heating due to forming of vacuum bubbles. If the temperature is still below the glass-transition temperature of polystyrene (100 °C) and the reaction takes place in viscous solution of the polymer in monomer, then vacuum bubbles may occur. To prevent this phenomenon fast increase of temperature reaction above 100 °C is applied to small samples up to 100 grams. The second step involves polymerization at 140 °C for approximately 3 days and ensures complete conversion from monomer to polymer. Following the main polymerization step, slow cooling is applied (third step). Further annealing (fourth step) of polymer scintillators under glass-transition temperature at 90 °C for 4 hours is required because rapid cooling can crack the polymer sample due to internal stresses from shrinking with decreasing temperature [152]. Finally, the fifth step is related to cooling to room temperature.

Obtained rods were cut to cylinders with desired dimensions 25 mm diameter and 25 mm height. Top part of rods were cut off and were not used in research because sometimes scintillator was yellowed probably from traces of oxygen in ampoule. Samples have also concave meniscus from polymer shrinkage. Styrene density is 0.91 g/cm<sup>3</sup> and polystyrene density is 1.06 g/cm<sup>3</sup>. Plastic scintillator contains mainly polystyrene (>95%) and typical volume shrinkage after polymerization is 17% [153], [154].

Cylinders have smooth and shining side surface from glass ampoule. Raw machined top and bottom part of cylinders were manually polished using sandpaper in water as cooling medium. Increasingly fine grades 1200, 2500 and 4000 of abrasive papers were used. The abrasive papers were glued to wooden blocks to ensure that the scintillator and sandpaper surfaces are kept plane.



## 4.2. Plates

Strip J-PET scanner is built from long plastic scintillator strips. To obtain many strips for radiation detector construction plates are manufactured which next can be cut to strips of desired dimensions. Cell-cast sheet has superior optical properties and light transmittance as well as smoother surfaces. For research and development purposes 10 mm thick plate was chosen.

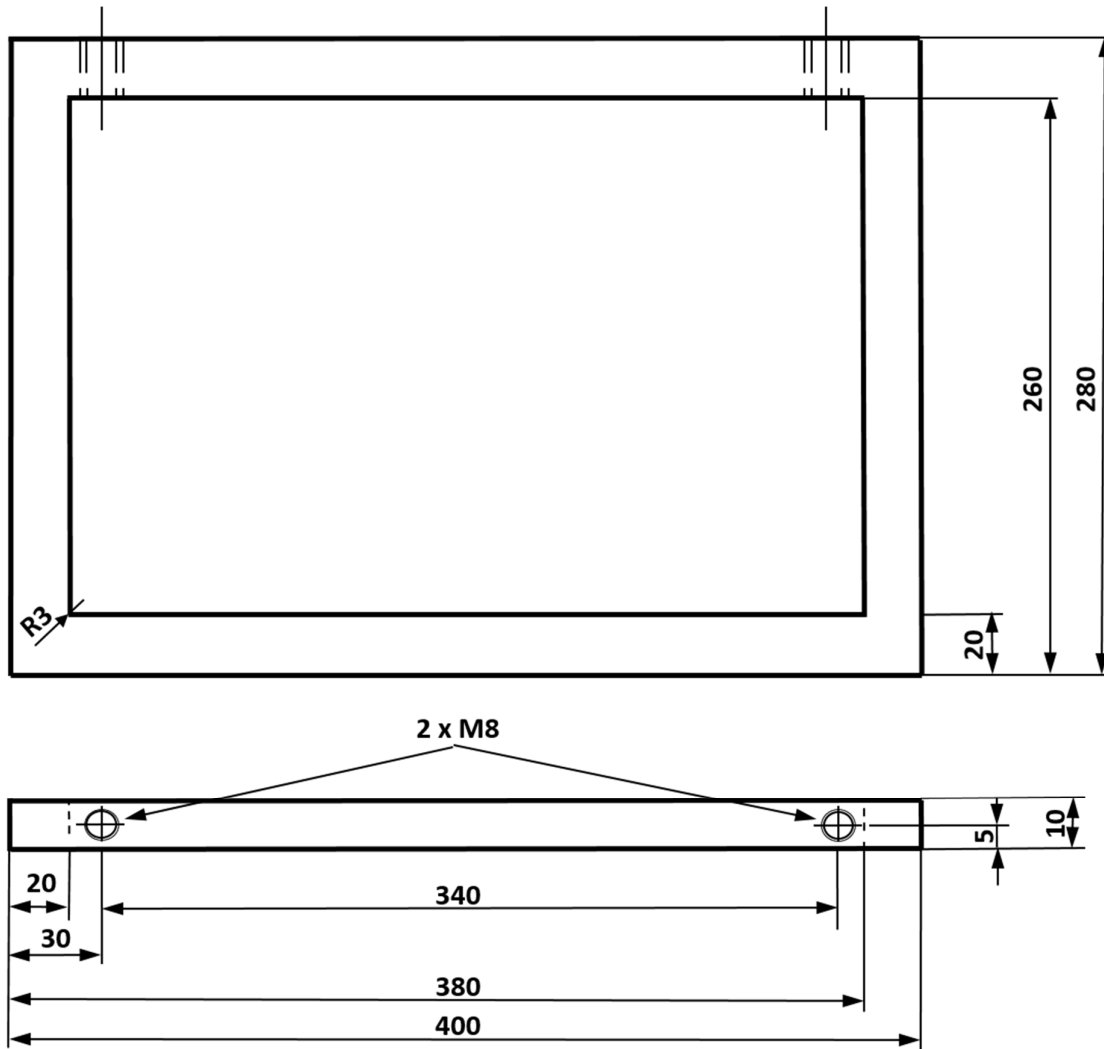
Cast sheet is made in a batch process within a mold or cell. Basically the processing cells consist of two pieces of polished plate glass slightly larger in area than the finished sheet is to be. Procedure is to pour the monomers or partially polymerized syrups into suitably designed molds and heating to complete the polymerization. A large reduction in volume, about 17%, takes place during the cure. The reaction also is accompanied by the liberation of a substantial amount of heat. At conversions above 20%, the polymerization becomes accelerated, and the rate rises rapidly until gelation occurs at about 90% conversion. Thereafter, the reaction slows down and a post cure may be needed to complete the polymerization [155].

During the accelerated phase, the rapid increase in viscosity and liberation of heat can raise the internal temperature and elevate the reaction rate. In extreme cases, a violent runaway polymerization can occur. During this cure cycle the effects of shrinkage and interrupting the polymerization to form syrup containing 25 to 50 wt% polymers can control acceleration. Amounts of shrinkage and heat production drop during polymerization cure in accordance with the polymer content. Using syrups also shortens the time in the mold, decreases the tendency to leakage from the molds, and greatly decreases the chance of dangerous polymerization runaways [155].

The monomer styrene (99.8%) was obtained from the Brenntag [145]. Polymerization inhibitor 4-tert-butylcatechol (TBC) from monomer, water and other impurities like ethylbenzene and benzaldehyde were removed by storing monomer in glass bottle filled with activated alumina balls (aluminum oxide,  $\text{Al}_2\text{O}_3$  [148]) during 12 hours. In order to remove dust particles from activated alumina balls styrene was filtered by ceramic sinter. Primary and secondary solutes were purchased from Sigma-Aldrich and were not purified (>99% purity grade, suitable for scintillation).

Thermal activated polymerization process was divided into two phases. In first phase prepolymer was made. A prepolymer is a polymer in some stage between that of the monomer and the final polymer. Thus it is a polymer that has not completely finalized its polymerization process and grown to full molecular weight [156]. In other words prepolymer is a solution of polymer in monomer, e.g. partially polymerized monomer with additions of fluorescent compounds. Primary and secondary solutes were weighted and dissolved in an appropriate volume of styrene monomer in round-bottom flask. Styrene solution of fluorescent additives was heated and stirred on magnetic stirrer under argon flow with use of Teflon stir bar. Water-cooled condenser was used to condense styrene vapors. Preparation of prepolymer was carried out during about 90 minutes at 120 °C. Prepolymer was ready to pour to the mold after it started increasing viscosity like in form of viscous syrup.

Manufacturing of plates was performed in rectangular glass mold consisting of two 4 mm thick flat glass plates, one 10 mm thick and 20 mm wide at sides aluminum frame (see Figure 20), 0.2 mm thick white insulating Teflon tape and steel spring clamps. Surfaces of glass plates were washed with water solution of dish soap, rinsed with water and were dried in an oven in 120 °C. Aluminum frame has two threaded screw holes in top part of the mold. One hole is for pouring prepolymer into the mold and the second is for air removing. One layer of 0.2x19 mm<sup>2</sup> Teflon tape gasket are placed between glass plates and aluminum frame to prevent leakage from the mold. The mold is clamped with steel spring clamps and closed at top part by two stainless steel screws, see Figure 21.



**Figure 20. Technical drawing of aluminum frame used in mold designed and constructed for polystyrene scintillator cast sheet manufacturing. Dimensions are in millimeters. Symbol M8 means threaded hole for screw with 8 mm diameter thread. Symbol R3 means 3 mm radius of edge rounding inside the frame.**



**Figure 21. Photograph of mold consisting two 280x400 mm glass plates, aluminum frame, white teflon gasket and steel spring clamps.**

Second phase of thermal activated polymerization process was performed in electric furnace (Figure 22) with automatic control of temperature with an accuracy of 1 °C [157]. Furnace has hot air circulation with temperature regulation from room temperature to 300 °C and 15 time-temperature steps per cycle. Dimensions of the working chamber are 200x500x1000 mm<sup>3</sup>.



**Figure 22. Furnace for plastic scintillator plates manufacturing [157]**

The biggest challenge in casting process was to obtain a nice look of polystyrene scintillator sheets without optical defects, bubbles inside and cracks on surfaces. Few time-temperature cycles from the literature were tested [33], [106], [158], [159], [160], [161]. All of them are probably intended for polymerization of small samples under total mass of 100 grams in sealed glass ampoules. Two polymerization cycles from mentioned publications were carried out in a silicone oil bath where heat transfer from ampoules with monomer to silicone oil is faster and more uniform. Polymerization took place in aluminum ampoules where heat transfer between polymer and surrounding medium was better because aluminum is a good thermal conductor. Small diameter of synthesized samples, usually about 25 mm, also facilitated heat removing from exothermic reaction in glass vials to surrounding thermostatic bath or oven.

Application of these settings in furnace with hot air circulation and mold with glass plates cause bubbles appearance during first 24 hours due to overheating and boiling of the monomer. Polystyrene is a thermal insulator and heat flow inside bulk polymerized sample depends from thickness of the sheet. Thermal initiated bulk polymerization process in bigger volumes needs different time-temperature cycle than the one used in small cylinder synthesis. Speed of heating at the beginning of the polymerization process should be smaller (less than 5 °C per hour) and initial temperature of heating should also be below 100 °C to prevent boiling of the styrene monomer at 145 °C (see Table 9).

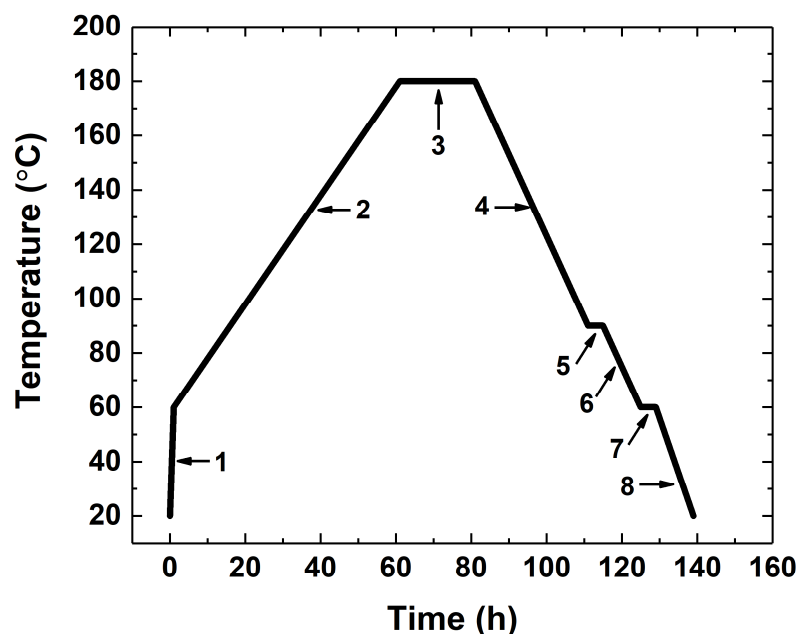
Lower initial temperature causes also higher average molar mass of polymer thus allowing to obtain polystyrene scintillator with increased light output, see Figure 9. On the other hand heating up to 180 °C and polymerization at that high temperature

reduces the presence of residual styrene monomer in plastic scintillator. High content of unreacted styrene monomer may cause damage of plastic scintillators optical properties. Evaporating of remaining styrene causes cracks on the surfaces, deteriorate light output and optical transparency of polystyrene scintillator.

The polymerization reaction can be accelerated by two heat sources. The first one is related to the furnace temperature and is well controlled by time-temperature cycle set in furnace controller. The second heat source is related to the exothermic polymerization reaction (process accompanied by the release of heat) and is more difficult to control [158]. If the speed of the reaction becomes very high due to a rapid rise of the oven temperature at the beginning of the process, bubbles are observed in random parts inside casting mold. Combined heat from furnace and exothermic polymerization causes local overheated zone in the mold and boiling of the monomer. Generated vapor bubbles are trapped inside volume of a viscous polystyrene and styrene solution. About 17% volume contraction takes place during polymerization process and in the mold cooling phase also vacuum bubbles can appear. Both kinds of bubbles can be avoided by control of the temperature increase and decrease speed in heating cycle. Too fast heating may cause uncontrolled reaction, monomer leak from the mold and even lead to an explosion.

A series of experimental studies on the polymerization process were performed to evaluate the optimal time and temperature cycle conditions. A most optimal temperature cycle established in this work is shown in Figure 23. Polymerization was carried out with the following steps:

1. fast heating from room temperature 20 °C to 60 °C in 1 hour, 40 °C/h,
2. slow heating from 60 °C to 180 °C in 60 hours, 2 °C/h,
3. polymerization in 180 °C during 20 hours,
4. cooling from 180 °C to 90 °C in 30 hours, 3 °C/h,
5. first annealing in 90 °C for 4 hours,
6. cooling from 90 °C to 60 °C in 10 hours, 3 °C/h,
7. second annealing in 60 °C for 4 hours,
8. cooling from 60 °C to 20 °C room temperature in 10 hours, 4 °C/h.



**Figure 23. Most optimal temperature cycle established in this work for plates manufacturing. Description in the text.**

Polymerization starts in first step during fast furnace heating to 60 °C. Prepolymer requires a slow heating due to forming of bubbles from monomer boiling. The second step is a slow heating from 60 °C to 180 °C in 60 hours. The third step involves polymerization at 180°C for approximately 20 hours and ensures complete conversion from monomer to polymer. Following the main polymerization step, slow cooling from 180 °C to 90 °C in 30 hours is applied (fourth step).

Further annealing at 90°C for 4 hours (fifth step) is required because rapid cooling can crack the polymer plate due to internal and surface stresses from shrinking with decreasing temperature. Annealing confers better dimensional stability on the pieces. In addition, the likelihood of cracks is reduced, thus increasing the useful life of plastic scintillator [152]. First annealing of polystyrene scintillator is few degrees under its glass-transition temperature at 98.5 °C (see chapter 5.1). After first annealing there is slow cooling from 90 °C to 60 °C in 10 hours (sixth step). Second annealing in 60 °C for 4 hours is added to anneal plate under softening point of polystyrene at about 70 °C. Finally, the eighth step is related to cooling to room temperature.

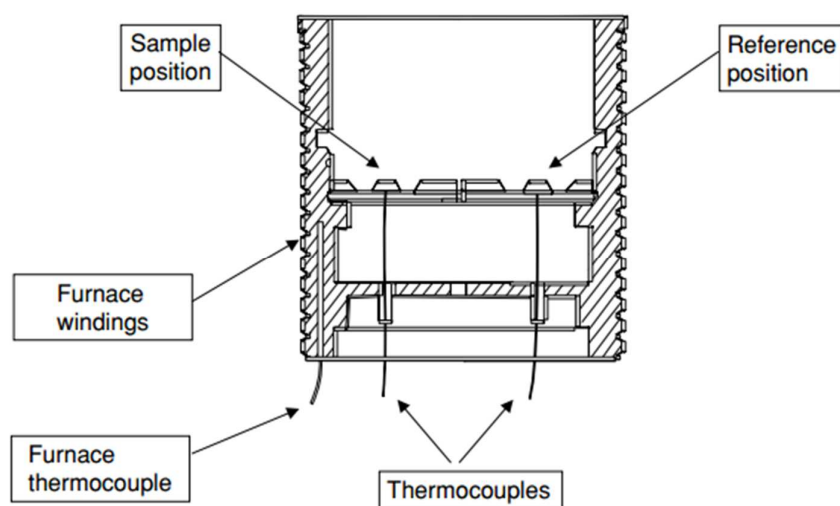
Plastic scintillators after polymerization between glass plates have smooth side surfaces. Only top part with concave meniscus with yellow discoloration from oxygen and side parts with Teflon gasket are cut away from the plate. Obtained plates were cut to strips. Side surface walls of strips were polished to optical grade in the same manner as in cylinders case.

## 5. Measurement of polystyrene scintillator structure

### 5.1. Glass transition temperature

Most polymers display a glass transition, in the course of which the material passes from a glassy to a rubbery state with a simultaneous increase in specific heat capacity. The glass transition ( $T_g$ ) is the temperature assigned to a region above which amorphous (non-crystalline) materials are fluid or rubbery and below which they are immobile and rigid, simply frozen in a disordered, non-crystalline state [162].

Differential scanning calorimetry (DSC) is the most widely used thermal technique in many applications including polymers and plastics [162]. Principle of operation of heat flux DSC is described in Figure 24.



**Figure 24. Diagram of a heat flux DSC. The sample and reference experience the same heat flux, but as energy demands differ, the heating or cooling effect will differ resulting in a difference in temperature between sample and reference. This difference in temperature is converted to an energy equivalent by the analyser giving the DSC signal in milliwatts (mW). The figure and caption are adapted from [162].**

A generalized DSC curve for a polymer is shown in Figure 25 and the main parameters used to characterize the glass transition are shown in Figure 26. For many applications it is important to know the temperature range  $T_{g,i}$  to  $T_{g,f}$  (see Figure 26) over which the substance vitrifies on cooling, or devitrifies on heating [163].

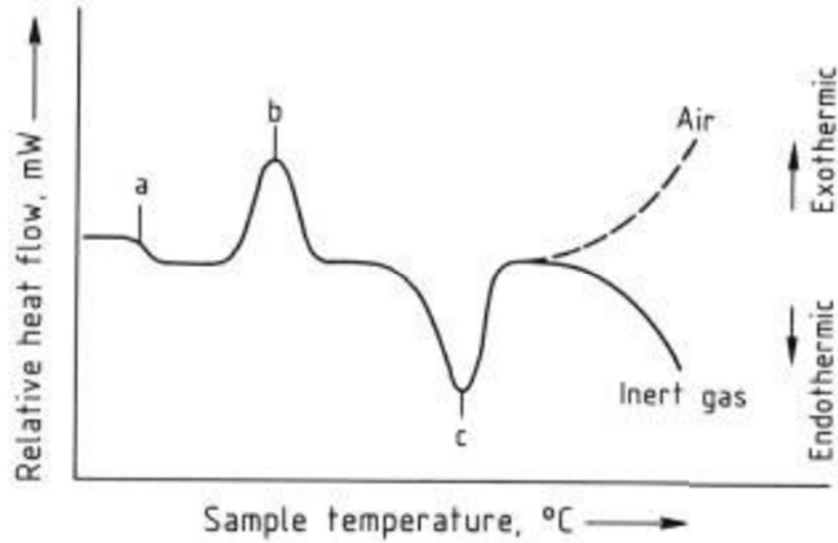


Figure 25. Generalized DSC curve for a polymer: a) glass transition; b) crystallization; c) melting. The subsequent reactions may be endothermic or exothermic. The figure is adapted from [164].

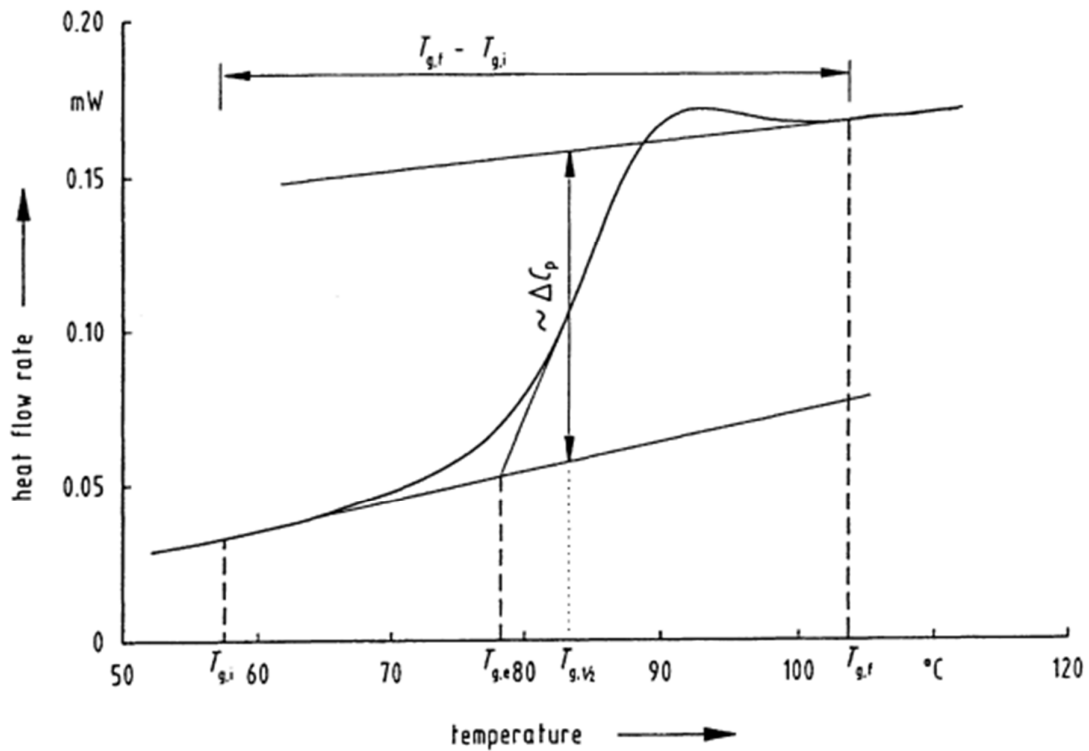


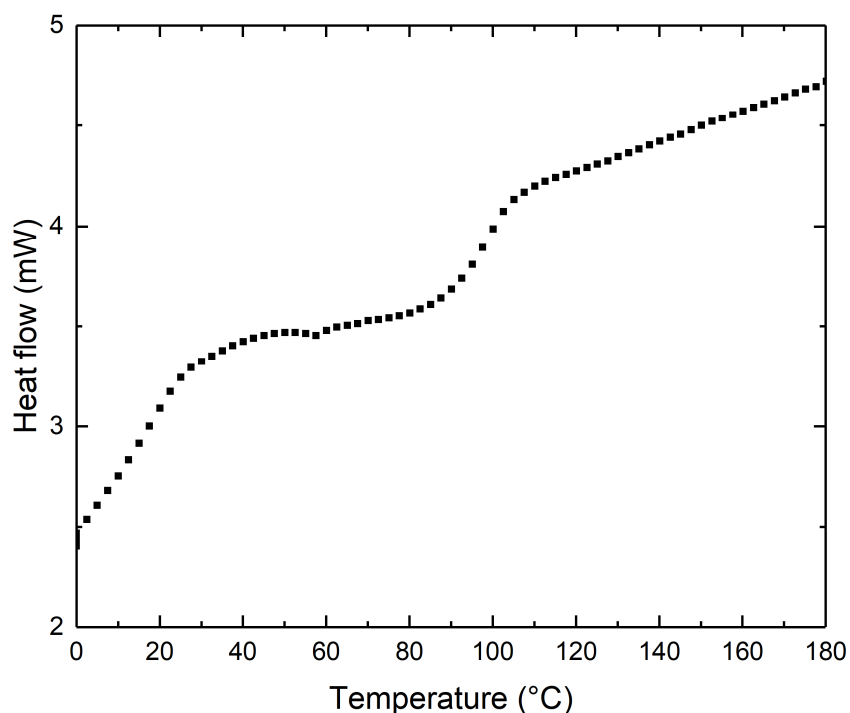
Figure 26. Definition of the most frequently used conventional quantities for characterization of the glass transition temperature.  $T_{g,e}$ : extrapolated onset temperature,  $T_{g,1/2}$ : half-step temperature,  $\Delta C_p$ : heat capacity change at the half-step temperature,  $T_{g,i}$  and  $T_{g,f}$ : initial and final temperatures of the glass transition,  $T_{g,f} - T_{g,i}$ : temperature interval of the glass transition. The figure is adapted from [163].



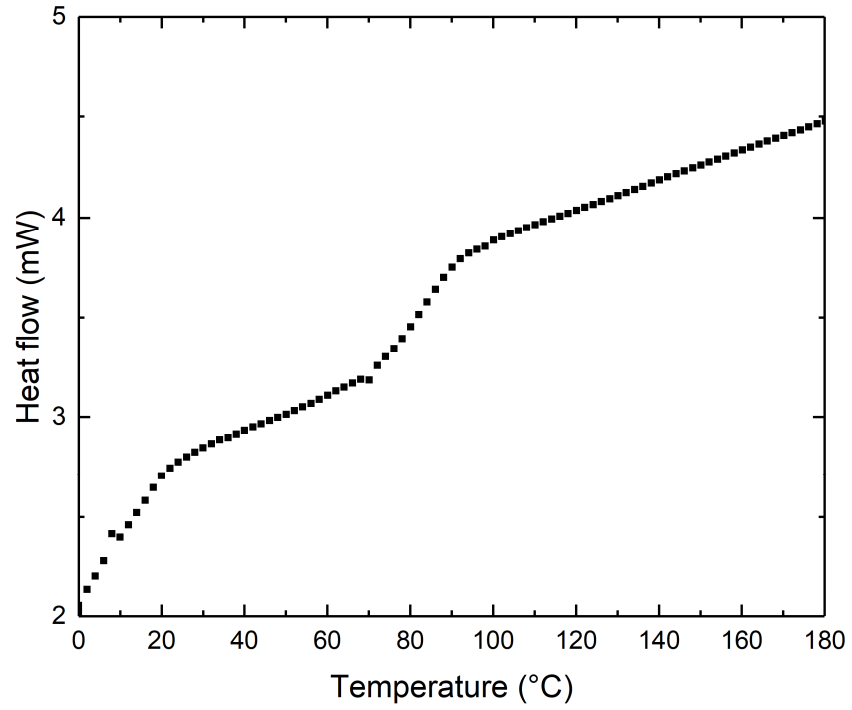
To measure glass transition temperature heat flux differential scanning calorimeter DSC1 from Mettler Toledo was used. Used samples were about 4 mg in weight. Measurement was done in 30 cm<sup>3</sup> per minute nitrogen flow with 10 Kelvin per minute heating speed.

Figure 27 and Figure 28 show obtained in this work DSC curves for polystyrene and polyvinyltoluene scintillators.  $T_{g,1/2}$  called also midpoint glass transition temperature was determined in Stare System program as described in Figure 26.

$T_g$  for polystyrene scintillator is 98.5°C and  $T_g$  for polyvinyltoluene scintillator is 86.65°C. Theoretical values from Table 3 are 100°C for polystyrene and 93-118°C for polyvinyltoluene. Differences between obtained and theoretical values are caused by manufacturing conditions during polymerization which effect on molar mass distribution and resulting  $T_g$  value.



**Figure 27. DSC curve for polystyrene scintillator. On a horizontal axis is temperature in °C and on vertical axis is heat flow in milliwatts (mW).**

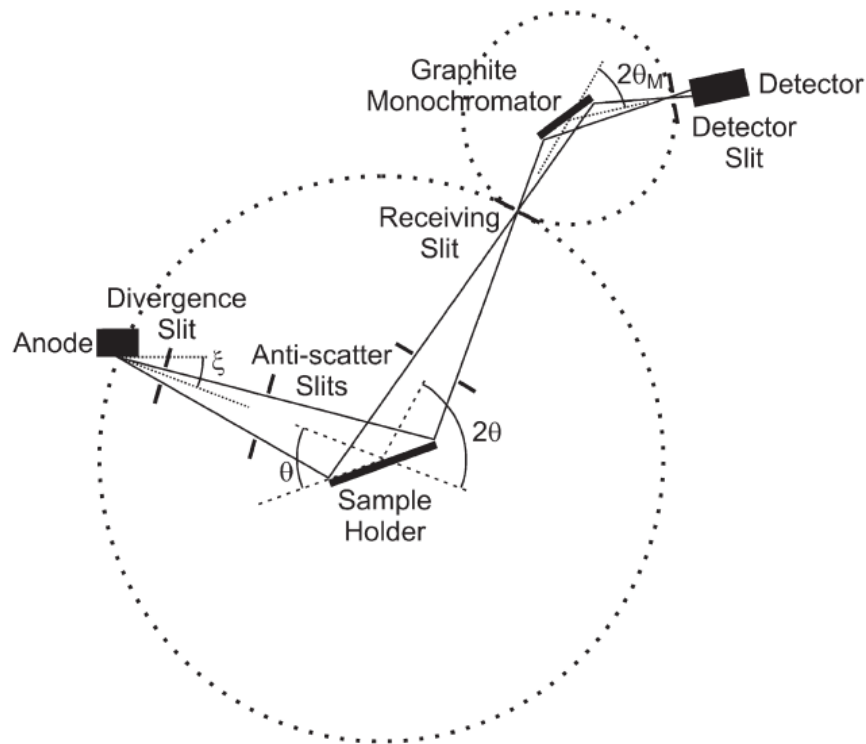


**Figure 28. DSC curve for polyvinyltoluene scintillator. On a horizontal axis is temperature in °C and on vertical axis is heat flow in milliwatts (mW).**

## 5.2. Amorphous state of polystyrene

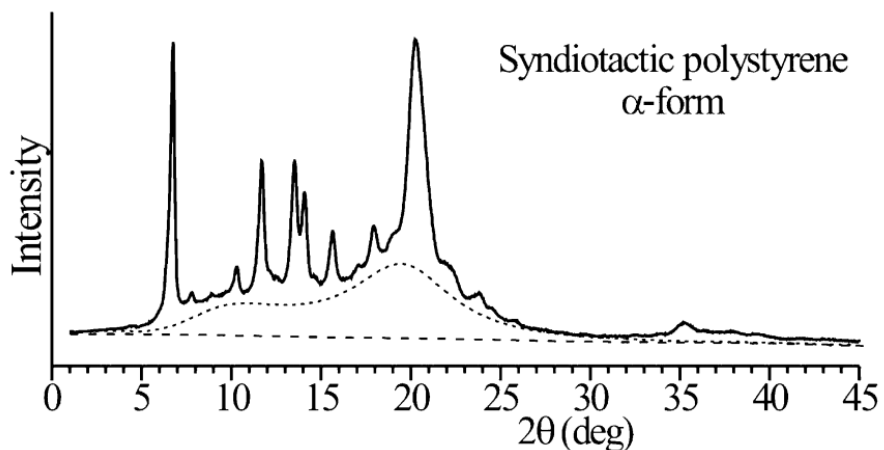
Powder X-ray diffraction (PXRD) offers a convenient method to characterize materials via their constituent crystal structures. When a crystal containing regular repeating arrays of atoms is irradiated by a monochromated X-ray beam, it generates diffraction peaks used to identify crystalline components of a sample [165].

The essential features of an x-ray powder diffractometer using the Bragg–Brentano focusing geometry are shown in Figure 29. The divergent incident X-ray beam produced by anode in lamp is reflected from the surface of the sample and converges at a fixed radius from the center of the sample position. The tube is aligned so that the beam divergent on the sample is at angle  $\xi$  to the anode surface and the divergence of the beam is controlled by one or more slits after the source [166]. After diffraction by the sample, the diffracted beam passes through the receiving slit. A post-sample graphite monochromator is employed with detector at the end [167].



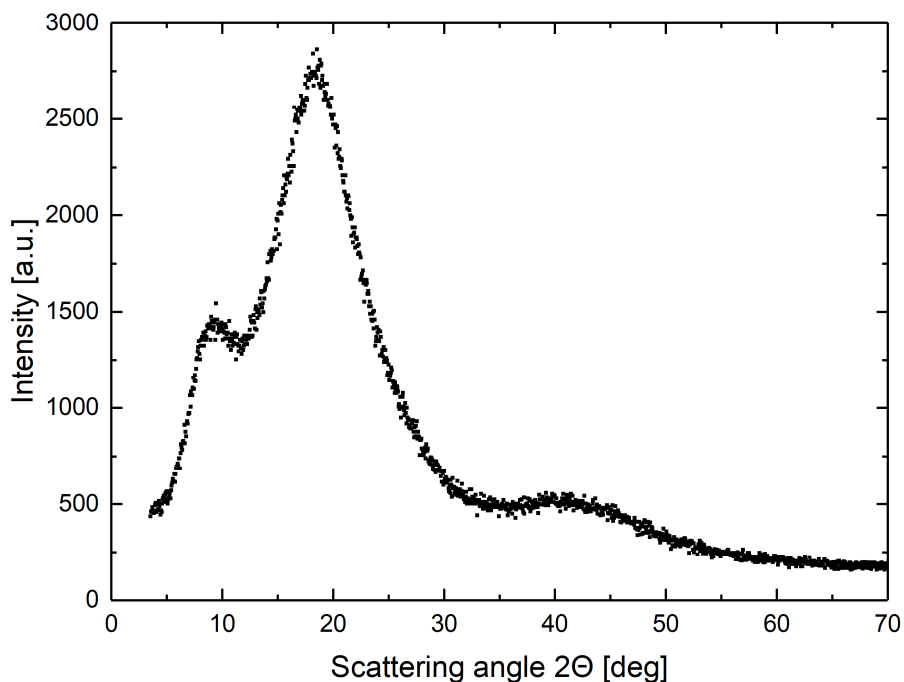
**Figure 29.** Scheme of a standard powder diffractometer with Bragg-Brentano geometry with a diffracted beam monochromator. The dotted circle centered on the sample position represents the goniometer circle on which the image of the divergent source of X-rays is focused by diffraction from the flat plate sample. The figure is adapted from [166].

The crystalline material shows a series of sharp peaks, or reflections, due to diffracted beams arising from different lattice planes. Whereas amorphous material shows broad peaks [168]. The X-ray powder diffraction profiles of partly crystalline polymers also clearly show the presence of a large contribution to the diffraction due to the amorphous phase, indicated by the dotted curves in Figure 30. Syndiotactic polystyrene with the phenyl groups positioned on alternating sides of the hydrocarbon backbone is an example of highly crystalline polymer with sharp peaks in diffractogram.



**Figure 30. X-ray powder diffraction profile of partly crystalline syndiotactic polystyrene (the figure is adapted from [169]). Contribution of amorphous phase is indicated by the dotted lines. The background intensity, approximated as a straight line, is indicated by the dashed lines.**

In this work, the diffractogram of polystyrene scintillator (Figure 31) was obtained using Philips X-ray powder diffractometer with  $K\alpha$  radiation from copper X-ray lamp. Sample was a 3 millimeters thick and 25 millimeters diameter disc.



**Figure 31. X-ray powder diffraction profile of amorphous polystyrene scintillator**

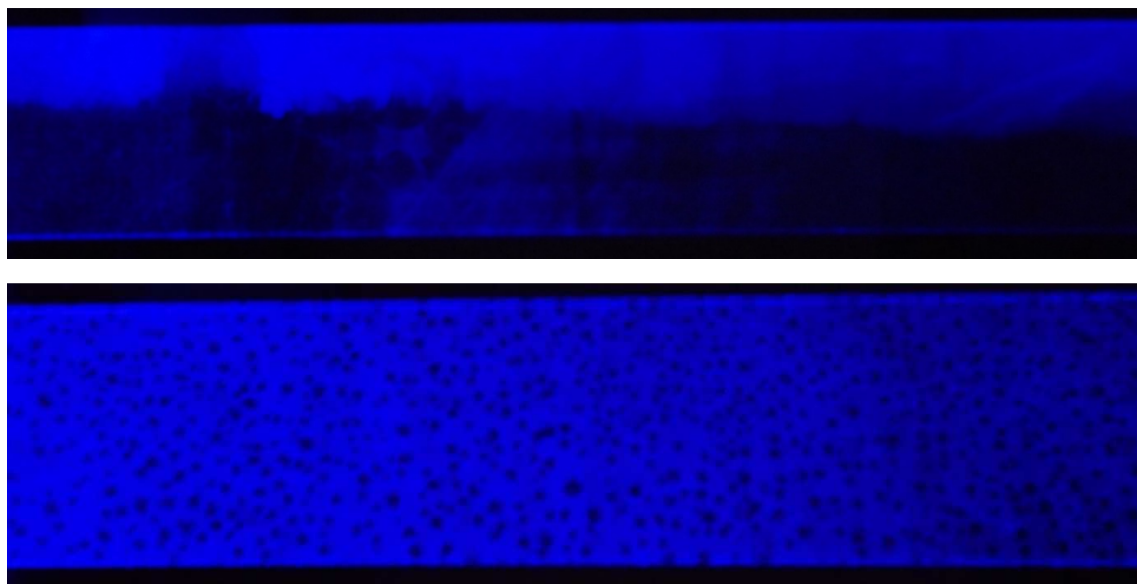
Polymers are composed of long molecular chains normally arranged in a random way. In some polymers, particularly those with simple linear conformations, the chains can become organized into ordered regions called crystallites [168]. Polystyrene in scintillator is atactic and amorphous. Random positioning of phenyl group on both sides of the hydrocarbon backbone prevents the chains from aligning with sufficient regularity to achieve high degree of crystallinity. Broad peaks in Figure 31 with maxima at 9, 18 and 41 degree show amorphous state of polystyrene manufactured in this PhD research. Amorphous polystyrene allows visible light to be propagated inside of plastic scintillator. Polystyrene with low degree of crystallinity (amorphous state) is transparent to visible light.

## 6. Quality control of plastic scintillators

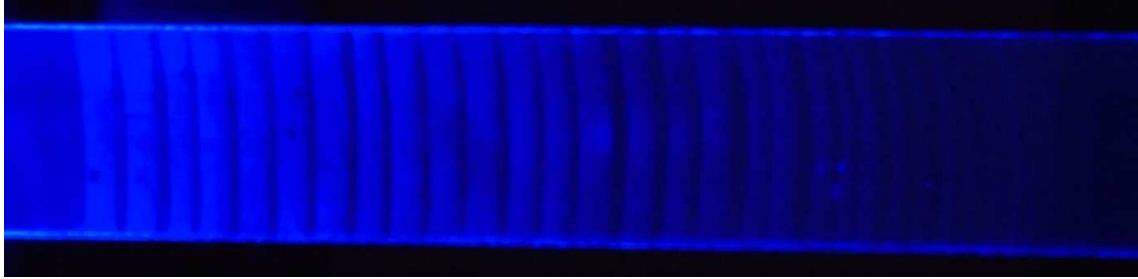
One of the aims of this work was to determine optical quality of manufactured and purchased plastic scintillator strips and wavelength shifter bars. Fast method of optical quality evaluation is required in view of building of new positron emission tomograph prototype based on plastic scintillator strips. A large number of strips must be examined in fast and easy way. For this purpose a new method of quality control of plastic scintillators was developed.

Three types of tests were performed. First was measuring dimensions of strip to check compatibility of obtained scintillators with thickness tolerance. Width and thickness were measured from both sides near edges with caliper with electronic readout with accuracy 0.01 mm and length was measured with aluminum ruler with precision 1 mm.

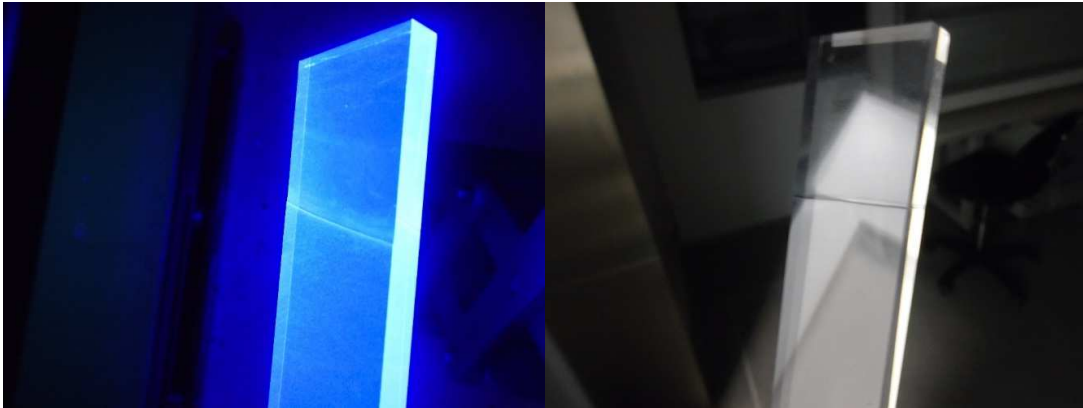
Second test for scintillator strip was its examination by eye under UV light which allows to detect scratches, cracks on the surface of scintillator, mat surface (Figure 32) and stains (Figure 33). Watermarks (Figure 34) and white spots on surface or in volume of the strip (Figure 35) are also easy to notice. These points inside of the strip are probably some dust or contamination from manufacturing process. The worst defects are bright volumes with irregular shapes on edges of the damaged scintillators (Figure 36). Strongly glowing areas under UV lamp are inhomogeneities in volume of strip caused by improper mixing of fluorescent additives in monomer. Strips are made from cutting plates into pieces. During polymerization some part of mixture separates from the rest of solution and falls to the bottom of mold.



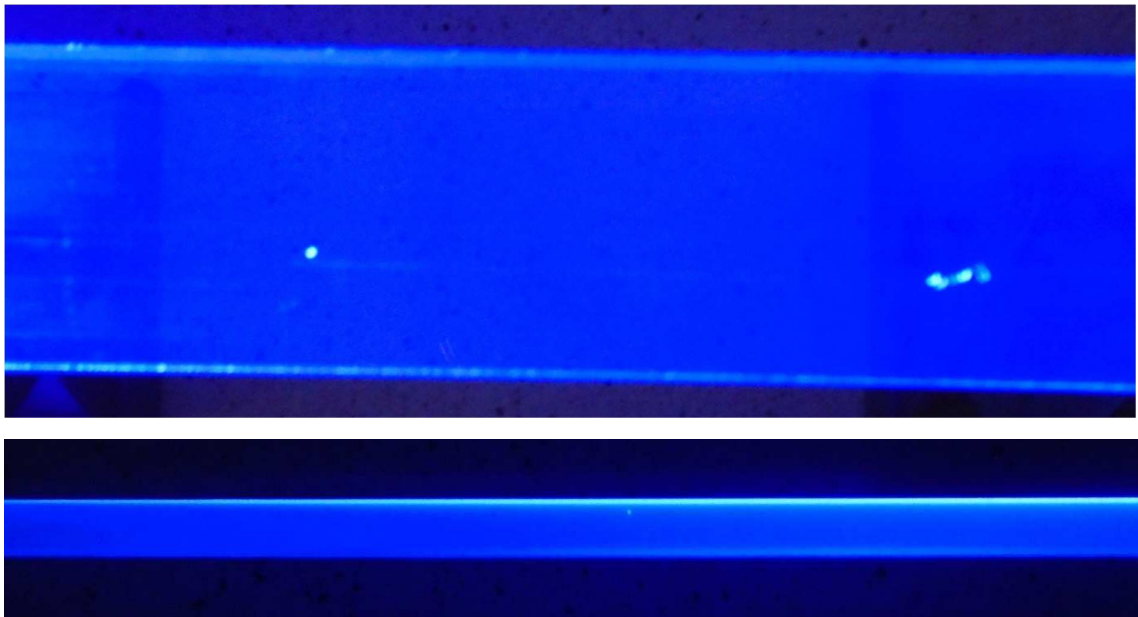
**Figure 32. Strips with surface defects as seen under UV light: mat surface visible under UV light – many small glowing spots and haze; probably microcracks from manufacturing process**



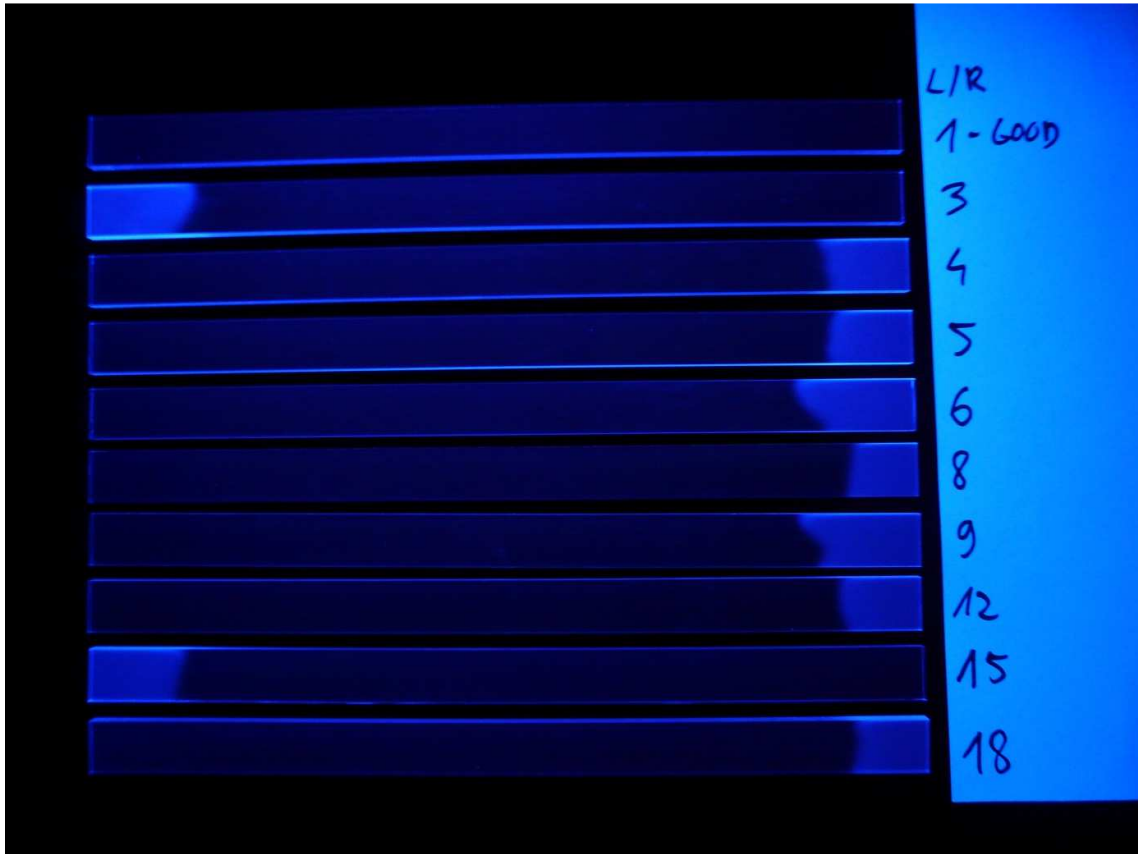
**Figure 33. Strips with surface defects seen under UV light: stains – glowing areas with random shapes; probably from sticky removable plastic foil or damages from mold surface**



**Figure 34. Strips with surface defects: transparent mark or watermark at one end of strip, barely visible curved line on surface under UV light (left) and under ambient light (right)**



**Figure 35. Strips with surface defects seen under UV light: white spots on surface or in volume of strip; some dust or contamination during manufacturing process**



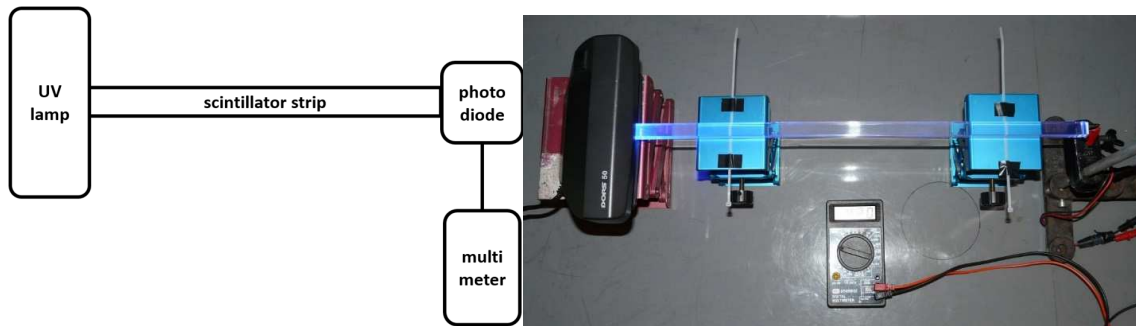
**Figure 36. BC-420 strips with rectangular cross-section  $5 \times 19 \times 500 \text{ mm}^3$  with volume defects under UV light. A strip without defects (labeled as 1) is shown for comparison.**

Optical properties were measured in third test. Scintillation strips were illuminated from one side (50 mm area from edge) by UV lamp and resulting blue light was read with photodiode at the second side (Figure 37). The photodiode converts the incoming light into electric pulses which amplitudes were measured by means of multimeter. Every strip was examined two times with photodiode coupled to the left and right side.

In measurement the following equipment was used:

- standard UV lamp for banknotes checking with Philips TL 4W/08 F4T5 BLB fluorescent lamp with 365 nm wavelength of maximum emission [170];
- laser pointer with 405 nm wavelength of maximum emission and 5 mW output power;
- silicon PIN photodiode S3590-06 from Hamamatsu [171];
- digital multimeter DT-830BUZ;
- 4 jacks.





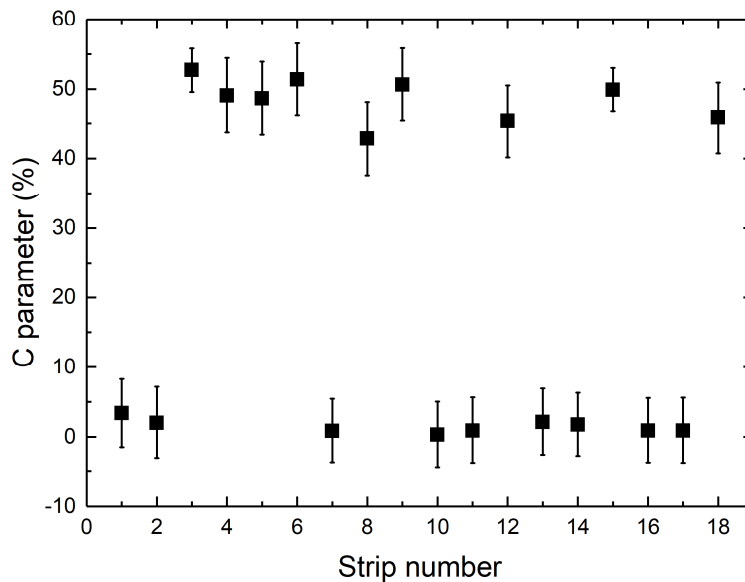
**Figure 37. Scheme of the experimental setup (left) and its photograph (right) used in quality assurance measurements**

A fractional changes of the voltage measured on left and right side can be used as a measure of the scintillator optical inhomogeneity:

$$C = \frac{|V_L| - |V_R|}{0,5 * (|V_L| - |V_B| + |V_R| - |V_B|)} * 100\% \quad (1)$$

where  $V_L$ ,  $V_R$ ,  $V_B$  denotes voltage measured on left side, right side and background voltage respectively.  $V_B$  was read out without plastic scintillator in experimental setup.

The value of  $C$  determined for eighteen tested scintillators is shown in Figure 38. The figure indicates that the values of  $C$  form two well separated regions grouped around 2% and 45%. This gives us possibility for univocal identification of scintillators with optical inhomogeneity.



**Figure 38. C parameter for all BC-420 (5x19x500 mm<sup>3</sup>) strips measured in quality control. Values of C parameter about 45% indicate optical inhomogeneity in strips.**

The big difference (more than 20% value of C parameter) of amplitudes measured at both ends indicates presence of some defects in scintillators volume. This method detects only defects in volume of scintillator. Strips with heterogeneities in optical properties and with not symmetrical response from left and right side were excluded from further research.

Optical test for wavelength shifter (WLS) bars was performed with the same setup except UV lamp that was replaced with laser pointer. UV lamp with optical filter cut off UV light at 380 nm and does not match WLS with absorption peak around 420 nm. Instead laser pointer was used with 405 nm emission wavelength (blue light) that overlaps absorption spectrum of WLS bar. Pointer was set perpendicularly to WLS bar at 10 mm from the end of the bar (Figure 39). Every bar was examined two times with photodiode coupled to the left and right side.



**Figure 39. Photograph of experimental setup used in measurement for wavelength shifter bars: top view (left) and side view (right)**

Results obtained from measurements with photodiode and UV lamp were cross-checked using alternative method. For two strips: one classified with UV lamp test as 'good' and one as 'bad', amplitude spectra of signals registered irradiating the scintillator in the middle of the strip with collimated beam from  $^{22}\text{Na}$  radioactive source were measured, see Figure 40. Two photomultiplier tubes (PMT) R5320 from Hamamatsu were used. For signal analysis LeCroy Waverunner LT375 oscilloscope was used. Na-22 source emits gamma quanta with two different energies: 511 keV originate from annihilation of positron with electron and 1.274 keV coming from deexcitation of neon. Reference detector was employed with appropriate oscilloscope settings to get rid of higher energy gamma quanta.

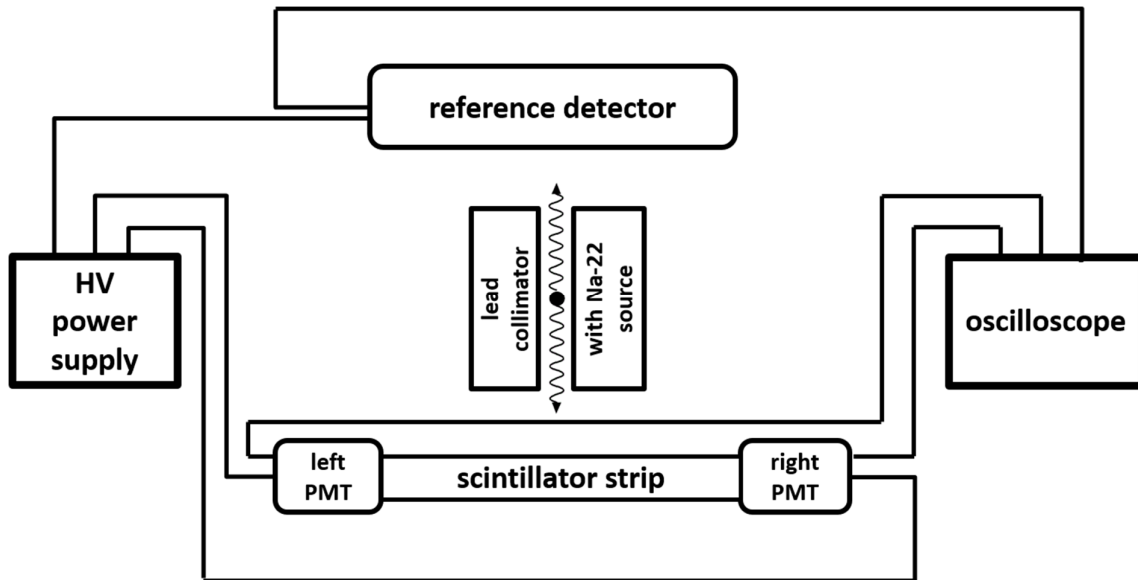


Figure 40. Scheme of setup used in plastic scintillator strip quality control experiment. HV denotes high voltage, PMT is photomultiplier tube and Na-22 is sodium-22 gamma radiation source.

Radiation was collimated in the middle of the strip, thus the amplitude spectra measured on both sides should be the same. Figure 41 shows these spectra for strips labelled as 14 and 18 (in Figure 38). For strip No. 14 amplitude spectra measured at the left and right side of strip are equal (spectra are equal within 10% error as expected from the gain variation of the photomultipliers), so this strip has no any optical defect. Comparison of spectra from strip 18 shows big difference in signal amplitudes obtained from left and right side, which indicates optical defect in one side.

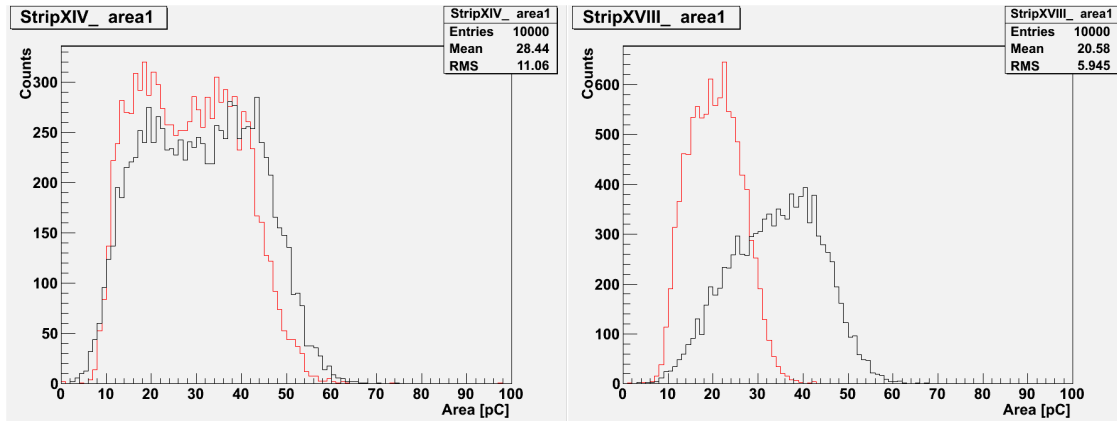
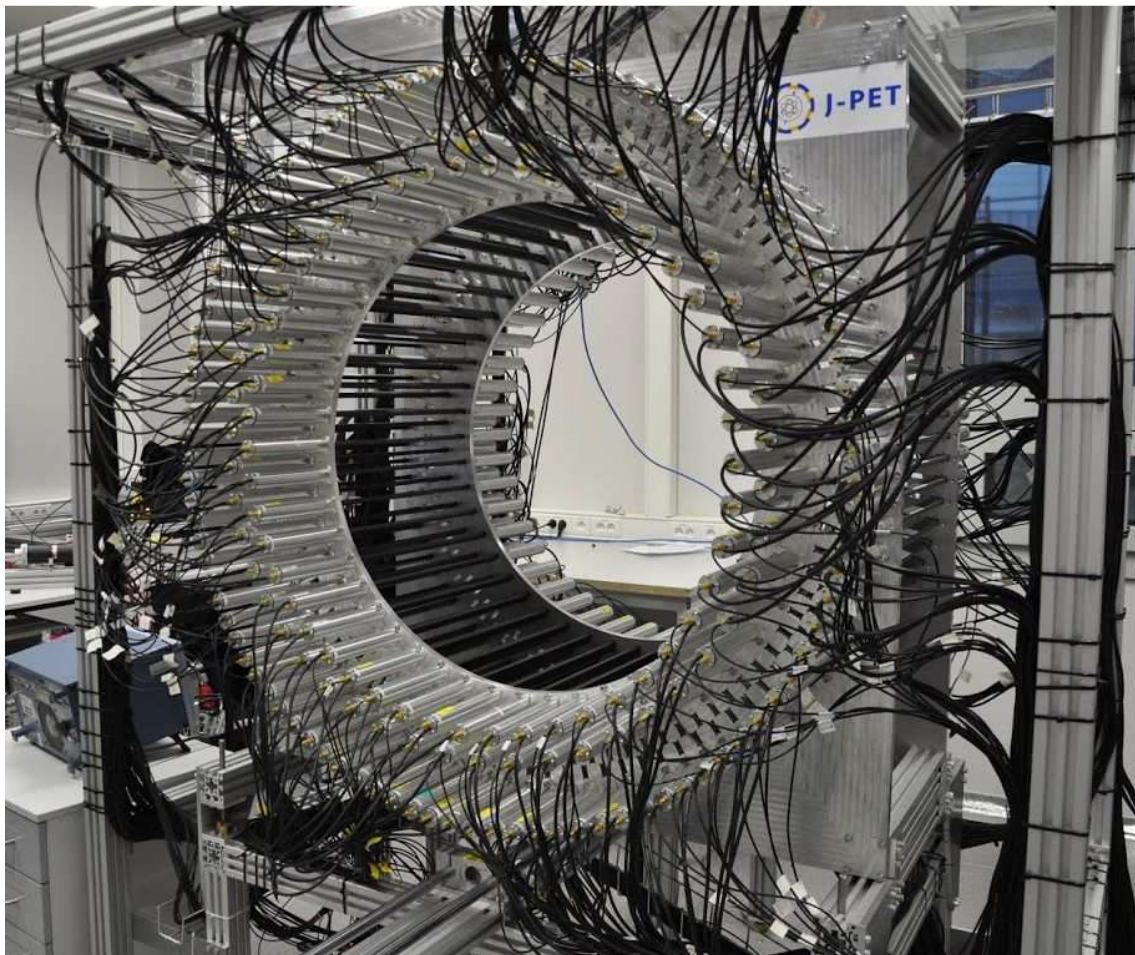


Figure 41. Comparison of charge spectra of signals from strips no 14 (left) and 18 (right). On the vertical axis is number of counts, on the horizontal axis is area under signals registered form radiation detector made from measured scintillator and photomultiplier. Red and black curves denote signals from left and right photomultipliers, respectively [172].

A developed method was used for the tests and quality control of 250 plastic scintillator strips of EJ-230 purchased for the construction of the first J-PET tomograph prototypes and 380 strips of BC-404 purchased for the construction of the new modular J-PET tomograph with the SiPM readout. The method allowed to make the test within few days. It occurred to be extremely important because out of 380 strips delivered by the producer Saint-Gobain Crystals 41% were found to be wrong and were send back to the company for the replacement. The first full scale J-PET tomograph built from the plastic scintillators [173] with the significant contribution of the author of this thesis is shown in Figure 42.



**Figure 42. Photo of the J-PET scanner prototype. The active inner part of the detector has a cylindrical shape with the length of 500 mm and diameter of 850 mm. The J-PET tomography scanner is made of three layers of plastic scintillator strips wrapped with the Vikuiti specular foil covered with an additional light-tight foil (black strips). The scintillators are optically connected at two ends to Hamamatsu R9800 vacuum tube photomultipliers in aluminum housing (gray pipes).**

## 7. Measurement of plastic scintillators optical properties

The aim of this research was to synthesize polystyrene scintillator with the best possible composition of the fluorescent additives in polystyrene scintillator for the detection of gamma radiation in J-PET scanner. Light output of developed scintillators should be high relative to stilbene crystal with not worsened of other parameters like decay time and light attenuation length. Equally important parameter is to match wavelength of maximum emission of polystyrene scintillators with maximum of quantum efficiency of light detectors used in J-PET scanner.

Fluorescent compounds for polystyrene scintillator synthesis were selected from many common fluorescent substances used in plastic scintillator manufacturing. In Table 4 and Table 5 can be found list of primary and secondary additives. From such group the best fluorescent substances were selected with highest fluorescence quantum yield close to 1.0 and shortest decay time with value less than 2 ns. As primary additive PPO, PTP and BPBD were selected and as the secondary additive (wavelength shifter) POPOP, DM-POPOP and bis-MSB were selected. Mentioned wavelength shifters were used because they have maxima of emission spectra around 430 nm. Wavelength of maximum emission in that region is well matched with highest quantum efficiency of light detectors used in first J-PET scanner prototype. Vacuum photomultiplier tubes have usually maximum quantum efficiency around 400 nm [174].

High fluorescence quantum yields of chosen substances ensure efficient conversion of energy from polystyrene to primary additive, from primary additive to wavelength shifter and finally efficient light emission by wavelength shifter (see energy transfer mechanism in Figure 4 and Figure 5). Emission spectra of primary additives are matched with absorption spectra of wavelength shifters like in case in Figure 7. Matching of these spectra are needed also for efficient energy transfer between used fluorescent substances. Short decay time of manufactured polystyrene scintillators are needed for achieving good resolution in novel time of flight J-PET scanner. Concentration of selected fluorescent additives was chosen based on literature review in chapter 2.6. Optimal concentration of primary additives is around 2 wt% and for wavelength shifters it is about 0.06 wt%.

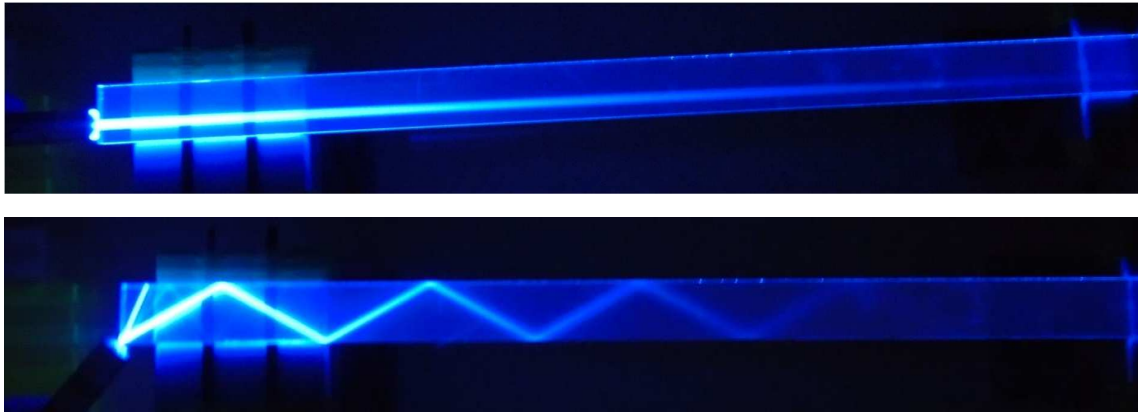


## 7.1. A method for light attenuation length measurement

The scintillation material for the time of flight (TOF) systems must have an attenuation length at least at the same order as the length of the scintillator. Time resolution depends on the number of photons arriving to the photomultipliers. Large attenuation length with respect to the length of the scintillator strip ensures that the photon statistics at the edges of the scintillator does not vary strongly as a function of the interaction position. Technical attenuation length (TAL) measurement is also important during verifying that the attenuation length of each scintillator meets the required specifications.

Light propagation in plastic scintillators may be characterized by light attenuation lengths BAL and TAL. Bulk attenuation length (BAL) depends on the material of scintillator. Technical attenuation length (TAL) depends on the geometry of the scintillator. The transparency of the scintillator material is determined by the so-called bulk attenuation length (BAL) – the scintillator's length which reduces the initial light intensity by factor  $e$  according to the Beer–Lambert law [95]. Initial light intensity drops from 100% to 36.8% after passing BAL inside plastic scintillator volume. The phenomenon of light attenuation is visualized in Figure 43.

The technical attenuation length (TAL) of a plastic scintillator bar is defined as the length of scintillator reducing the light signal by a factor of  $e$  and depending upon bulk transmission of the scintillator, its thickness, shape and reflective properties of the surfaces [95]. The use of light guides and reflectors also can alter the measured technical attenuation length of a plastic scintillator.



**Figure 43. Light propagation in rectangular shaped BC-404 plastic scintillator strip (6x24x500 mm<sup>3</sup>). Visual comparison of bulk attenuation length where light goes straight through strip (upper photo) and technical attenuation length where light reflects many times at polished strip surfaces (bottom photo). Plastic scintillator strip was illuminated by blue laser pointer.**

Measured TAL is strongly influenced by geometry of the plastic scintillator. For example the effect of thickness on the measured TAL is demonstrated by the following data on 120 mm wide and 2000 mm long sheets of BC-408 taken from Saint-Gobain

brochure [30]: for 5 mm thick scintillator the TAL = 1900 mm, for 10 mm thick TAL = 2100 mm, and for 20 mm thick TAL = 2750 mm. This data was taken using a 50 mm diameter bi-alkali photomultiplier tube coupled to one end of the scintillator by a light guide and with the opposite end of the scintillator blackened. In actual practice, however, the far end is not blackened resulting in much better light collection performance and bigger TAL value.

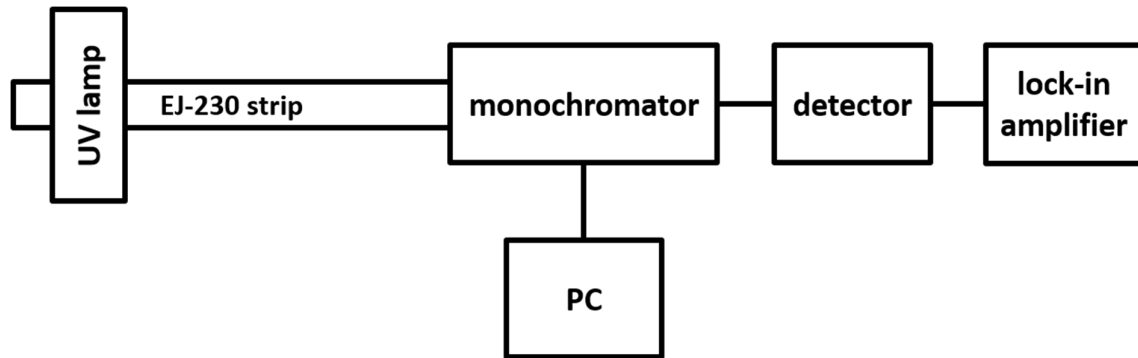
In addition it is important to stress that the attenuation of light depends on the wavelength of photons and so the energy spectrum of photons will change while they propagate through the scintillator.

The aim of this work was to determine how the emission spectrum at the edge of the EJ-230 plastic scintillator strip changes with the distance of the excitation point to the edge. Measured scintillator was polished at all sides and was not covered by any reflecting foil.

Following equipment was used in this measurements:

- plastic scintillator strip EJ-230, dimensions: 5x19x500 mm<sup>3</sup>
- monochromator Oriel Cornerstone 260 1/4 m
- grating between monochromator and scintillator Dual Grating Assemblies 74163
- amplified UV Silicon Photodetector Newport 71889
- UV light lamp Spectroline ENF-260C/FE
- lock-in amplifier
- personal computer, PC.

EJ-230 strip was connected through the grating and monochromator to the silicon detector, see Figure 44. Scintillator was excited by UV lamp (365 nm) covered by aluminum foil and black tape with 2x20 mm<sup>2</sup> slot. Lamp was moved along the strip in 50 mm steps. Monochromator let through only small range of emitted spectra (1 nm) and collected results were in 5 nm steps. Monochromator and detector were controlled by computer. For each wavelength interval an output voltage from detector read by amplifier was measured.

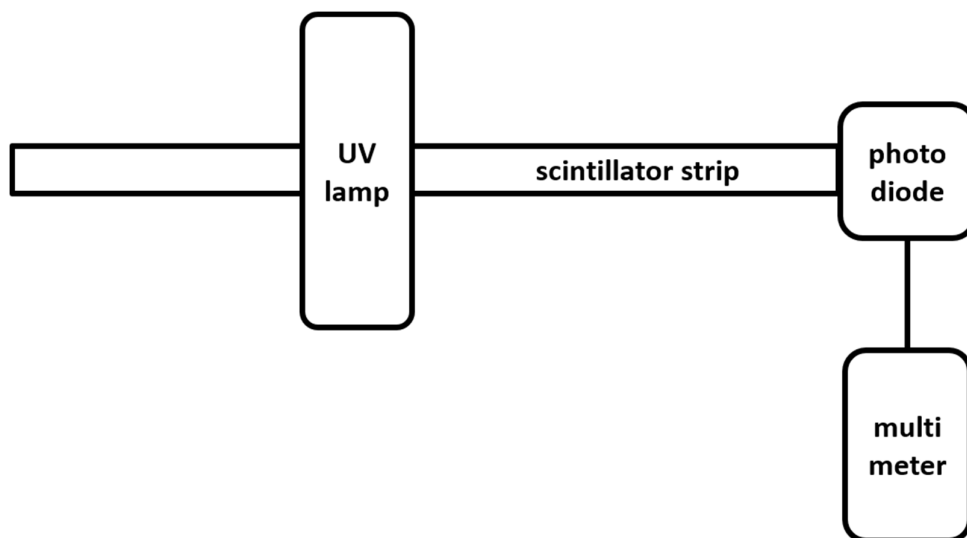


**Figure 44. Scheme (upper panel) and photo (lower panel) of the experimental setup used in measurement of emission spectra of 5x19x500 mm<sup>3</sup> EJ-230 plastic scintillator strip. UV lamp exciting scintillator was moved along the scintillator strip. Numbers on lower panel photo denote 1 scintillator, 2 UV lamp, 3 monochromator, 4 detector, 5 lock-in amplifier, 6 PC to control the monochromator [175].**

In order to measure light attenuation length of large number of different plastic scintillator strips faster method was used. Experimental setup (see Figure 45) consisted of:

- standard UV lamp for banknotes checking with 365 nm wavelength of maximum emission [170];
- UV lamp with 311 nm wavelength of maximum emission;
- UV lamp with 254 nm wavelength of maximum emission;
- silicon PIN photodiode S3590-06 from Hamamatsu [171];
- digital multimeter DT-830BUZ;
- 4 jacks.





**Figure 45. Scheme of experimental setup used in light attenuation length measurement of plastic scintillator strip. UV lamp exciting scintillator was moved alongside to the scintillator strip.**

UV lamps with different wavelengths of maximum emission were selected to match with absorption spectra of fluorescent additives used in plastic scintillators. Most of the fluorescent compounds in organic scintillators with blue light emission have absorption spectra from 230 to 400 nm, see Table 4, Table 5 and Figure 7.

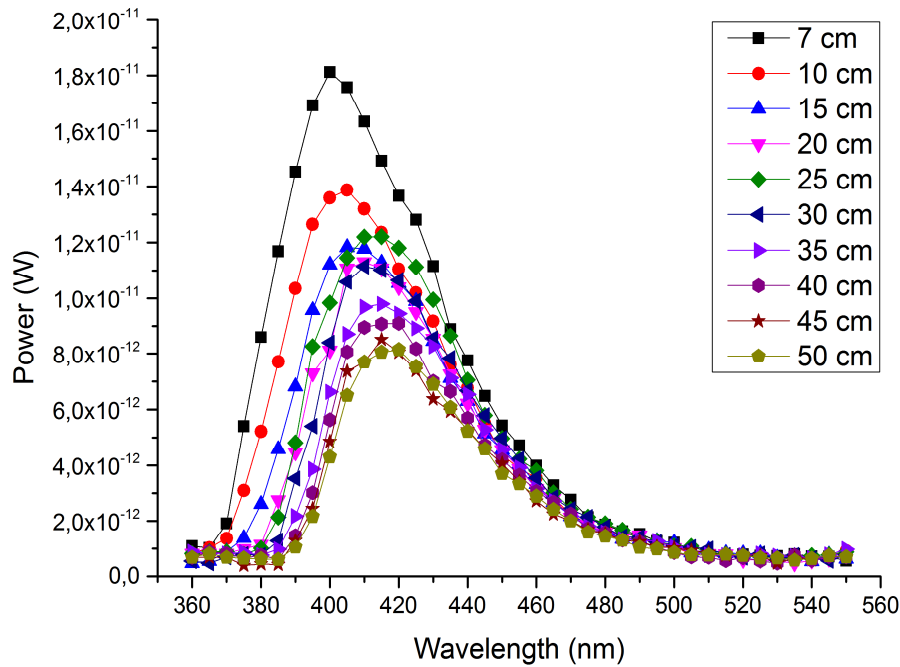
Plastic scintillator strip was connected to silicon PIN photodiode. Scintillator was excited by UV lamp with wavelength of maximum emission at 254 or 311 nm covered by aluminum foil and black tape with 5x20 mm<sup>2</sup> slot. UV lamp was moved along the strip in 20 mm steps. Light reflecting inside the strip was converted to voltage by silicon photodiode. Voltage was read out by multimeter.

Plastic scintillators in shape of strip allow to measure light attenuation length - the length of scintillator reducing the light signal by a factor of  $e$ . Few commercial plastic scintillator strips were tested before use of them in J-PET scanner prototypes.

Light attenuation length is composed of mainly two components accounting for the absorption of short-wavelength UV light component and long-wavelength blue light component [176]. Light attenuation length in scintillator strip depends on wavelength of light [11]. In emission spectrum of typical plastic scintillator light photons are emitted at wavelengths from 360 nm to 500 nm. If light is traveling in scintillator then UV light is more attenuated in scintillator bulk material than blue part of its spectrum. Maximum of emission spectra is shifted to the longer wavelengths as light length path in scintillator increases. This phenomenon is associated with higher absorption of shorter wavelengths ( $< 400$  nm) by polymer and with partially light absorption of fluorescent compound in plastic scintillator caused by overlapping of absorption and emission spectra of this fluorescent additive.

Obtained results from emission spectra measurements described in Figure 44 were corrected for responsivity factor of silicon detector. Corrected spectra are shown

in Figure 46. Intensity of light reaching to detector is proportional to the power from detector in watt unit because area of which light come from scintillator to monochromator and detector is constant ( $5 \times 19 \text{ mm}^2 = 95 \text{ mm}^2$ ). Scintillator was placed few centimeters from grating and only unknown part of light from scintillator reaches to detector. However, since the conditions were the same for each position we may assume that the intensity of light for each position was reduced by the same factor allowing for the determination of the light attenuation coefficients as a function of the wavelength.



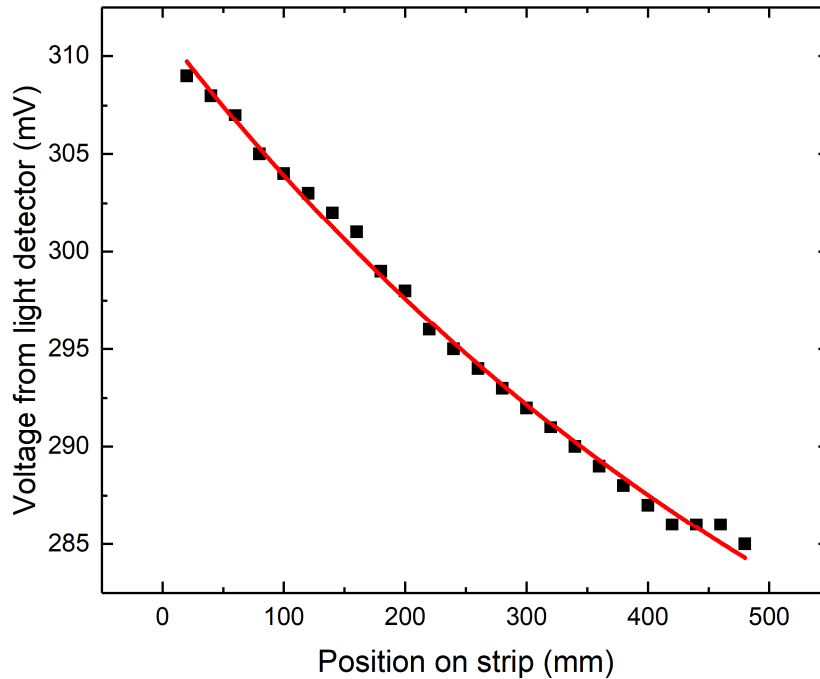
**Figure 46. Emission spectra of  $5 \times 19 \times 500 \text{ mm}^3$  EJ-230 strip determined using experimental setup shown in Figure 44. Subsequent points from 7 cm to 50 cm denote distance between UV lamp excitation point and light detector.**

One can see that as path length between UV lamp and detector is increased, not only a decrease in the spectrum intensity but also the rapid degradation of its short-wave part is observed. Maximum of spectra shifts to the longer wavelength. The reason of the observed effect is rapid increase in absorption in the short-wave part of the emission spectrum.

Effectively, the intensity of light traveling through plastic scintillator follows a relation of the form of sum of two exponential functions [177] given by the formula:

$$I(x) = C_1 * e^{\left(\frac{-x}{\lambda_1}\right)} + C_2 * e^{\left(\frac{-x}{\lambda_2}\right)} \quad (2)$$

where  $\lambda_1$  and  $\lambda_2$  are long and short components of light attenuation lengths, respectively. TAL was measured with experimental setup shown in Figure 45. Example of fitted function to experimental point is shown in Figure 47. Summarized results from TAL measurement are in Table 11.



**Figure 47. Function given by formula (2) fitted (red line) to experimental points for EJ-230 strip with dimensions 14x14x500 mm<sup>3</sup>. Measurement with UV lamp with 254 nm emission maximum.**

**Table 11. Technical attenuation length of selected plastic scintillator strips**

Scintillator strip and its dimensions in mm <sup>3</sup>	TAL measured by producer [mm]	TAL measured in this experiment [mm]	
		UV lamp 254 nm	UV lamp 311 nm
EJ-230 5x19x500	1200	483.1±1.4	301.7±1.6
EJ-230 14x14x500	1200	647.1±5.3	787.5±2.6
BC-404 6x24x500	1600*	842.9±1.4	324.6±77.6
RP-408 14x14x500	4000	-	1152.9±6.1

\* BAL

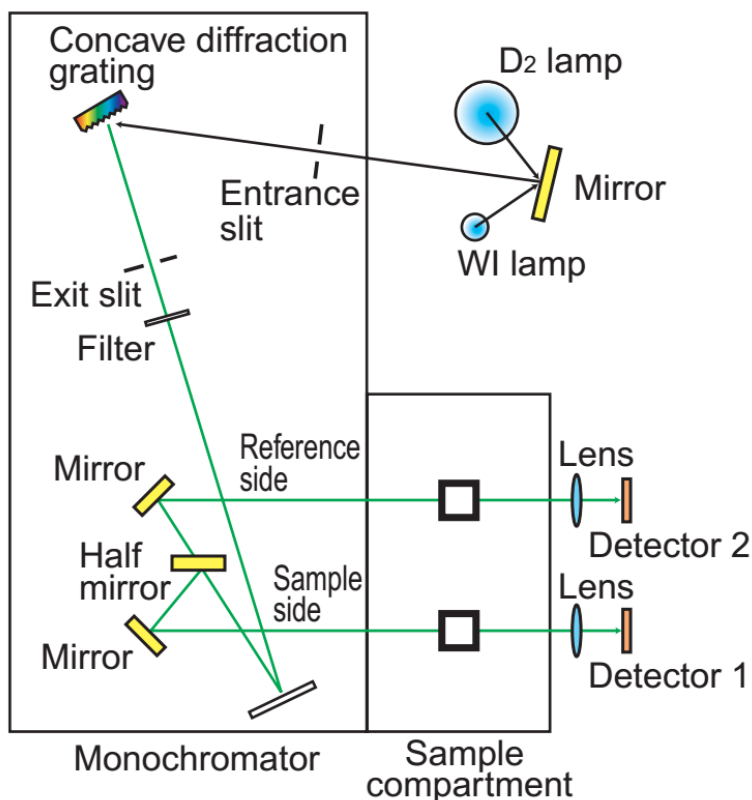
Obtained results of TAL measurement depend strongly on the wavelength of the light emitted by the UV lamp used in experimental setup. Received values of TAL are smaller than TAL measured by plastic scintillators given by manufacturers. Smaller value of TAL in plastic scintillator strips results from the more light reflection in small strip. Light emitted by scintillator reflects on surfaces more times in small strip than thick plate or block. Imperfections on surface may cause light scattering and smaller part of light emitted at excitation point reaches to the photodetector.

Outcome of TAL measurement conducted in this research can be compared to results from two doctoral dissertations [177] and [178]. EJ-230 and BC-420 are commercial equivalents manufactured by two independent companies and they have similar optical properties. In both mentioned thesis BC-420 plastic scintillator strips with rectangular cross-section and dimensions  $5 \times 19 \times 300 \text{ mm}^3$  and  $5 \times 19 \times 250 \text{ mm}^3$  were measured. Scintillators were wrapped in Vikuiti specular reflective foil. Measurements were done with use of Na-22 radioactive gamma source and two vacuum photomultiplier tubes connected at both ends of the scintillator strip. Two values of TAL originate from left and right photomultiplier tubes measurements. For 300 mm long BC-420 scintillator long components of TAL are  $370 \pm 5 \text{ mm}$  and  $377 \pm 7 \text{ mm}$ . For 250 mm long BC-420 scintillator long components of TAL are  $492 \pm 60 \text{ mm}$  and  $308.6 \pm 8.2 \text{ mm}$ . Big differences in TAL values obtained in the quoted works suggest that TAL measurement is very sensitive to the experimental conditions. However, it is important to stress that the results for EJ-230 and BC-420 scintillators obtained in this and previous work are comparable.

Factors that contribute to technical attenuation length of plastic scintillator sheets and strips are: bulk transmission of the material, thickness and shape of the sheet and reflective properties of the surfaces. The use of light guides and wrapping scintillator in different reflective foils also can alter the measured TAL of a plastic scintillator. Type of used light detectors: photomultiplier tube or silicon photodiode also can influence on TAL results measurement because these two kind of detectors have different quantum efficiency for light detecting. Choice of gamma radiation source for plastic scintillator excitation will give different results because gamma radiation reacts directly with polymer and UV lamp excites fluorescent additives in plastic scintillator. UV sources in experimental setup also affect TAL results because of its different emission spectrum maxima which excite different part of absorption spectra of fluorescent compounds inside plastic scintillator.

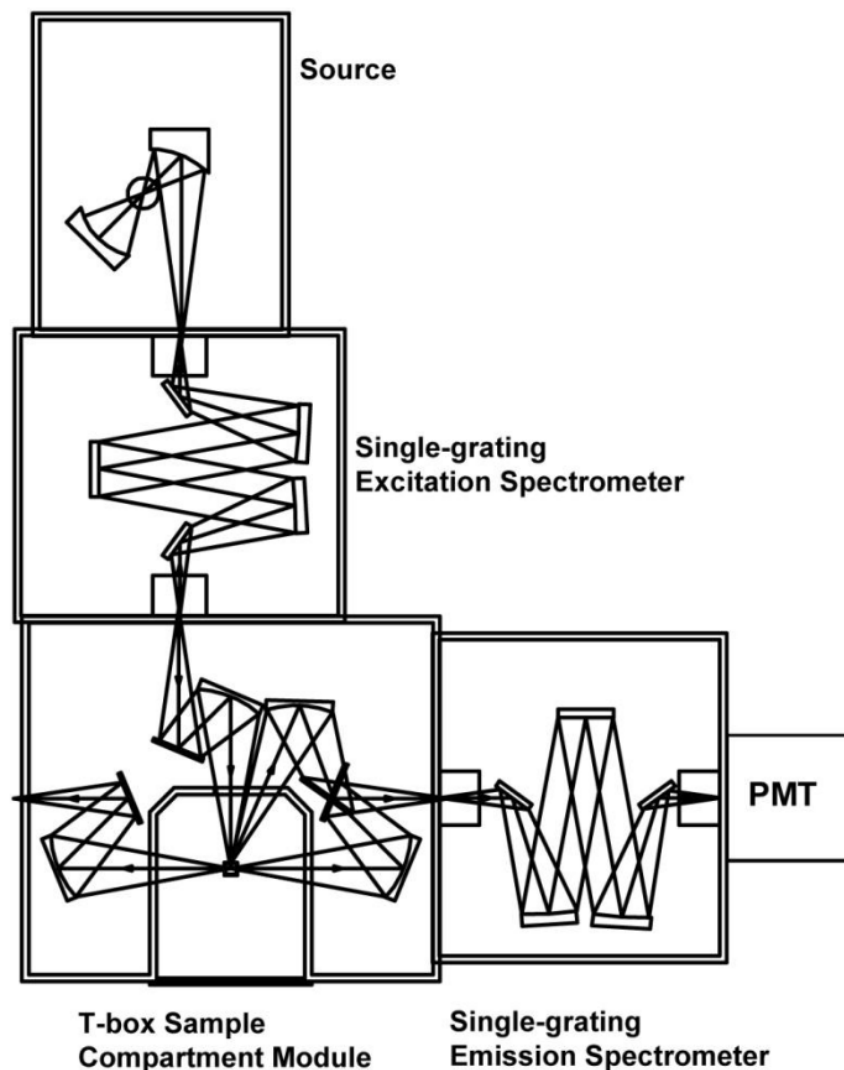
## 7.2. Emission spectra

Emission spectra of primary and secondary solutes in toluene were measured with Hitachi double beam spectrophotometer U-2900, see Figure 48. Concentration of fluor was  $10^{-6}$  mol. As is described in details in [179] the beam of light is filtered by an excitation monochromator and it is divided into two with a half mirror so that one passes through the reference side, and the other through the sample. Sample responds to the incoming light from lamp resulting in fluorescent light emission registered by detector.



**Figure 48. Scheme of double beam U-2900 spectrophotometers optics. D2 is deuterium lamp and WI is tungsten lamp. The figure is adapted from [179].**

Photo-induced emission spectra were measured using Horiba Jobin-Yvon FluoroLog-3 spectrofluorometer, see Figure 49. The light source is generally a high-pressure xenon arc lamp, which offers the advantage of continuous emission from about 250 nm to the infrared. A monochromator is used to select the excitation wavelength. Fluorescence is collected at right angles with respect to the incident beam and detected through a monochromator by a photomultiplier. Automatic scanning of wavelengths is achieved by the motorized monochromators, which are controlled by the electronic devices and the computer [180].



**Figure 49. Scheme of FluoroLog-3 spectrofluorometer optics. PMT is photomultiplier tube light detector. The figure is adapted from [181].**

The emission signal was detected using a PMT R928P (Hamamatsu Photonics). Measurement was done in reflecting mode. Plastic scintillators samples disc with diameter 25 mm and 2 mm thickness were excited on surface by continuous wave xenon source with monochromator located at 45 degree from the normal to the surface. Emission light was collected by photomultiplier tube (PMT) at the opposite side of surface at the same angle.

Table 12 contains results from measurement of emission maxima of fluorescent additives in toluene, polystyrene and in polystyrene scintillators.

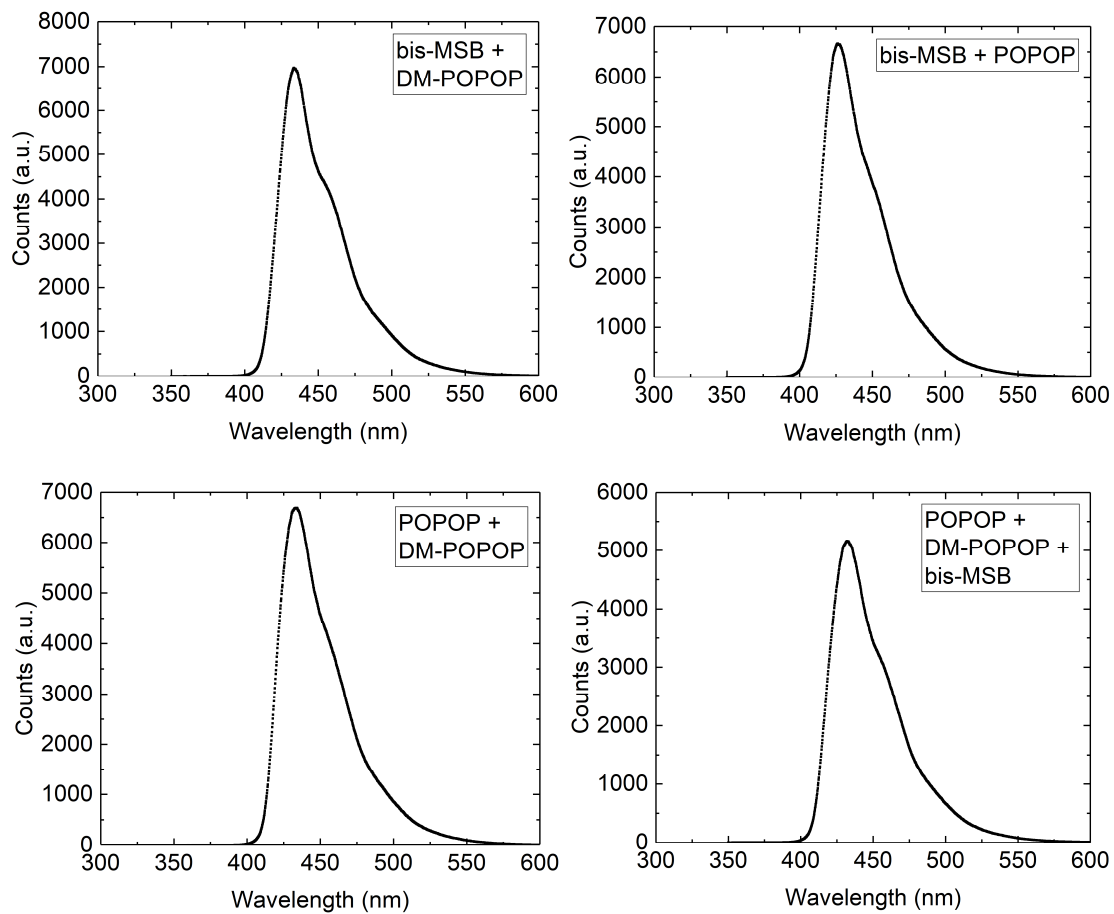
Emission maxima of fluorescent substances in polystyrene are shifted to the longer wavelength comparing to emission maxima in toluene solution. Short wavelengths of emission spectra are more attenuated in polystyrene matrix and left part of spectra is cut. Overlapping of wavelength shifters emission spectra causes

small difference of maxima of emission spectra of polystyrene scintillators with mixtures of wavelength shifters.

**Table 12. Emission maxima of fluorescent additives in toluene solution, pure polystyrene and in polystyrene scintillator**

<b>Compound</b>	<b>Emission maximum in toluene [nm]</b>	<b>Emission maximum in pure polystyrene [nm]</b>	<b>Emission maximum in polystyrene scintillator [nm]</b>
PPO	364	430	-
PTP	344	344	-
BPBD	365	363	-
POPOP	418	479	422
DM-POPOP	430	497	435
bis-MSB	423	464	429
POPOP + DM-POPOP	-	-	434
bis-MSB + POPOP	-	-	423
bis-MSB + DM-POPOP	-	-	433
POPOP + DM-POPOP + bis-MSB	-	-	433

Spectra obtained for all substances listed in Table 12 are given in Appendix A. Here, as an example only emission spectra of mixed secondary fluorescent additives in polystyrene scintillator are shown in Figure 50.



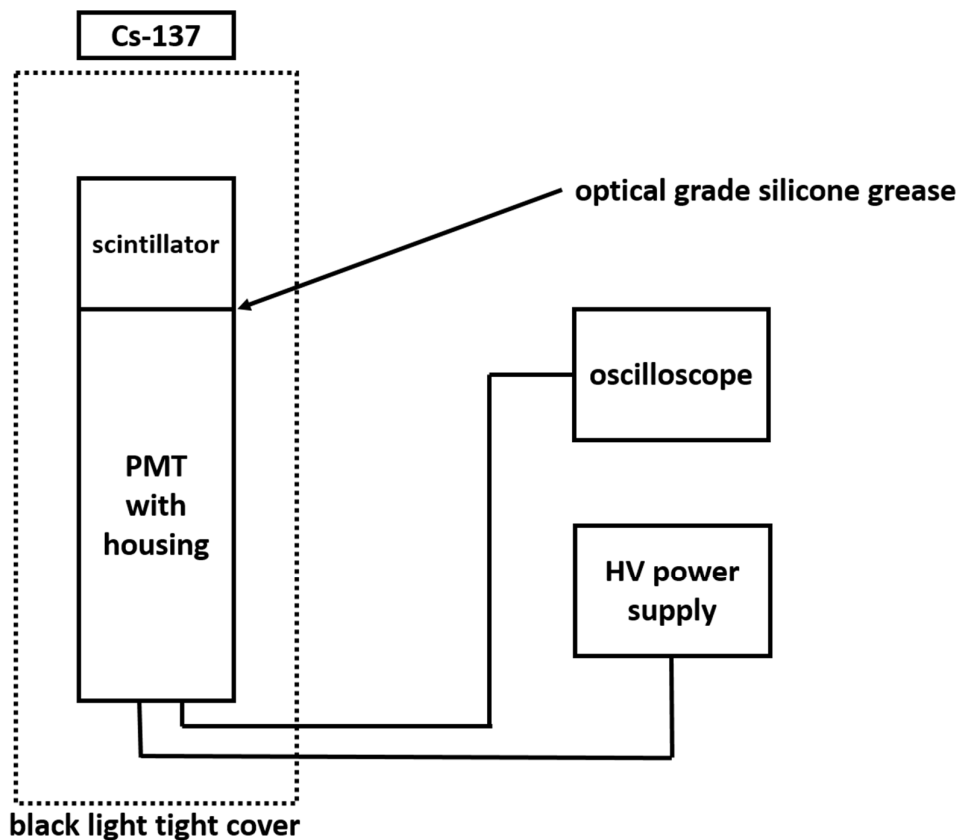
**Figure 50. Emission spectra of mixed secondary fluorescent additives in polystyrene scintillator**



### 7.3. Relative light output

Light yield or light output is a conversion efficiency of radioactive energy deposited in scintillator into light and is expressed in light photons generated per megaelectronvolt of deposited energy (ph/MeV) by radiation quanta or particle. Comparing light output of produced plastic scintillators to light output of anthracene or stilbene crystal scintillators is known as relative light output.

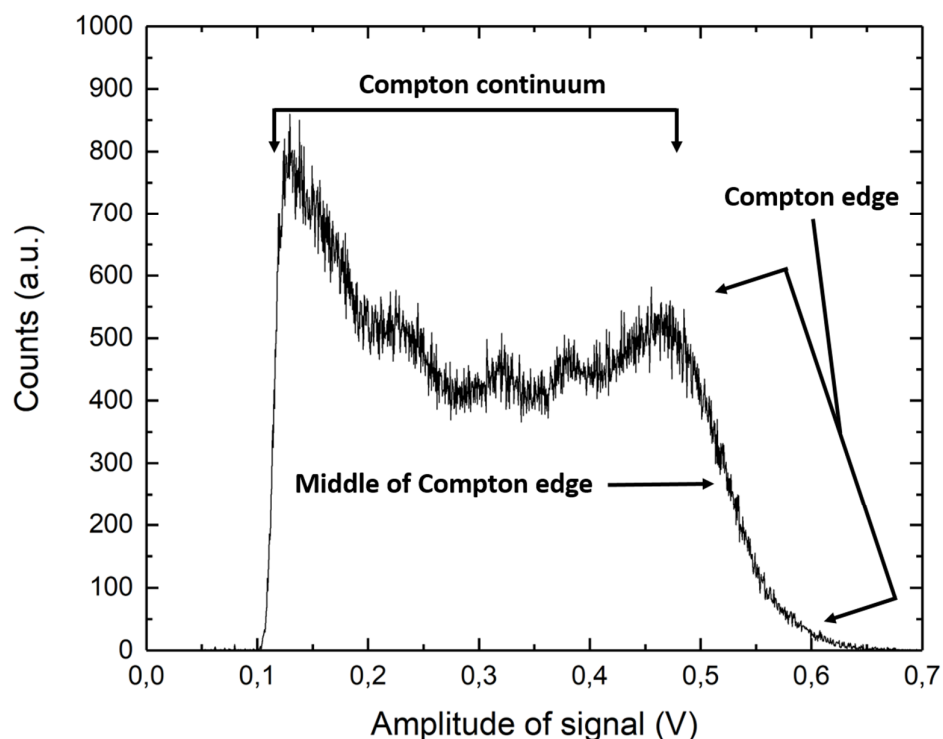
Relative light output, of samples studied in this thesis, was measured with oscilloscope LeCroy SDA 6000A, see Figure 51. Cylindrical shape scintillator samples with diameter 25 mm and height 25 mm (polished all sides) were wrapped with three layers of white Teflon tape and coupled to photomultiplier R5320 (Hamamatsu Photonics) with bialkali photocathode using optical grade silicone grease EJ-550 (Eljen Technology). Radioactive source Cs-137 was placed on top of the black light tight cover. Cesium-137 was chosen because its nuclei decay to an excited state of barium-137 which then emits 0.662 MeV gamma quanta which energy is close to 0.511 MeV as used in the PET scanner measurements.



**Figure 51. Setup for relative light output measurement. PMT is photomultiplier tube, Cs-137 caesium-137 gamma radiation source, HV high voltage.**

Amplitude spectra from synthesized polystyrene scintillator samples were compared with spectra obtained from stilbene crystal [32] of the same shape and sizes, whose light yield was taken as 100%. Positions of middle of Compton edges for

stilbene crystal and measured polystyrene scintillators were compared to obtain relative light output, see Figure 52.



**Figure 52. Amplitude spectrum of Cs-137 gamma source measured by radiation detector with polystyrene scintillator as described in Figure 51. Amplitude of signal is proportional to energy deposited by gamma quanta in plastic scintillator. Cut off at beginning of the spectrum is caused by trigger set in oscilloscope.**

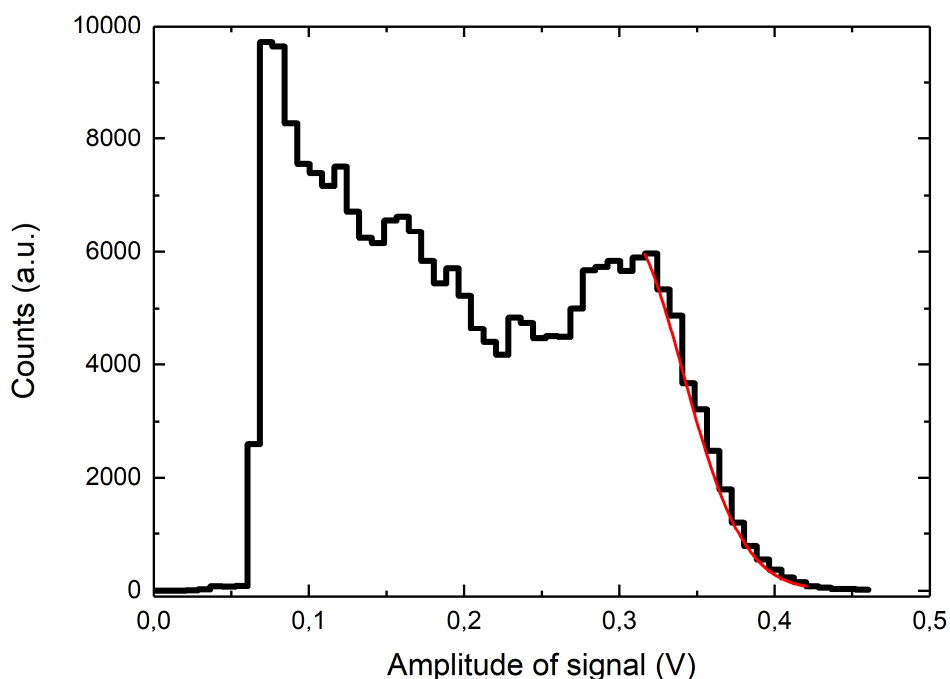
Plastic scintillators consist of low atomic number ( $Z$ ) elements like carbon ( $Z = 6$ ) and hydrogen ( $Z = 1$ ). Gamma quanta interact with electrons of low atomic number elements predominantly through Compton scattering and therefore the amplitude distribution is continuous. Photoelectric maximum typical for crystal scintillators with higher average atomic number is not observed in amplitude spectra.

Gamma rays scatter off the plastic scintillator and escape thus only some fraction of its energy is registered by the radiation detector. The amount of energy deposited in the detector depends on the scattering angle of the gamma photon leading to a continuous energy loss spectrum. The highest energy that can be deposited corresponding to full back-scatter is called the Compton edge. Amplitude of signals distribution from plastic scintillators is ended with Compton edge at the right side of spectrum as described in Figure 52.

Light output of manufactured polystyrene scintillators in form of cylinders was determined with respect to known light output of stilbene crystal scintillator with the same shape and dimensions.

The amplitude of registered signals is proportional to the number of scintillation photons which in turn is proportional to the energy transferred by gamma quantum to an electron in plastic scintillator during Compton scattering.

The middle of the Compton edge of each spectrum was determined by fitting the Gaussian function to the right edge of amplitude spectrum, see Figure 53.



**Figure 53. Amplitude spectrum of stilbene crystal (black histogram) registered with Cs-137 gamma radiation source. Superimposed Gaussian function (red line) is fitted at the Compton edge.**

Relative light output (RLO) was calculated as a ratio of the middle of Compton edge positions of tested plastic scintillator ( $MCE_{PS}$ ) sample and stilbene crystal ( $MCE_{stilbene}$ ):

$$RLO = \frac{MCE_{PS}}{MCE_{stilbene}} \times 100\% \quad (3)$$

The ratio is interpreted as the relative light output. Knowing the light output of stilbene crystal 14,000 photons/MeV [32], light output of synthesized polystyrene

scintillators were calculated. Values of polystyrene scintillators relative light output determined using this method are given in Table 13.

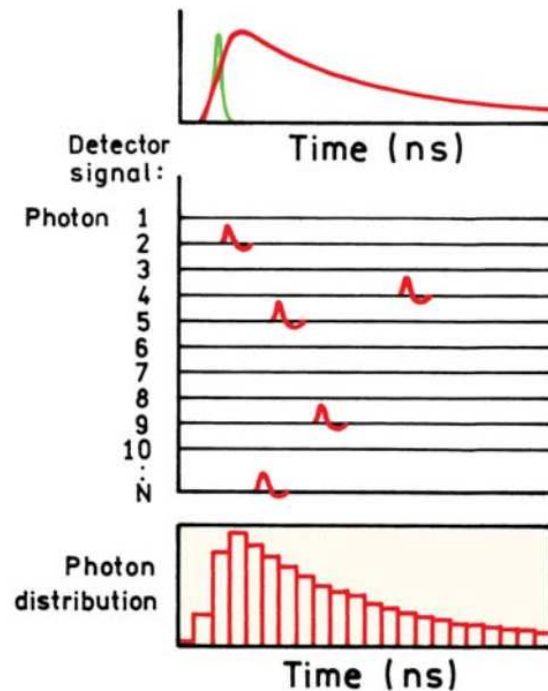
**Table 13. Relative light output of polystyrene scintillators determined with respect to the stilbene crystal scintillator**

Sample No.	Primary solute	Secondary solute	Relative light output [% of stilbene]	Light output [photons/MeV]
1	2% PPO	0.06% POPOP	66.9	9370
2		0.06% DM-POPOP	51.1	7151
3		0.06% bis-MSB	70.1	9809
4		0.03% POPOP + 0.03% DM-POPOP	63.2	8845
5		0.03% DM-POPOP + 0.03% bis-MSB	56.8	7946
6		0.03% bis-MSB + 0.03% POPOP	80.1	11212
7		0.02% POPOP + 0.02% DM-POPOP + 0.02% bis-MSB	76.2	10672
8	2% PPO	0.06% POPOP	66.8	9346
9	2% PTP		68.7	9611
10	2% BPBD		76.9	10772
11	1% PPO + 1% PTP		72.4	10141
12	1% PTP + 1% BPBD		62.3	8727
13	1% BPBD + 1% PPO		73.8	10336
14	0.67% PPO + 0.67% PTP + 0.67% BPBD		70.3	9846

The best chemical composition of polystyrene scintillators are: 2% PPO with 0.03% bis-MSB and 0.03% POPOP; 2% PPO with 0.02% POPOP, 0.02% DM-POPOP and 0.02% bis-MSB; 2% BPBD with 0.06% POPOP.

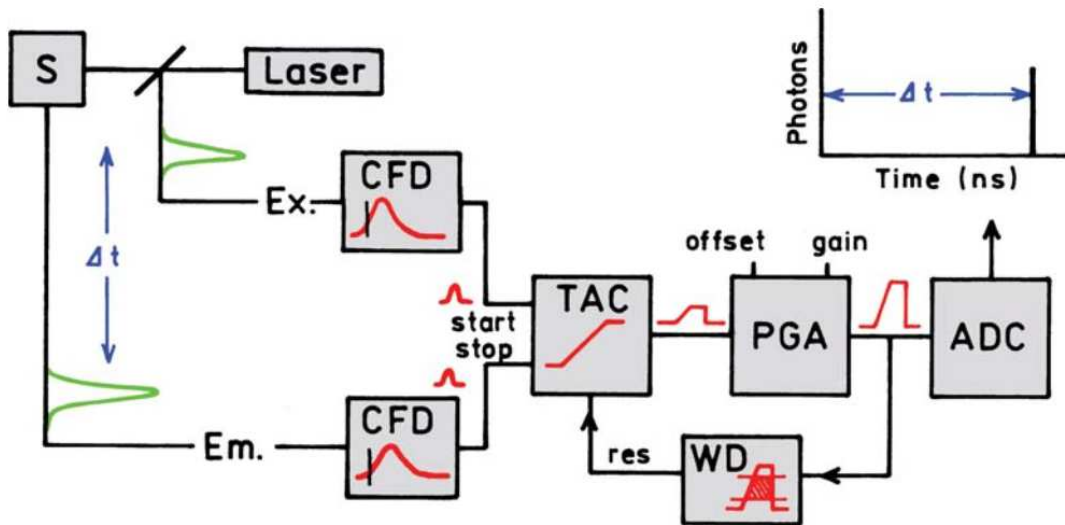
## 7.4. Decay time

Decay time can be roughly defined as time over which the light signal from scintillator decreases to  $1/e$  of its maximum value. To measure decay time of plastic scintillators time-correlated single photon counting (TCSPC) was used. The sample is excited with a pulse of light, resulting in the waveform shown at the top of the Figure 54 when many fluorophores are excited and many photons are observed. However, for TCSPC the conditions are adjusted so that on the average less than one photon is detected per laser pulse. The time is measured between the excitation pulse and the observed photon and stored in a histogram. The x-axis is the time difference and the y-axis the number of photons detected for this time difference [98].



**Figure 54. Principle of TCSPC. The pulses in the middle panel represent the output from a constant fraction discriminator. Green impulse in the upper panel is excitation pulse. The figure is adapted from [98].**

Dedicated electronics are used for measuring the time delay between the excitation and emission in TCSPC measurement (Figure 55). As it is described in reference [98]: the excitation pulse and the pulse from the single detected photon are send to the constant fraction discriminators (CFD) and the difference in time between these pulses is converted by time-to-amplitude converter (TAC) to the signal whose amplitude is proportional to the time delay ( $\Delta t$ ) between the excitation and emission signals. This signal after amplification by programmable gain amplifier (PGA) is digitized by analog-to-digital converter (ADC). The time range of event is limited by the a window discriminator (WD). A histogram of the decay is measured by repeating this process many times.



**Figure 55. Electronic schematic for time-correlated single photon counting.  $\Delta t$  is time delay between the excitation and emission signals (green impulses). The rest of the symbols are explained in the text. The figure is adapted from [98].**

Fluorescence decay time was acquired with spectrofluorometer FluoroLog-3, (Horiba Jobin-Yvon) using NanoLED diode (Horiba Jobin-Yvon) with 340 nm emission maximum and 1.3 ns pulse full width at half maximum (FWHM).

In ternary plastic scintillators the distribution of the time of photon emission followed by the interaction of the gamma quantum at time  $\Theta$ , is given by the following convolution of two exponential and Gaussian terms [182]:

$$f(t) = K \int_{\Theta}^t \left( e^{-\frac{t-\tau}{t_d}} - e^{-\frac{t-\tau}{t_r}} \right) \cdot e^{-\frac{(\tau-\Theta-2.5\sigma)^2}{2\sigma^2}} d\tau, \quad (4),$$

where following symbols denote:

K - normalization constant

$\Theta$  – time of the gamma quantum interaction with scintillator

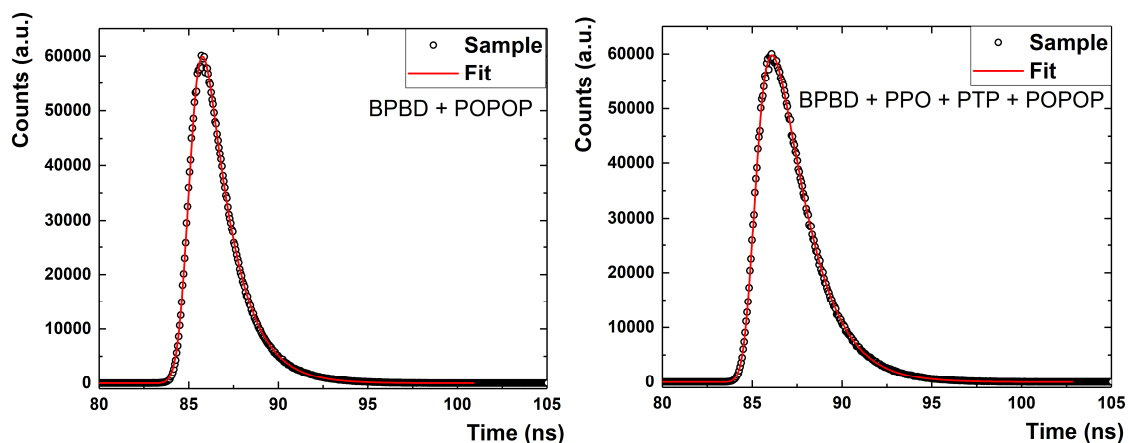
t - time

$t_d$  - decay time of the final light emission

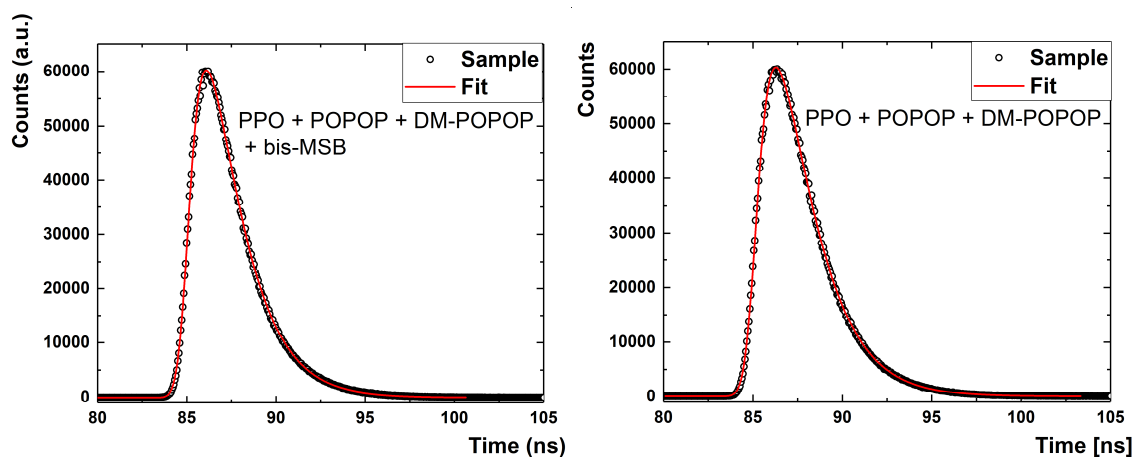
$t_r$  - average time of the energy transfer to the wavelength shifter

$\sigma$  - standard deviation reflects total uncertainty of light emission from scintillator and TCSPC components: excitation diode, photomultiplier tube and electronics.

Decay time was determined by fitting equation (4) to the experimental data with K,  $\Theta$ ,  $t_d$ ,  $t_r$ , and  $\sigma$  treated as a free parameters of the fit [183]. Gaussian part of equation (4) reflects effectively a spread of the signal due to the light emission from scintillator, density distribution of photons emitted by UV diode excitation, transit time spread in photomultiplier tube detector and broadening of the signal due to electronics in TCSPC measurement. The measurement was performed for all investigated compositions (listed in Table 10). Exemplary experimental results (dots) with superimposed lines denoting the result of the fit are presented in Figure 56 and Figure 57.



**Figure 56. Decay time fit for polystyrene scintillators with 2% BPBD, 0.06% POPOP and with 0.67% BPBD, 0.67% PPO, 0.67% PTP, 0.06% POPOP**



**Figure 57. Decay time fit for polystyrene scintillators with 2% PPO, 0.02% POPOP, 0.02% DM-POPOP, 0.02% bis-MSB and with 2% PPO, 0.03% POPOP, 0.03% DM-POPOP**

The determined decay times for the studied samples together with the estimated statistical errors are given in Table 14. Statistical errors were estimated as one standard deviation of the fitted parameter. In addition, systematical errors were estimated as a difference in the determined decay times for two samples prepared with the same fluorescent content. The difference in decay times was found to be smaller than  $\pm 0.05$  ns.

**Table 14. Decay time of polystyrene scintillators obtained after deconvolution of TCSPC measurement**

Scintillator sample composition [wt%]	Decay time [ns]
0.06% POPOP	1.55 ± 0.01
2% PPO + 0.06% POPOP	1.66 ± 0.02
2% PPO + 0.06% POPOP	1.76 ± 0.02
2% PPO + 0.06% DM-POPOP	1.96 ± 0.02
2% PPO + 0.06% bis-MSB	1.62 ± 0.02
2% PPO + 0.03% POPOP + 0.03% DM-POPOP	1.81 ± 0.02
2% PPO + 0.03% POPOP + 0.03% DM-POPOP	1.95 ± 0.02
2% PPO + 0.03% DM-POPOP + 0.03% bis-MSB	1.81 ± 0.02
2% PPO + 0.03% POPOP + 0.03% bis-MSB	1.80 ± 0.02
2% PPO + 0.02% POPOP + 0.02% DM-POPOP + 0.02% bis-MSB	1.80 ± 0.02
2% PTP + 0.06% POPOP	1.59 ± 0.01
1% BPBD + 1% PTP + 0.06% POPOP	1.62 ± 0.02
0.67% BPBD + 0.67% PPO + 0.67% PTP + 0.06% POPOP	1.66 ± 0.02
2% BPBD + 0.06% POPOP	1.51 ± 0.02
1% PPO + 1% PTP + 0.06% POPOP	1.58 ± 0.01
1% PPO + 1% BPBD + 0.06% POPOP	1.87 ± 0.03
1% BPBD + 1% PTP + 0.03% POPOP + 0.03% DM-POPOP	1.71 ± 0.01

The fastest polystyrene scintillator is composition with 2% BPBD primary solute and 0.06% POPOP wavelength shifter. Decay time of this sample is  $1.51 \pm 0.02$  ns. The lowest value of decay time is connected with its composition of only two fluorescent substances. Energy transfer between first and second dyes in samples containing only two fluorescent additives are faster than in other compositions with multiple of dyes.

Other sample with only one primary solute and one wavelength shifter composed of 2% PTP + 0.06% POPOP has decay time equal to  $1.59 \pm 0.01$  ns, and sample with 2% PPO + 0.06% POPOP has decay time  $1.66 \pm 0.02$  ns.

In group of samples with 2% PPO as primary solute the slowest are those of DM-POPOP in their compositions with decay times from 1.80 to 1.96 ns. DM-POPOP with own slow decay time affects the rest of fastest fluorescent ingredients.



## 8. Discussion and conclusions

The aim of the thesis was to develop polystyrene scintillator for use in the novel time of flight J-PET scanner which is being elaborated for the whole-body PET imaging. To achieve this goal, scintillators with the different chemical compositions were produced. Spectroscopic and optical properties of these polystyrene scintillators were measured. Relative light output, decay time, emission spectra and technical attenuation lengths were measured to develop best composition.

Optimization of the conditions of styrene polymerization for the production of gamma radiation detectors was conducted. As a result of the work presented in this thesis the time-temperature cycles were established: (i) for polymerization in small cylinders as well as (ii) for polymerization in the glass mold allowing to manufacture plastic scintillator strips.

This thesis presents also a new method developed for the fast quality control of plastic scintillator strips. The method was successfully applied during J-PET prototype building. Several hundred of plastic scintillator strips can be optically checked in short time. Measurement of technical attenuation length also was accelerated by UV lamp use instead of radioactive sources.

Structure of manufactured scintillators were studied using two methods: powder X-ray diffraction (PXRD) and differential scanning calorimetry (DSC). Amorphous state of polystyrene was confirmed by PXRD. Polystyrene in scintillator is atactic and amorphous. Random positioning of phenyl group on both sides of the hydrocarbon backbone prevents the chains from aligning with sufficient regularity to achieve high degree of crystallinity. Broad peaks in PXRD diffractogram show amorphous state of polystyrene manufactured in this PhD research. Amorphous polystyrene allows visible light to be propagated inside of plastic scintillator. Glass transition temperature ( $T_g$ ) of polystyrene scintillator was determined as 98.5°C and for polyvinyltoluene scintillator is 86.65°C. The glass transition temperature  $T_g$  value was determined and used for design of annealing phase in polymerization cycle in furnace.

Wavelengths of maximum emission of produced plastic scintillators are in the range from 422 nm to 435 nm. This polystyrene scintillator emission spectra are well matched with vacuum photomultiplier tubes used in J-PET scanner prototype. Vacuum photomultiplier tubes have maximum quantum efficiency for light detecting around 400 nm. Developed polystyrene scintillators are also well matched with the silicone photomultipliers which have broad spectrum of quantum efficiency with maximum at 450 nm [184].

Decay time of investigated polystyrene scintillator samples are in the range from 1.51 ns to 2.00 ns. Decay time  $1.51 \pm 0.02$  ns of the fastest polystyrene scintillator is for composition with 2% BPBD primary solute and 0.06% POPOP wavelength shifter. The lowest value of decay time is connected with its composition of only two fluorescent substances. Sample contains two fluorescent additives and energy transfer between first and second dyes are faster than in other compositions with multiple of dyes.

Relative light output values of polystyrene scintillators were also studied in this thesis and they are determined to be between 51.1 and 80.1 percent compared to stilbene crystal. The best chemical composition of polystyrene scintillators are: 2% PPO with 0.03% bis-MSB and 0.03% POPOP; 2% PPO with 0.02% POPOP, 0.02% DM-POPOP and 0.02% bis-MSB; 2% BPBD with 0.06% POPOP. Among them polystyrene scintillator with 2% PPO primary solute and 0.03% bis-MSB and 0.03% POPOP wavelength shifters is characterized by the best light output of over 11200 photons per MeV which is comparable with light output of BC-420 with value 10240 photons per MeV.

Properties of polystyrene scintillators manufactured and investigated in this thesis are given in Table 15. Obtained values of light output, decay time and wavelength of maximum emission spectra are very similar to properties of commercially available plastic scintillators based on polyvinyltoluene [30].

**Table 15. Summarized results from synthesized polystyrene scintillators**

Sample No.	Primary solute	Secondary solute	$\lambda_{em}$ [nm]	$\tau$ [ns]	Light output [photons/MeV]
1	2% PPO	0.06% POPOP	422	1.66	9370
2		0.06% DM-POPOP	435	1.96	7151
3		0.06% bis-MSB	429	1.62	9809
4		0.03% POPOP + 0.03% DM-POPOP	434	1.81	8845
5		0.03% DM-POPOP + 0.03% bis-MSB	433	1.81	7946
6		0.03% bis-MSB + 0.03% POPOP	423	1.80	11212
7		0.02% POPOP + 0.02% DM-POPOP + 0.02% bis-MSB	433	1.80	10672
8	2% PPO	0.06% POPOP	-	1.76	9346
9	2% PTP		-	1.59	9611
10	2% BPBD		-	1.51	10772
11	1% PPO + 1% PTP		-	1.58	10141
12	1% PTP + 1% BPBD		-	1.62	8727
13	1% BPBD + 1% PPO		-	1.87	10336
14	0.67% PPO + 0.67% PTP + 0.67% BPBD		-	1.66	9846
15	2% PPO	-	-	2.00	-
16	2% PTP	-	-	1.47	-
17	2% BPBD	-	-	1.46	-
18	-	0.06% POPOP	-	1.53	-
19	-	0.06% DM-POPOP	-	1.80	-
20	-	0.06% bis-MSB	-	1.64	-

The research presented in this thesis resulted also in the concept of a method and a system for determining parameters of a position of a gamma quantum reaction within a scintillator detector of a PET scanner. The concept is based on measurement with two photomultiplier tubes with different quantum efficiency of light detection. This method uses the fact that light attenuation strongly depends on its wavelength. The method is beyond the scope of this thesis and for details the interested reader is referred to the patent publication [185].

## 9. Appendix A

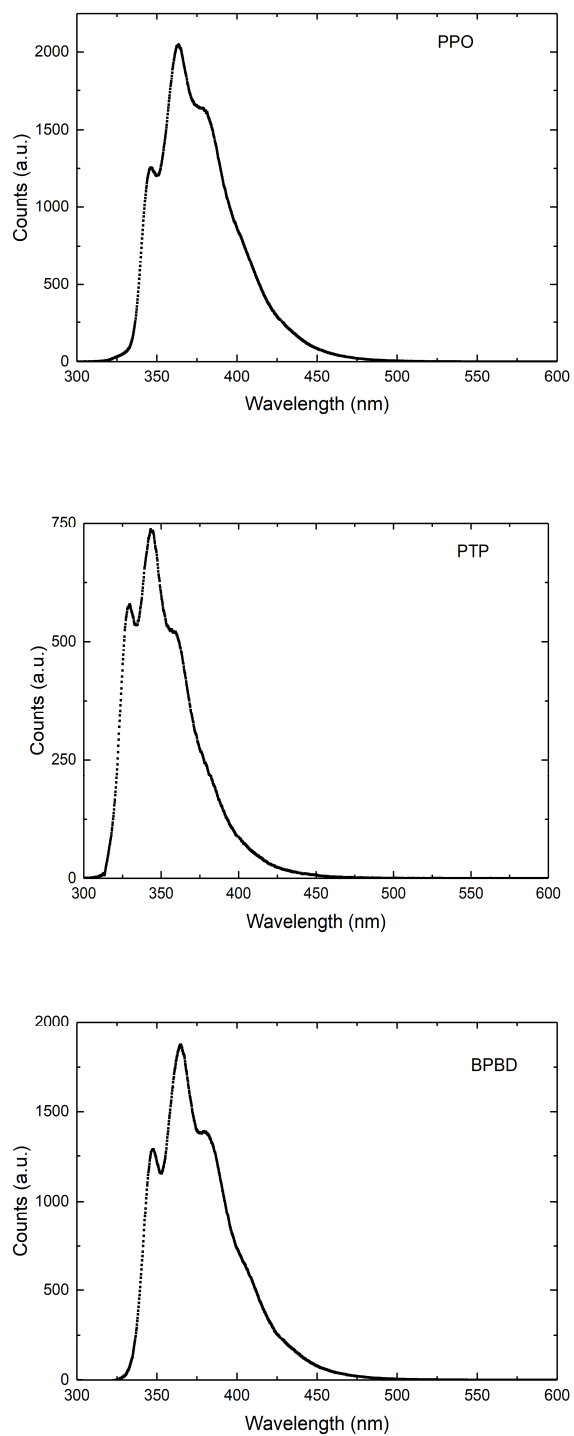
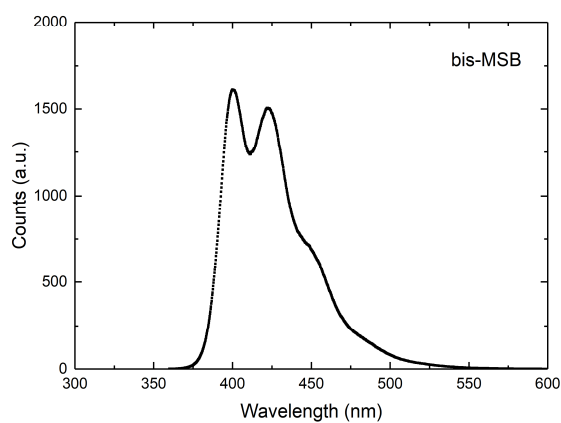
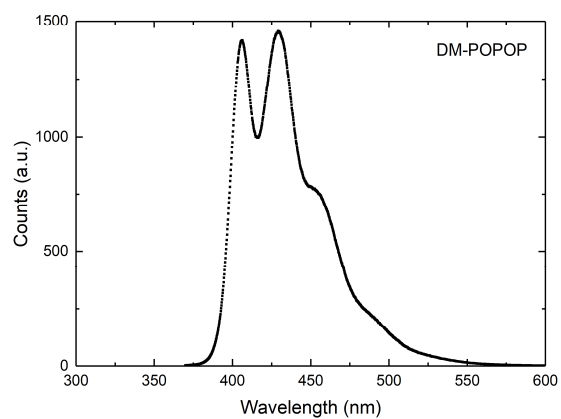
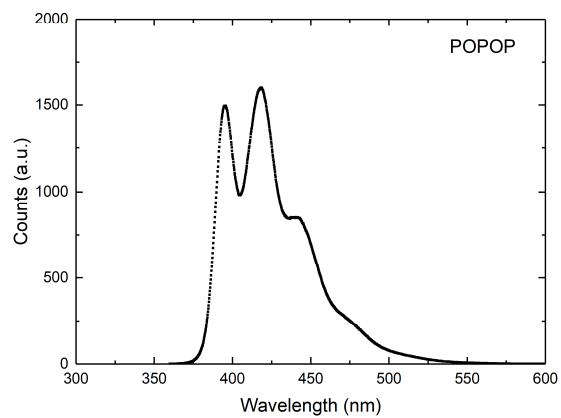
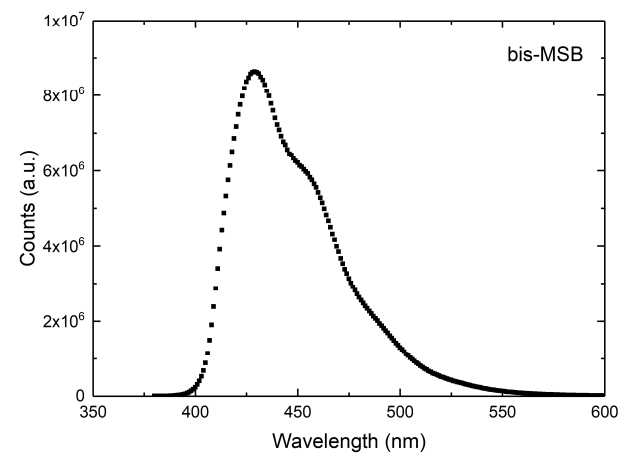
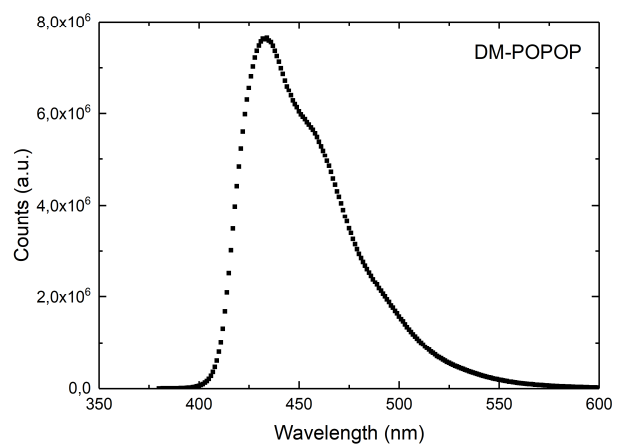
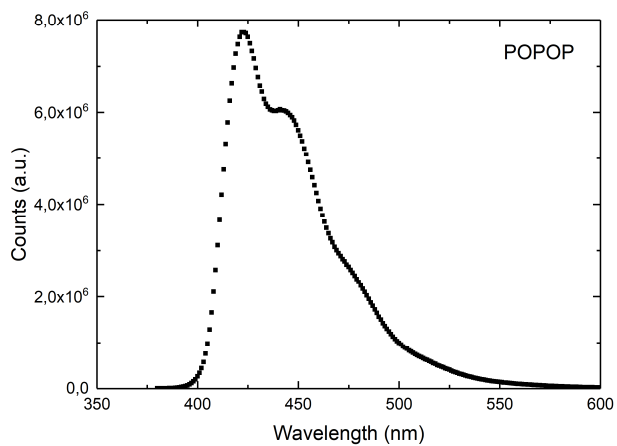


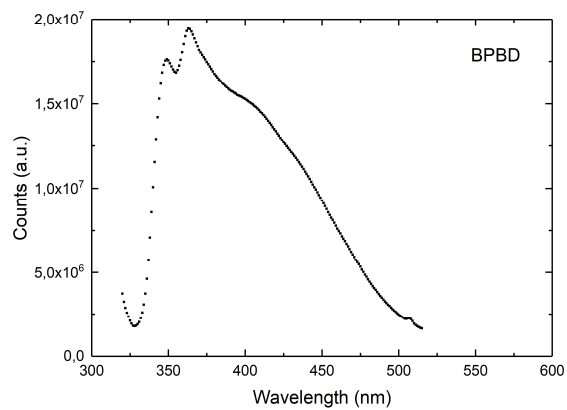
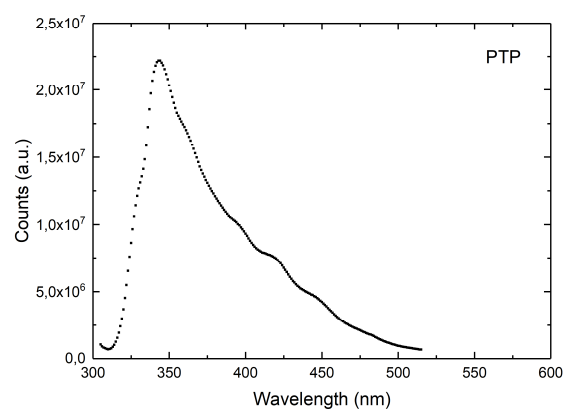
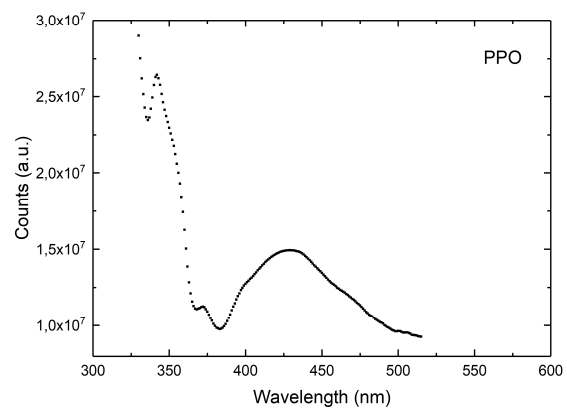
Figure 58. Emission spectra of primary fluorescent additives in toluene



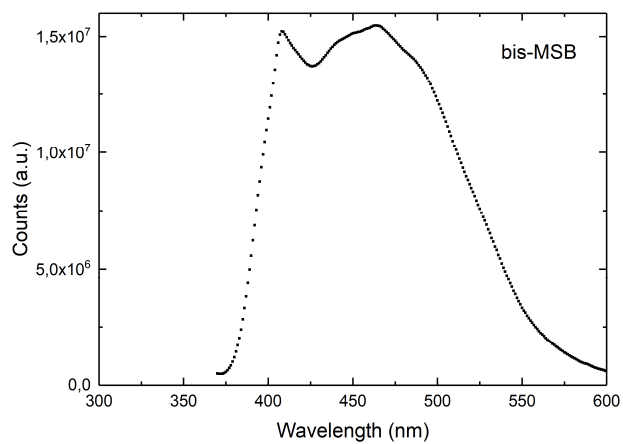
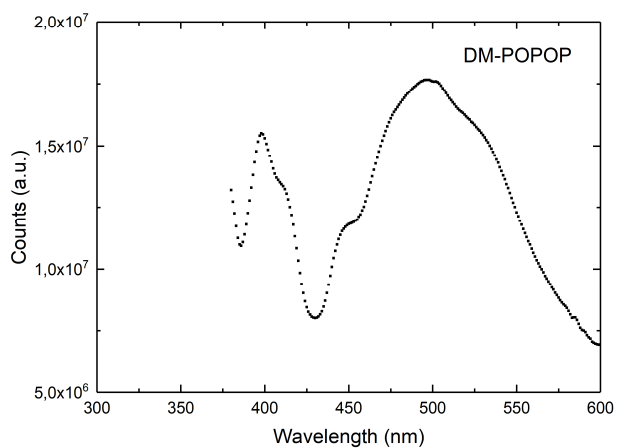
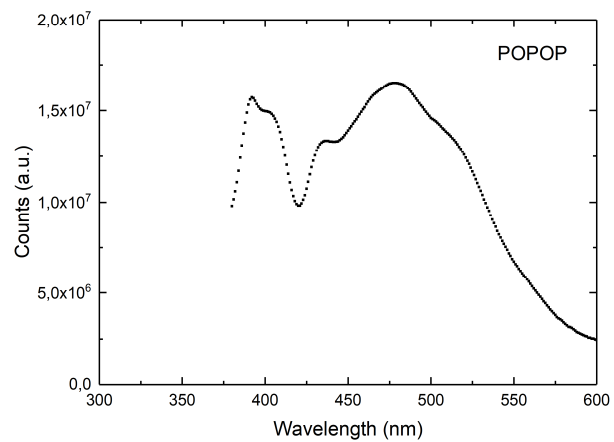
**Figure 59. Emission spectra of secondary fluorescent additives in toluene**



**Figure 60. Emission spectra of secondary fluorescent additives in polystyrene scintillator**



**Figure 61. Emission spectra of primary fluorescent additives in pure polystyrene**



**Figure 62. Emission spectra of secondary fluorescent additives in pure polystyrene**



## 10. References

- [1] P. Slomka et al., Recent advances and future progress in PET instrumentation, *Seminars in Nuclear Medicine* 46 No. 1 (2016) 5.
- [2] S. Vandenberghe et al., Recent developments in time-of-flight PET, *EJNMMI Physics* 3:3 (2016).
- [3] X. Zhang et al., Quantitative image reconstruction for total-body PET imaging using the 2-meter long EXPLORER scanner, *Physics in Medicine and Biology* 62 (6) (2017) 2465.
- [4] S. Cherry et al., Total-body imaging: Transforming the role of positron emission tomography, *Science Translation Medicine* 9 (2017) 381 .
- [5] J. Lacy et al., High sensitivity, low cost PET using lead-walled straw detectors, *Nuclear Instruments and Methods in Physics Research Section A* 471 (2001) 88.
- [6] N. Shehad et al., Novel lead-walled straw PET detector for specialized imaging applications, *Nuclear Science Symposium Conference Record IEEE* 4 (2005) 2895.
- [7] G. Belli et al., RPC: From high energy physics to positron emission tomography, *Journal of Physics: Conference Series* 41 (2006) 555.
- [8] A. Blanco et al., Efficiency of RPC detectors for whole-body human TOF-PET, *Nuclear Instruments and Methods in Physics Research Section A* 602 (2009) 780.
- [9] P. Moskal et al., Novel detector systems for the positron emission tomography, *Bio-Algorithms and Med-Systems* 14 (2011) 73.
- [10] P. Moskal, ..., Ł. Kapłon et al., Test of a single module of the J-PET scanner based on plastic scintillators, *Nuclear Instruments and Methods in Physics Research Section A* 764 (2014) 317.
- [11] P. Moskal, ..., Ł. Kapłon et al., Time resolution of the plastic scintillator strips with matrix photomultiplier readout for J-PET tomograph, *Physics in Medicine & Biology* 61 (2016) 2025.
- [12] P. Moskal, ..., Ł. Kapłon et al., Strip-PET: a novel detector concept for the TOF-PET scanner, *Nuclear Medicine Review* 15 (2012) Supplement C 68.
- [13] P. Moskal, ..., Ł. Kapłon et al., TOF-PET detector concept based on organic scintillators, *Nuclear Medicine Review* 15 (2012) Supplement C 81.
- [14] Jagiellonian-PET collaboration, <http://koza.if.uj.edu.pl/>.

- [15] P. Moskal, A hybrid TOF-PET/MRI tomograph, patent application No. PCT/EP2014/068373.
- [16] P. Moskal, A hybrid TOF-PET/CT tomograph, patent application No. PCT/EP2014/068363.
- [17] G. F. Knoll, Radiation Detection and Measurement, 4th ed., John Wiley & Sons 2010.
- [18] C. Fabjan and H. Schopper (Eds.), Elementary Particles: Detectors for Particles and Radiation, Part 2: Systems and Applications, Springer 2011.
- [19] C. Grupen, I. Buvat (Eds.), Handbook of Particle Detection and Imaging, Springer 2012.
- [20] John Caunt Scientific, Scintillation detectors, <http://www.johncaunt.com/detectors/scintillation-detectors/applications-general-properties/>.
- [21] R. Zaleski et al., Macro- and nanoscopic studies of porous polymer swelling, *Macromolecules* 50 (13) (2017) 5080.
- [22] B. Jasińska, ..., Ł. Kapłon et al., Determination of the 3gamma fraction from positron annihilation in mesoporous materials for symmetry violation experiment with J-PET scanner, *Acta Physica Polonica B* 47 (2016) 453.
- [23] E. Kubicz, ..., Ł. Kapłon et al., Studies of unicellular micro-organisms *Saccharomyces cerevisiae* by means of positron annihilation lifetime spectroscopy, *Nukleonika* 60 (4) (2015) 749.
- [24] A. Wieczorek, ..., Ł. Kapłon et al., PALS investigations of free volumes thermal expansion of J-PET plastic scintillator synthesized in polystyrene matrix, *Nukleonika* 60 (4) (2015) 777.
- [25] Ludlum Measurements, <http://safeguard.ludlums.com/solutions>.
- [26] Saint-Gobain Oil and Gas Group, Crystals detectors, <http://www.oilandgas.saint-gobain.com/scintillation-detectors.aspx>.
- [27] S. Tavernier, Radiation Detectors for Medical Applications, Springer 2006.
- [28] Scintillation Properties, <http://scintillator.lbl.gov/>.
- [29] Scintillation Technologies, Plastic scintillators, [www.scintitech.com](http://www.scintitech.com).
- [30] Saint-Gobain, Plastic product materials, [http://www.crystals.saint-gobain.com/Plastic\\_Material.aspx](http://www.crystals.saint-gobain.com/Plastic_Material.aspx).
- [31] Eljen Technology, Liquid scintillators, <http://www.eljentechnology.com/index.php/products/liquid-scintillators>.

- [32] Cryos-Beta, Organic molecular single crystals, <http://www.cryos-beta.kharkov.ua/organic.php>.
- [33] J. Birks, *The Theory and Practice of Scintillation Counting*, Pergamon Press 1964.
- [34] O. Sytnik, et al., Polymer composite based on polystyrene containing GdF<sub>3</sub> nanoparticles, *Functional Materials* 20 No. 2 (2013) 243.
- [35] W. Cai et al., Synthesis of bulk-size transparent gadolinium oxide-polymer nanocomposites for gamma ray spectroscopy, *Journal of Materials Chemistry C* 1 (2013) 1970.
- [36] N. Galunov et al., Single-layer and multilayer composite scintillators based on organic molecular crystalline grains, *IEEE Nuclear Science Symposium Conference Record* (2011) 1869.
- [37] G. Britvich et al., New scintillation materials for particle detectors, *Instruments and Experimental Techniques* 44 No. 4, (2001) 472.
- [38] Z. Kang et al., CdTe quantum dots and polymer nanocomposites for x-ray scintillation, *Applied Physics Letters* 98 (2011) 181914.
- [39] Y. Sun et al., High-energy X-ray detection by hafnium-doped organic-inorganic hybrid, *Applied Physics Letters* 104 (2014) 174104.
- [40] J. Park et al., Scintillation properties of quantum-dot doped styrene based plastic scintillators, *Journal of Luminescence* 146 (2014) 157.
- [41] Saint-Gobain, Organic scintillation materials, <http://www.crystals.saint-gobain.com/uploadedFiles/SG-Crystals/Documents/SGC%20Organics%20Brochure.pdf>.
- [42] D. Bailey, *Positron Emission Tomography Basic Sciences*, Springer 2005.
- [43] Hamamatsu Product Catalog: Photomultiplier Tubes and Assemblies. For Scintillation Counting and High Energy Physics, 2012.
- [44] K. Iniewski, *Medical Imaging: Principles, Detectors and Electronics*, Wiley 2009.
- [45] L. Raczyński, ..., Ł. Kapłon et al., Novel method for hit-positron reconstruction using voltage signals in plastic scintillators and its application to the positron emission tomography, *Nuclear Instruments and Methods in Physics Research A* 764 (2014) 186.
- [46] L. Raczyński, ..., Ł. Kapłon et al., Compressive sensing of signals generated in plastic scintillators in a novel J-PET instrument, *Nuclear Instruments and Methods in Physics Research A* 786 (2015) 105.

- [47] P. Moskal, ..., Ł. Kapłan et al., A novel method for the line-of-response and time-of-flight reconstruction in TOF-PET detectors based on a library of synchronized model signals, *Nuclear Instruments and Methods in Physics Research A* 775 (2015) 54.
- [48] A. Wieczorek, ..., Ł. Kapłan et al., A pilot study of the novel J-PET plastic scintillator with 2-(4-styrylphenyl)benzoxazole as a wavelength shifter, *Acta Physica Polonica A* 127 (2015) 1487.
- [49] G. Korcyl, ..., Ł. Kapłan et al., Sampling FEE and trigger-less DAQ for the J-PET scanner, *Acta Physica Polonica B* 47 (2016) 491.
- [50] A. Gajos, ..., Ł. Kapłan et al., Trilateration-based reconstruction of ortho-positronium decays into three photons with the J-PET detector, *Nuclear Instruments and Methods in Physics Research A* 819 (2016) 54.
- [51] D. Kamińska, ..., Ł. Kapłan et al., Searches for discrete symmetries violation in ortho-positronium decay using the J-PET detector, *Nukleonika* 60 (4) (2015) 729.
- [52] N. G. Sharma, ..., Ł. Kapłan et al., Reconstruction of hit-time and hit-position of annihilation quanta in the J-PET detector using the Mahalanobis distance, *Nukleonika* 60 (4) (2015) 765.
- [53] W. Krzemień, ..., Ł. Kapłan et al., Processing optimization with parallel computing for the J-PET tomography scanner, *Nukleonika* 60 (4) (2015) 745.
- [54] P. Kowalski, ..., Ł. Kapłan et al., Multiple scattering and accidental coincidences in the J-PET detector simulated using GATE package, *Acta Physica Polonica A* 127 (2015) 1505.
- [55] P. Białas, ..., Ł. Kapłan et al., GPU accelerated image reconstruction in a two-strip J-PET tomograph, *Acta Physica Polonica A* 127 (2015) 1500.
- [56] Saint-Gobain Crystals, BC-418, BC-420, BC-422, BC-422Q Plastic Scintillators, <http://www.crystals.saint-gobain.com/products/BC418-BC420-BC422-BC422Q>.
- [57] Y. Arikawa et al., Characterization of the plastic scintillator BC-422 and BC-422Q for neutron measurement, Institute of Laser Engineering, Osaka University 2007.
- [58] M. Moszyński et al., Status of timing with plastic scintillation detectors, *Nuclear Instruments and Methods* 158 (1979) 28.
- [59] Particle detectors for accelerators - Particle Data Group, <http://pdg.lbl.gov/2011/reviews/rpp2011-rev-particle-detectors-accel.pdf>.
- [60] B. Valeur, *Molecular Fluorescence. Principles and Applications*, Wiley 2002.
- [61] S. Majewski, C. Zorn, *Fast scintillators for high radiation levels [in:] F. Sauli, Instrumentation in High Energy Physics*, World Scientific 1992.

- [62] M. Sauer, J. Hofkens and J. Enderlein, Handbook of Fluorescence Spectroscopy and Imaging, Wiley 2011.
- [63] S. Beddar, L. Beaulieu (Eds.), Scintillation Dosimetry, CRC Press 2016.
- [64] J. Birks, K. Kuchela, Energy transfer in fluorescent plastic solutions, Discussions of the Faraday Society 27 (1959) 57 [in:] J. Birks, The Theory and Practice of Scintillation Counting, Pergamon Press 1964.
- [65] T. Adam et al., The OPERA experiment target tracker, Nuclear Instruments and Methods in Physics Research A 577 Issue 3 (2007) 523.
- [66] S. Moser et al., Principles and practice of plastic scintillator design, Radiation Physics and Chemistry 41 No. 1/2 (1993) 31.
- [67] J. Mark, Polymer Data Handbook, Oxford University Press 1999.
- [68] J. Brandrup et al., Polymer Handbook, John Wiley & Sons 1999.
- [69] H. Mark, Encyclopedia of Polymer Science and Technology, 3rd ed., Wiley 2004.
- [70] Nuvia Group, Scintillation detectors, [www.nuvia.cz/en/produkty/89-scintillation-detectors](http://www.nuvia.cz/en/produkty/89-scintillation-detectors).
- [71] EPIC Crystal, Plastic scintillator, [www.epic-crystal.com/shop\\_reviews/plastic-scintillator](http://www.epic-crystal.com/shop_reviews/plastic-scintillator).
- [72] Amcrys, [www.amcrys.com](http://www.amcrys.com).
- [73] SRC IHEP facilities, <http://exwww.ihep.ru/scint/bulk/product-e.htm>.
- [74] Kuraray Co., Plastic scintillating fibers, <http://kuraraypsf.jp/index.html>.
- [75] Saint-Gobain Crystals, Scintillating fiber, [www.crystals.saint-gobain.com/products/scintillating-fiber](http://www.crystals.saint-gobain.com/products/scintillating-fiber).
- [76] V. Salimgareeva, S. Kolesov, Plastic scintillators based on polymethyl methacrylate: a review, Instruments and Experimental Techniques 48 No. 3 (2005) 273.
- [77] W. Kienzle et al., Scintillator development at CERN, NP Internal Report 75-12, Geneva 1975.
- [78] T. Ferbel, Experimental Techniques in High-Energy Nuclear and Particle Physics, World Scientific Publishing 1991.
- [79] Eljen Technology, Light guides and acrylic plastics, <http://www.eljentechnology.com/index.php/products/light-guides-and-acrylic-plastic>.

- [80] N. Barashkov, Factors determining radiation stability of plastic scintillators, *Applied Radiation and Isotopes* 47 Issue 11–12 (1996) 1557.
- [81] J. Simonetti, High temperature plastic scintillator, US patent No. US 4713198, 1987.
- [82] J. Simonetti, High temperature scintillator, US patent No. US 6884994 B2, 2005.
- [83] B. Rupert et al., Bismuth-loaded plastic scintillators for gamma-ray spectroscopy, *Europhysics Letters* 97 (2012) 22002.
- [84] H. Nakamura et al., Undoped polycarbonate for detection of environmental radiation, *Japanese Journal of Health Physics* 49 (2) (2014) 98.
- [85] H. Nakamura et al., Radiation measurements with heat proof polyethylene terephthalate bottles, *Proceedings of the Royal Society of London A* 466 (2010) 2847.
- [86] H. Nakamura et al., Evidence of deep-blue photon emission at high efficiency by common plastic, *Europhysics Letters* 95 (2011) 22001.
- [87] Revolutionary radiation-sensitive plastic, <http://www.nirs.go.jp/ENG/press/110629.shtml>.
- [88] H. Nakamura et al., Polysulfone as a scintillation material without doped fluorescent molecules, *Nuclear Instruments and Methods in Physics Research A* 797 (2015) 206.
- [89] H. Nakamura et al., Poly (ether sulfone) as a scintillation material for radiation detection, *Applied Radiation and Isotopes* 86 (2014) 36.
- [90] H. Nakamura et al., Undoped poly (phenyl sulfone) for radiation detection, *Radiation Measurements* 73 (2015) 14.
- [91] A. Quaranta et al., Optical and scintillation properties of polydimethyl-diphenylsiloxane based organic scintillators, *IEEE Transactions of Nuclear Science* 57 No. 2 (2010) 891.
- [92] Poly(2-vinylnaphthalene), Sigma-Aldrich, <http://www.sigmaaldrich.com/catalog/product/aldrich/461946?lang=pl&region=PL>.
- [93] J. Dharia et al., Synthesis and characterization of wavelength-shifting monomers and polymers based on 3-hydroxyflavone, *Macromolecules* 27 (1994) 5167.
- [94] N. Zaitseva et al., Plastic scintillators with efficient neutron-gamma pulse shape discrimination, *Nuclear Instruments and Methods in Physics Research A* 668 (2012) 88.

- [95] A. Artikov et al., Properties of the Ukraine polystyrene-based plastic scintillator UPS 923A, *Nuclear Instruments and Methods in Physics Research A* 555 (2005) 125.
- [96] D. Horrock, Chin-Tzu Peng (Eds.), *Organic Scintillators and Liquid Scintillation Counting*, Academic Press 1971.
- [97] W. Selove et al., Fluorescent-wave-shifters and scintillators for calorimeters, *Nuclear Instruments and Methods* 161 (1979) 233.
- [98] J. Lakowicz, *Principles of Fluorescence Spectroscopy*, Springer 2006.
- [99] I. Berlman, *Handbook of Fluorescence Spectra of Aromatic Molecules*, Academic Press 1971.
- [100] J. Birks, *Solutes and Solvents for Liquid Scintillation Counting*, Koch-Light Laboratories 1969.
- [101] Exciton, Laser dyes, <http://www.exciton.com/laserdyeslist.html>.
- [102] U. Brackmann, *Lambdachrome Laser Dyes*, 3rd ed., Lambda Physik AG, Germany 2000.
- [103] American Dye Source, OLED & PLED materials, <http://www.adsdyes.com/oled.htm>.
- [104] Luminescence Technology Corp., OLED materials, <http://www.lumtec.com.tw/product1.asp?id=94>.
- [105] H. Gusten, PMP, a novel solute for liquid and plastic scintillation counting, *Advances in Scintillation Counting* (1984) 330.
- [106] A. Pla-Dalamu, *Design of fluorescent compounds for scintillation detection*, Doctoral dissertation, Northern Illinois University, USA 1990.
- [107] H. Gusten, J. Mirsky, PMP, a Novel Scintillation Solute with a Large Stokes' Shift, 1989 [in:] H. Ross et al., *Liquid Scintillation Counting and Organic Scintillators*, Lewis Publishers 1991.
- [108] F. Sguerra et al., Thermo- and radioluminescent polystyrene based plastic scintillators doped with phosphorescent iridium(iii) complexes, *Journal of Materials Chemistry C* 2 (2014) 6125.
- [109] B. Rupert et al., Bismuth-loaded plastic scintillators for gamma-ray spectroscopy, *Europhysics Letters* 97 (2012) 22002.
- [110] E. Velmozhnaya et al., Mixed-ligand complexes of gadolinium carboxylates containing unsaturated bonds in plastic scintillators, *Functional Materials* 22 No. 2 (2015) 274.

- [111] Saint-Gobain, Plastic scintillator BC-422Q, <http://www.crystals.saint-gobain.com/uploadedFiles/SG-Crystals/Documents/SGC%20BC422Q%20Data%20Sheet.pdf>.
- [112] Eljen Technology, Fast timing plastic scintillator EJ-232Q, <http://www.eljentechnology.com/index.php/products/plastic-scintillators/ej-232-ej-232q>.
- [113] Current Manufacturing Techniques, <http://vclendenen.tripod.com/id4.html>.
- [114] F. Markley et al., Development of radiation hard scintillators, *Radiation Physics and Chemistry* 41 No. 1/2 (1993) 135.
- [115] V. Senchishin, A new radiation stable plastic scintillator, *Nuclear Instruments and Methods in Physics Research A* 364 (1995) 253.
- [116] Eljen Technology, boron loaded plastic scintillator EJ-254, <http://www.eljentechnology.com/index.php/products/plastic-scintillators/ej-254>.
- [117] G. Britvich et al., A neutron detector on the basis of a boron-containing plastic scintillator, *Nuclear Instruments and Methods in Physics Research A* 550 (2005) 343.
- [118] Z. Bell et al., Boron-loaded silicone rubber scintillators, *IEEE Transactions on Nuclear Science* 51 No. 4 (2004) 1773.
- [119] R. Breukers et al., Transparent lithium loaded plastic scintillators for thermal neutron detection, *Nuclear Instruments and Methods in Physics Research A* 701 (2013) 58.
- [120] A. Mabe et al., Transparent lithium-6 based polymer scintillation films containing a polymerizable fluor for neutron detection, *Radiation Measurements* 66 (2014) 5.
- [121] Z. Bell et al., Organic scintillators for neutron detection, *Proceedings of SPIE* 4784 (2003) 150.
- [122] A. Bedrik et al., Plastic scintillator with gadolinium phenylpropionate, *Functional Materials* 18 (4) (2011) 470.
- [123] S. Sandler, K. Tsou, Quenching of the scintillation process in plastics by organometallics, *The Journal of Physical Chemistry* 68 (2) (1964) 300.
- [124] K. Tsou, Evaluation of organometallic compounds for gamma detection in plastic scintillators, *IEEE Transactions on Nuclear Science* 12 (1965) 28.
- [125] J. Dannin, S. Sandler, B. Baum, The use of organometallic compounds in plastic scintillators for the detection and resolution of gamma rays, *The International Journal of Applied Radiation and Isotopes* 16 (1965) 589.



- [126] G. Britvich et al., New heavy plastic scintillators, *Instruments and Experimental Techniques* 43 No. 1 (2000) 36.
- [127] M. Hamel et al., Preparation and characterization of highly lead-loaded red plastic scintillators under low energy x-rays, *Nuclear Instruments and Methods in Physics Research Section A* 660 (2011) 57.
- [128] Saint-Gobain, BC-452 Lead-loaded plastic scintillators, <http://www.crystals.saint-gobain.com/uploadedFiles/SG-Crystals/Documents/SGC%20BC452%20Data%20Sheet.pdf>.
- [129] B. Rupert et al., Bismuth-loaded plastic scintillators for gamma-ray spectroscopy, *Europhysics Letters* 97 (2012) 22002.
- [130] N. Cherepy et al., Bismuth- and lithium-loaded plastic scintillators for gamma and neutron detection, *Nuclear Instruments and Methods in Physics Research A* 778 (2015) 126.
- [131] K. Bower, Y. Barbanel, Y. Shreter, G. Bohnert (Eds.), *Polymers, Phosphors, and Voltaics for Radioisotope Microbatteries*, CRC Press 2002.
- [132] B. Funt, A. Hetherington, The influence of chain length on the luminescent output of plastic scintillators, *The International Journal of Applied Radiation and Isotopes* 4 (1959) 189.
- [133] R. Swank, W. Buck, The scintillation process in plastic solid solutions, *Physical Review* 91 (1953) 927.
- [134] A. Adadurov et al., Optimizing concentration of shifter additive for plastic scintillators of different size, *Nuclear Instruments and Methods in Physics Research A* 599 (2009) 167.
- [135] R. Swank, W. Buck, The scintillation process in plastic solid solutions, *Physical Review* 91 (1953) 931.
- [136] J. Marchant et al., PVT scintillators with very-high fluorescent dye concentrations, *IEEE Nuclear Science Symposium Conference Record* (2009) 1555.
- [137] Ł. Kapłon et al., Plastic scintillators for positron emission tomography obtained by the bulk polymerization method, *Bio-Algorithms and Med-Systems* 10 (2014) 27.
- [138] E. Arndt, K. Parrish, A. Seidel, *Processing and Finishing of Polymeric Materials*, Wiley 2011.
- [139] Machery-Nagel GmbH & Co, *Derivatization in gas chromatography*, <http://www.mn-net.com/tabid/12428/default.aspx>.
- [140] SubsTech (Substances&Technologies). Information about methods of polymers fabrication, <http://www.substech.com/dokuwiki/doku.php>.

- [141] A. Karyukhin et al., Injection molding scintillator for ATLAS tile calorimeter, ATLAS internal note, CERN, Geneva 1996.
- [142] J. Thevenin et al., Extruded polystyrene, a new scintillator, Nuclear Instruments and Methods in Physics Research Section A 169 (1980) 53.
- [143] A. Pla-Dalmau et al., Low-cost extruded plastic scintillator, Nuclear Instruments and Methods in Physics Research Section A 466 (2001) 482.
- [144] V. Senchyshyn et al., Influence of polystyrene scintillator strip methods of production on their main characteristics, Radiation Measurements 42 (2007) 911.
- [145] Brenntag, Styrene monomer, <http://www.brenntag.be/prd/product/styrenestyrenestyreenen.php>.
- [146] Sigma-Aldrich, Methylstyrene monomer, <http://www.sigmaaldrich.com/catalog/product/aldrich/522864?lang=pl&region=PL>.
- [147] W. Armarego, Purification of Laboratory Chemicals, Butterworth-Heinemann 2017.
- [148] HEK, Activated alumina sorbent, <http://www.hek.com.pl/program-produktow/adsorbent-granulat-osuszajacy>.
- [149] P. Zhmurin et al., Organization of production of large-size plastic scintillators for physical experiments, Institute for Scintillation Materials of NAS of Ukraine.
- [150] Sigma-Aldrich, Scintillation reagents, <http://www.sigmaaldrich.com/>.
- [151] Czylok, Split tubular furnace on stand, <http://czylok.com.pl/en/dla-laboratoriow/tubular-type-rsd/split-tubular-furnace-on-stand>.
- [152] L. Thornhill, Scintillation Counter Technology, CERN 1983.
- [153] Safe Handling and Storage of Styrene Monomer, Chevron Phillips Chemical Company 2010.
- [154] M. Gilbert (Ed.), Brydson's Plastics Materials, Butterworth-Heinemann 2017.
- [155] D. Rosato, D. Rosato, M. Rosato, Plastic Product Material and Process Selection Handbook, Elsevier Science 2004.
- [156] C. Harper, E. Petrie, Plastics Materials and Processes: A Concise Encyclopedia, John Wiley & Sons 2003.
- [157] Czylok, furnace DCF 420/spec, [www.czylok.com.pl/piece-i-urzadzenia-specjalne/urzadzenia-specjalne/dcf-420-spec-pl](http://www.czylok.com.pl/piece-i-urzadzenia-specjalne/urzadzenia-specjalne/dcf-420-spec-pl).

- [158] P. Rebourgeard et al., Fabrication and measurements of plastic scintillating fibers, Nuclear Instruments and Methods in Physics Research Section A 427 (1999) 543.
- [159] A. Kamieński et al., Preparation method of standard plastic scintillators on the base of polystyrene with improved light output, Institute of Nuclear Research, Warsaw, Poland 1975.
- [160] P. Zhmurin et al., Plastic scintillator for pulse shape neutrons and gamma quanta discrimination, Radiation Measurements 62 (2014) 1.
- [161] P. Zhmurin et al., Polystyrene-based plastic scintillator for n- $\gamma$ -discrimination, Functional Materials 21 No. 3 (2014) 282.
- [162] Paul Gabbott (Ed.), Principles and Applications of Thermal Analysis, Blackwell Publishing 2008.
- [163] G. Höhne, W. Hemminger, H. Flammersheim, Differential Scanning Calorimetry, Springer 2003.
- [164] Ullmann's Encyclopedia of Industrial Chemistry, Wiley 2007.
- [165] A. Clearfield, J. Reibenspies, N. Bhuvanesh (Eds.), Principles and Applications of Powder Diffraction, Wiley 2008.
- [166] R. Dinnebier, S. Billinge (Eds.), Powder Diffraction. Theory and Practise, RSC Publishing 2008.
- [167] E. Zolotoyabko, Basic Concepts of Crystallography, Wiley-VCH Verlag 2014.
- [168] C. Suryanarayana, M. Grant Norton, X-Ray Diffraction. A Practical Approach, Springer 1998.
- [169] C. De Rosa, F. Auriemma, Crystals and Crystallinity in Polymers. Diffraction Analysis of Ordered and Disordered Crystals, Wiley 2014.
- [170] Philips Lighting, TL miniature lamp 4W BLB,  
[http://www.lighting.philips.com/main/prof/conventional-lamps-and-tubes/special-lamps/colored-and-blacklightblue-blb/tl-mini-blacklight-blue/928000010803\\_EU/product](http://www.lighting.philips.com/main/prof/conventional-lamps-and-tubes/special-lamps/colored-and-blacklightblue-blb/tl-mini-blacklight-blue/928000010803_EU/product).
- [171] Silicon PIN photodiode S3590-06 data sheet,  
[http://www.datasheetlib.com/datasheet/1010023/s3590-06\\_hamamatsu-photonics.html](http://www.datasheetlib.com/datasheet/1010023/s3590-06_hamamatsu-photonics.html).
- [172] Ł. Kapłon, A. Wieczorek, E. Kubicz, S. Niedźwiecki, J-PET Report No. 25: Determining optical quality of plastic scintillator strips, Jagiellonian University 2013.

- [173] S. Niedźwiecki, ..., Ł. Kapłon et al., J-PET: A new technology for the whole-body PET imaging, *Acta Physica Polonica B* 48 (2017) 1567.
- [174] T. Hakamata (Ed.), *Photomultiplier Tubes. Basics and Applications*, Hamamatsu Photonics 2006.
- [175] P. Kowalski, Ł. Kapłon, J-PET Report No. 7: Dependence of absorption length of the EJ230 plastic scintillator on wavelengths of photons, Jagiellonian University 2014.
- [176] A. Baulin et al., Attenuation length and spectral response of Kuraray SCSF-78MJ scintillating fibres, *Nuclear Instruments and Methods in Physics Research A* 715 (2013) 48.
- [177] T. Bednarski, The energy calibration and timing synchronization of the modular scintillation detector system for TOF-PET tomograph, Doctoral dissertation, Jagiellonian University, Cracow, Poland 2016.
- [178] A. Wieczorek, Development of novel plastic scintillators based on polyvinyltoluene for the hybrid J-PET/MR tomograph, Doctoral dissertation, Jagiellonian University, Cracow, Poland 2017.
- [179] Double Beam Spectrophotometer U-2900/2910, [http://www.hitachi-hightech.com/global/product\\_detail/?pn=ana-u2900](http://www.hitachi-hightech.com/global/product_detail/?pn=ana-u2900).
- [180] B. Valeur, *Molecular Fluorescence. Principles and Applications*, Wiley 2002.
- [181] *Fluorolog-3 Operation Manual*, Horiba 2014.
- [182] M. Moszynski et al., Status of timing with plastic scintillation detectors, *Nuclear Instruments and Methods* 158 (1979) 1.
- [183] K. Dulski, private communication, Jagiellonian University, Cracow, Poland 2017.
- [184] MPPC module for PET, Hamamatsu Photonics 2016.
- [185] P. Moskal, Ł. Kapłon, A method and a system for determining parameters of a position of a gamma quantum reaction within a scintillator detector of a PET scanner, patent No. P.405188, PCT/EP2014/068382.